CHARACTERIZATION OF A NOVEL INTERACTION BETWEEN PRESENILIN-1 AND MONOAMINE OXIDASE-A

A Thesis Submitted to the
College of Graduate Studies and Research
in Partial Fulfillment of the Requirements
for a Master's Degree
in the Department of Psychiatry
University of Saskatchewan
Saskatoon

By
Geraldine Grace Gabriel

PERMISSION TO USE

In presenting this thesis in partial fulfillment of the requirements for a Master's degree from the University of Saskatchewan, I agree that the Libraries of this University make it freely available for inspection. I further agree that permission for copying of this thesis in any manner, in whole or in part, for scholarly purposes may be granted by Dr. Darrell D. Mousseau, who supervised my thesis work or, in his absence, the Head of the Department of Psychiatry at the University of Saskatchewan. It is understood that any copying, publication, or use of this thesis or parts thereof for financial gain shall not be allowed without my written permission. It is also understood that due recognition shall be given to me, to the Neuropsychiatry Research Unit of the Department of Psychiatry and to the University of Saskatchewan in any scholarly use which may be made of any material in my thesis.

Requests for permission to copy or to make other use of material in this thesis in whole or part should be addressed to:

Dr. Darrell D. Mousseau and/or

Head of the Department of Psychiatry

University of Saskatchewan

Saskatoon, Saskatchewan

Canada, S7N 5E4

ABSTRACT

The enzyme monoamine oxidase (MAO) is linked to mental disorders such as depression and neurodegenerative diseases. Our laboratory has recently demonstrated that increases in calcium (Ca^{2+}) can enhance MAO activity and that this might contribute to Alzheimer disease (AD). AD has been linked to gain-of-function mutations in the presenilin-1 (PS-1) protein that not only promote the generation of the toxic amyloid-β peptide, but that also alter intracellular Ca^{2+} availability.

Radioenzymatic MAO assays were used to demonstrate that over-expression of different AD-related PS-1 mutant proteins, *i.e.* Y115H, ΔEx9 and M146V, in hippocampal-derived HT-22 cells alter either basal and/or Ca^{2+}-sensitive MAO-A activity. The effects of PS-1 mutant proteins on the availability of intracellular Ca^{2+} are not consistent suggesting that this may not be the primary means of regulating MAO activity. The sensitivity of MAO to Ca^{2+} was also demonstrated in cortical (both MAO-A and MAO-B responded to Ca^{2+}) and cerebellar (only MAO-A responded to Ca^{2+}) samples from transgenic mice overexpressing the PS-1 (M146V) mutation. These changes in MAO coincided with changes in the availability of the neurotransmitters dopamine, noradrenaline and serotonin in the cerebellum, but not in the cortex, and reflect the known regional differences in neurotransmitter regulation. Immunoprecipitation studies and the observed increase in MAO-A activity following *in vitro* chemical inhibition of the γ-secretase complex (comprising several proteins including PS-1) support the notion that PS-1 constitutively associates with MAO-A. These effects on Ca^{2+}-sensitive MAO function could contribute to AD-related pathology and could also contribute to the depression often associated with AD.

ACKNOWLEDGMENTS

I would like to thank my research supervisor, Dr. Darrell D. Mousseau, for giving me the opportunity to pursue graduate studies at the University of Saskatchewan, and for all of his expert instruction and personal and financial support throughout my time here. I would also like to extend my thanks to my Advisory Committee members, Dr. Xin-Min Li and Dr. Adil Nazarali for their guidance of my research project during these years. In addition, I would like to thank my family and friends for their constant support in my pursuit of all of my degrees. I would also like to acknowledge the financial assistance that I have received through the College of Graduate Studies at the University of Saskatchewan and the Canadian Institutes of Health Research. Lastly, I would like to thank Dr. Glen Baker and his lab at the University of Alberta for generously collecting all of the HPLC data, and Dr. Xia Cao (University of Saskatchewan) for carrying out the subcellular fractionation procedure and collecting some of the cortical MAO data presented in my thesis.

TABLE OF CONTENTS

LIST OF FIGURES

LIST OF ABBREVIATIONS

3-MT	3-Methoxytyramine
5-HIAA	5-Hydroxyindoleacetic acid
5-HT	Serotonin
A	Adrenaline
Aβ	Amyloid-beta
AD	Alzheimer disease
ADH	Alcohol dehydrogenase
ADP	Adenosine diphosphate
APH-1	Anterior pharynx-defective 1
ANOVA	Analysis of variance
APP/hAPP	Amyloid precursor protein/ human amyloid precursor protein
APS	Ammonium persulfate
Asp	Aspartic acid
BSA	Bovine serum albumin
CB-28K	Calbindin D28K
CCE	Capacitative calcium entry
CMV	Cytomegalovirus
COMT	Catechol-o-methyltransferase
DA	Dopamine
DAPT	N-[N-(3,5-difluorophenacetyl)-L-alanyl]-S-phenylglycine t-butyl ester
DβH	Dopamine beta hydroxylase
DCF/DCFDA	2',7'-dichlorofluorescein
DMEM	Dulbecco's modified Eagle's medium
DMSO	Dimethyl sulfoxide
DNA	Deoxyribonucleic acid
DOPAC	3,4-Dihydroxyphenylacetic acid
E. coli	*Escherichia coli*
EDTA	Ethylenediaminetetraacetic acid
ECL	Enhanced chemiluminescent luminal

EOFAD	Early onset familial Alzheimer disease
ER	Endoplasmic reticulum
HEK	Human embryonic kidney
HPLC	High performance liquid chromatography
HVA	Homovanillic acid
IB	Immunoblot
IP	Immunoprecipitation
IP3	Inositol triphosphate
KUZ	Kuzbanian
LB	Loading buffer
MAO-A/MAO-B	Monoamine oxidase-A/ Monoamine oxidiase-B
MAP/MAPK	Mitogen activated protein/mitogen activated protein kinase
MCS	Multiple cloning site
ME	Metanephrine
MHPG	3-Methoxy-4-hydroxyphenylethyleneglycol
MPTP	1-methyl-4-phenyl-1, 2, 3, 6-tetrahydropyridine
mRNA	Messenger ribonucleic acid
MW	Molecular weight
NA	Noradrenaline
NICD	Notch intracellular domain
PAGE	Polyacrylamide gel electrophoresis
PBS	Phosphate buffered saline
PC	Phaeochromocytoma
PCR	Polymerase chain reaction
PEA	Phenylethylamine
PEN-2	Presenilin enhancer 2
PHF	Paired helical filaments
PNMT	Phenylethanolamine-N-methyltransferase
PS-1/PS-2	Presenilin-1/ Presenilin-2
RT	Room temperature
SDS	Sodium dodecyl sulfate

Swe	Swedish
TACE	TNF-alpha converting enzyme
TBE	Tris borate EDTA
TBS/TBS-T	Tris buffered saline (-Tween 20)
TCL	Total cell lysate
TEMED	N,N,N',N'-tetramethylethylenediamine
TRYP	Tryptophan
VMA	Vanillylmandelic acid
WT	Wild-type

1 INTRODUCTION

1.1 Alzheimer disease

Alzheimer disease (AD) is the most prevalent neurodegenerative disease today and the third most common affliction, apart from cancer and cardiovascular disease, in the elderly (1, 2). Two pathological hallmarks of AD are neurofibrillary tangles and amyloid plaques (3). Neurofibrillary tangles are comprised of tau protein. Tau is a microtubule associated protein that when phosphorylated dissociates from the microtubles forming insoluble paired helical filaments (PHF), which then combine to form intracellular neurofibrillary tangles. Amyloid plaques are extracellular and are comprised mostly of the protein amyloid beta (Aβ). Aβ, which can exist as a 40-mer or a 42-mer cleavage product derived from a precursor protein, is generally believed to be the main initiator of AD and promotes the amyloid cascade, which stimulates numerous cell pathways, including neurofibrillary tangle formation, to bring about neurodegeneration. AD can occur early in life (familial AD) or later on (sporadic AD). The direct cause of sporadic AD is still undetermined but is believed to arise from many factors including diet, age and stress. Familial AD is associated with three genes, *e.g. APP*, *PS-1*, *PS-2*. Mutations in the amyloid precursor protein (APP) can increase total Aβ or promote the longer (42-mer) plaque-associated Aβ over its shorter (40-mer) form but only few familial AD cases are because of APP mutations. The majority of the familial AD cases are due to mutations in either of two presenilin (PS) protein. The PS proteins, PS-1 or PS-2, provide the functional core of the gamma (γ)-secretase complex, which cleaves Aβ from APP (3). These two proteins are derived from two separate genes and share 60% sequence homology (4). Over 160 pathogenic PS-1

gene mutations have been found in people affected with familial AD, compared to PS-2 which has 10 associated familial AD mutations (3). Because of this and other reasons, which will be elaborated on in the subsequent sections, the current thesis focused on the PS-1 protein.

There are relatively few treatments available for AD, most of which involve slowing down the degradation of the neurotransmitter, acetylcholine. However, the effects of these drugs offer only modest symptomatic relief, so better treatments are needed. Some treatments currently in clinical trials include passive immunization of Aβ, Aβ aggregation inhibitors, γ-secretase inhibitors, nerve growth factor (NGF) therapy, antioxidants and calcium (Ca^{2+}) channel antagonists (5). Moreover because the onset of this disease is slow and insidious, and it is believed that Aβ plaques are only an end-point in the progression of the disease, earlier preventative measures are likely to be more beneficial. In order to develop these prophylactic treatments, it is critical to elucidate the mechanisms leading to Aβ plaque formation and neurodegeneration, through cellular and animal models. Familial AD models, which are more aggressive than sporadic AD but have the same disease progression, often offer great insight into AD pathology and etiology. As already mentioned, the most mutated gene in familial AD is *PS-1*, so examination of the role(s) of the PS-1 protein, beyond simply contributing to Aβ formation, is necessary for understanding the disease process and defining better preventative and chronic treatments.

1.2 Presenilin-1

1.2.1 Gene and protein structure of presenilin-1

In 1995, a gene, *S182*, on chromosome 14q24.3 was found to be associated with early-onset familial Alzheimer's disease (EOFAD), when mutated. This gene and the subsequent protein was later named presenilin-1 (PS-1) (6). The PS-1 gene is approximately 60 kilo-base pairs long and has a total of 12 exons with only 10 of those being coding exons (exons 3-12). These coding exons transcribe a 1403 base

pair (bp) PS-1 protein (7). Initial hydropathy plots revealed that PS-1 has at minimum seven hydrophobic transmembrane helical domains connected by hydrophilic domains which include one large hydrophilic loop between transmembrane domains six and seven (6) (Figure 1.1). Aside from all of the above findings, there is nothing else known about the 3-D structure of PS-1, because it is a relatively new protein and no one has been able to crystallize it yet.

1.2.2 Location of presenilin-1

Northern blot analysis has revealed that *PS-1* mRNA is found in equal amounts in many brain regions (6). In peripheral tissues such as the kidney, heart and skeletal muscle, *PS-1* mRNA is expressed at the same level as in the brain except in the liver where there is very low expression (6). Presenilin-2 (*PS-2*) mRNA, on the other hand, is expressed at a much lower level throughout the brain and is found at much higher levels in peripheral tissues (heart, skeletal muscle and pancreas) (8)

At the level of neurons, PS-1 is found mainly in neuronal dendrites and cell bodies and only somewhat in axons (9). In the cells (neuronal and non-neuronal) of the brain, immunofluorescence has revealed that PS-1 is found mainly in intracellular membrane systems such as the endoplasmic reticulum (ER) and golgi apparatus (10), but reports do confirm its existence in other cellular areas such as the cell (11), nuclear (12) and mitochondrial membranes (13). The entire γ-secretase complex, including the proteins APH-1, PEN-2 and nicastrin, is located at the mitochondria (14). Furthermore this complex was found to be functionally active as well (14). This is extremely relevant to the current thesis work.

1.2.3 Physiological functions of presenilin-1

1.2.3.1 Catalytic core of the γ-secretase complex

The most well-known function of PS-1 is its role as part of the γ-secretase complex; this complex includes the proteins PS-1, APH-1, PEN-2 and nicastrin (15). The combination of these proteins at the plasma membrane, in their mature and active form, allow cleavage of specific Type 1 single transmembrane proteins such

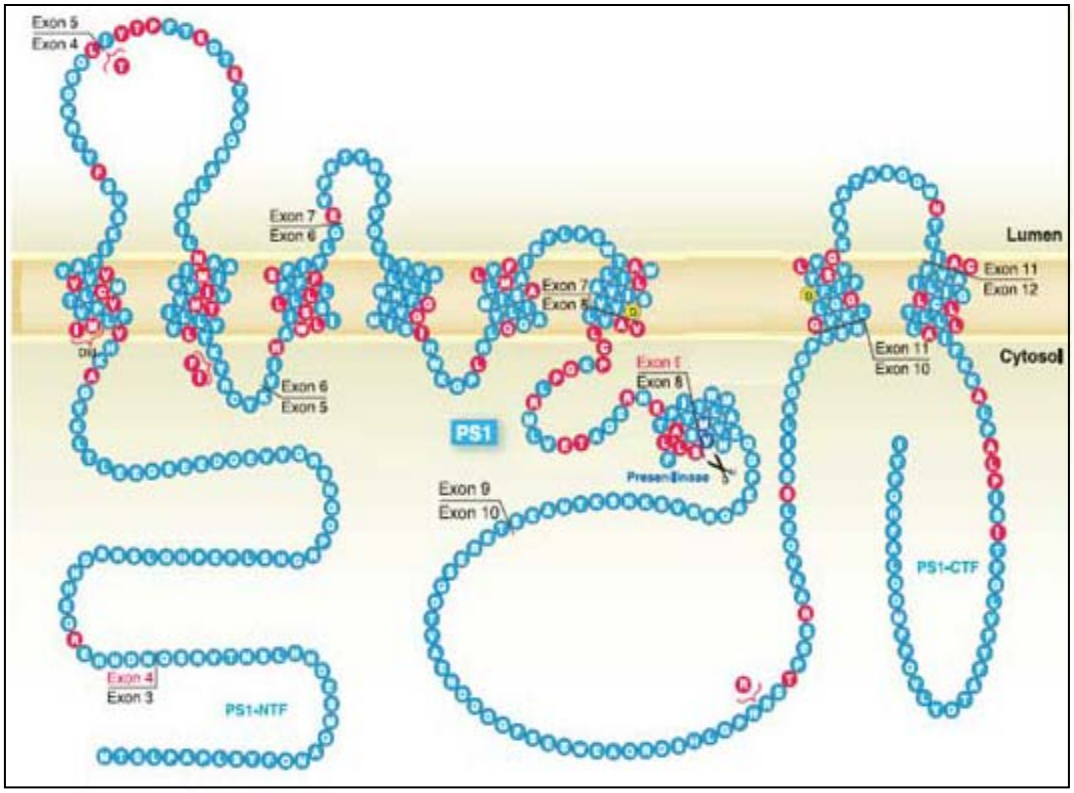

Figure 1.1: Protein structure of presenilin-1. Commonly mutated amino acids are in red, two catalytic aspartate residues are in yellow and the exon junctions are noted too (modified image is from Hardy J and Selkoe DJ (16); reprinted with permission from AAAS).

as APP, notch and cadherins (17, 18). For example, the first step in the formation of the Aβ peptide is the removal of APP's large extracellular N-terminal domain by β-secretase to form the transmembrane peptide fragment, C99 (Figure 1.2) (17). Once the large ectodomain is removed, γ-secretase is able to carry out intramembrane proteolysis of the C99 peptide and form amyloid-beta peptides ranging from 38-43 amino acids long (19). In low amounts and in the form $A\beta_{40}$ (*i.e.* the 40-mer) Aβ is believed to be involved in regulating ion channels and synaptic transmission (20) but, in AD γ-secretase is believed to decrease $A\beta_{40}$ production so that $A\beta_{42}$ (*i.e.* the 42-mer) is the predominant peptide (19). Once excreted from the cell, this form tends to be more fibrillogenic (21). PS-1, at the core of γ-secretase, accounts for approximately 80% of all Aβ produced in the brain and PS-2 accounts for the other 20% (22). Another important γ-secretase substrate is notch. Notch is a protein that is important in cell fate during development and similar to APP, the large ectodomain of Notch is removed by a metalloproteases such as KUZ or TACE (23, 24). Then the resulting transmembrane protein is cleaved by γ-secretase, and a protein called NICD (notch intracellular domain) is released and translocates to the nucleus to up-regulate specific genes (25).

In order for the γ-secretase complex to carry out proteolysis, it was originally believed that PS-1 first undergoes endoproteolysis and becomes a functionally active N- and C-terminal heterodimer that forms a catalytic core to bind γ-secretase substrates (26). A year later, it was discovered that PS-1 endoproteolysis occurs between threonine 291 and alanine 299 with the majority of cut sites at or around methionine 298 (27). Furthermore, this group quantified the number and size of peptide fragments from a PS-1 familial AD mutant, Cys410Tyr (meaning that Cysteine410 was substituted with a Tyrosine in the PS-1 protein), and they discovered that this mutant was similar to PS-1 WT concerning its endoproteolysis (27), but was unable to process Notch (28). This illustrates that not all familial AD mutants alter PS-1 endoproteolysis and that PS-1 endoproteolysis may not guarantee an active γ-secretase. Concerning PS-1's catalytic core, it is a GxGD-type aspartyl protease that has two aspartic acid (Asp) residues, Asp257 and Asp385, found on PS-1's transmembrane 6 and 7 domains, respectively (29, 30). These residues are

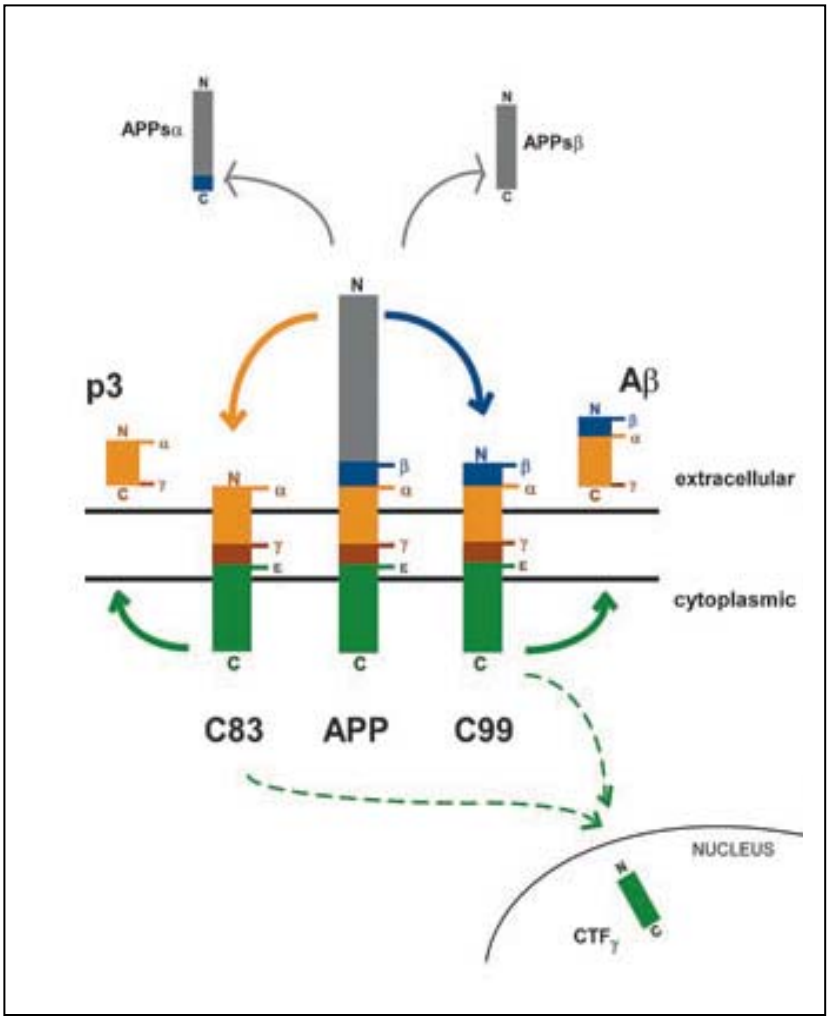

Figure 1.2: APP proteolysis by different secretases. The Aβ peptide is produced first by removal of the APP N-terminal domain by β-secretase, then by intramembrane proteolysis *via* γ-secretase (modified image is from Brunkan and Goate (17); reprinted with permission from Wiley-Blackwell Publishing Ltd).

required for γ-secretase activity and if they are mutated then γ-secretase-mediated proteolytic processing cannot occur (29).

For the other proteins in the γ-secretase complex, their characteristics and roles are not well-established yet. What is known about these proteins is that nicastrin is a single transmembrane protein with a large extracellular domain, APH-1 has seven transmembrane domains and PEN-2 has two transmembrane domains (19). Moreover, PEN-2 is believed to bind to PS-1's N-terminal fragment and activate PS-1 endoproteolysis, while APH-1 acts as a scaffold for the entire γ-secretase complex, first binding to nicastrin and then to PS-1 and PEN-2 (31). Finally, nicastrin uses its large ectodomain to recognize γ-secretase substrates that are bound to PS-1 and then moved to PS-1's catalytic area to be cleaved (19).

1.2.3.2 Regulator of Ca^{2+} homeostasis

Although most of PS-1's roles are related to its proteolytic activity, some groups have shown that PS-1 has functions not related to γ-secretase. For example, full-length WT (wildtype) PS-1 in mouse embryonic fibroblasts (MEFs) can form low conductance Ca^{2+} channels in the ER, which is an organelle that stores Ca^{2+} (32). Moreover, these channels are responsible for the majority of passive Ca^{2+} that is leaked out of the ER. In addition these same authors demonstrated that the catalytically inactive PS-1 mutant D257A has the same level of cation conductance as PS-1 WT, while two FAD associated mutants M146V and Exon 9 deletion (ΔEx9) had a lower or higher level of cation conductance, respectively (32). A second research group found that WT PS-1 is involved in regulating Capacitative Calcium Entry or CCE (33). CCE is believed to involve Ca^{2+} conducting membrane channels, located at the plasma membrane, that are physically linked to the inositol triphosphate (IP3) receptors on the ER membrane. This interaction allows extracellular Ca^{2+} to enter the ER lumen and fill its Ca^{2+} store whenever IP3 receptor agonists stimulate ER Ca^{2+} release. Yoo and colleagues (2000) found that when PS-1 was knocked out in PS-1 mice or when cells were expressing the inactive PS-1 D257A protein, there was a drastic increase in CCE compared to that observed in WT PS-1 mice (33). Even more surprisingly was the finding that a CCE inhibitor,

SKF96365, was able to dose-dependently increase $A\beta_{42}$ levels and other Ca^{2+} influx inhibitors, nifedipine and ω-conotoxin GVIA did not affect $A\beta_{42}$ levels. In contrast, increasing $A\beta_{42}$ levels did not affect CCE (33). These results demonstrate that WT PS-1 has a normal physiological role in CCE regulation and mutated PS-1 in familial AD may alter CCE leading to increased $A\beta_{42}$.

1.2.3.3 Neuroprotection

A recent study has provided evidence that the presence of WT PS-1 in heterozygous familial AD animals helps to guard against senile plaque formation (34). These authors noted that transgenic APP mice that were heterozygous for PS-1 WT and M146V (APP/PS-$1^{M146V/+}$) has 3-4 times less plaque deposits than transgenic APP/PS-1 heterozygous null mice (APP/PS-$1^{M146V/-}$) at 3 and 12 months of age. Additionally the APP/PS-$1^{M146V/-}$ had a lower γ-secretase activity resulting in less $A\beta_{40}$ formation and no changes in $A\beta_{42}$ formation (34). These results support a neuroprotective role for WT PS-1.

1.2.4 Mutations in the presenilin-1 gene and their effects

There has been over 160 pathogenic PS-1 gene mutations found to date in people affected with familial Alzheimer's disease (FAD), compared to PS-2 which has 10 associated FAD mutations (4). Although there have been findings of people with sporadic AD to have the PS-1 gene mutated, the cases are few (35). Almost all of the PS-1 mutations are point mutations with the greater part being the missense type, meaning that one nucleotide is different from the normal PS-1 gene and this single change codes for a different amino acid. Even with such a minute alternation there can be an immense effect seen at the cellular and organism level.

1.2.4.1 Cellular effects in AD

The two hallmarks of AD are neurofibrillary tangles and amyloid plaques, both of which are found, to various extents, in individuals with PS-1 mutations.

For the most part, PS-1 missense mutations will increase the production of the more fibrillogenic $A\beta_{42}$ (the formation of this peptide was discussed in section

1.2.3.1.) (36, 37) and this will lead to the formation of amyloid plaques. $A\beta_{42}$ peptides oligomerize extracellularly and aggregate with other factors to form amyloid plaques. These plaques then activate astrocytes and microglia to cause neuron dysfunction and eventually neuron death (16). PS-1 mutations are also associated with the other hallmark of AD pathology. As previously discussed, neurofibrillary tangles (NFTs) are formed from hyperphosphorylation of tau protein, which is thought to occur through many paths, one of which is Aβ initiated (38). Thus, mutated PS-1 proteins can increase Aβ production which leads to stimulation of kinases that phosphorylate tau. Moreover, the specific PS-1 mutants M139V, I143F, G209V, R269H and E280A are all shown to promote neurofibrillary tangles at a much higher rate than in sporadic AD (39).

Other less common neuropathological changes associated with PS-1 mutations are amyloid angiopathy, Pick bodies and cortical Lewy bodies (40).

1.2.4.2 Clinical phenotype effects in AD

There are a vast amount of clinical symptoms that present to different degrees in each patient with EOAD associated with PS-1 mutations. These symptoms are mostly the same symptoms which are found in sporadic AD, although some PS-1 mutations have been found to be linked to one or two of these characteristics more prominently. For example, there have been over 30 familial AD PS-1 mutations such as M139V, M146V, G209V, ΔEx9 and E280A each connected to prominent seizures, myoclonus, parkinsonism, extrapyramidal signs and spastic paraparesis, and over 20 other PS-1 familial AD mutations such as M146I, M146L, L250S, R269H and ΔEx9 that are related to obvious psychiatric symptoms (agitations, hallucinations, depression and delusions) and aphasia (40). Other phenotypic effects such as cerebellar ataxia are not as prevalent, with only 10 or less PS-1 familial AD mutations showing a higher incidence of these signs (40).

Because of the abundant symptoms that EOAD patients have, one of the easiest ways to categorize familial AD mutations is by the age of onset of clinical features. For example, some people with the more aggressive gene mutations such as M233L, M233V, L235P and Y256S are observed to have decreased cognition

before age 30, while others have an age of onset just before 60 years old (40). Surprisingly, even with the earlier age of onset these PS-1 mutation usually do not produce more $A\beta_{42}$ than the other familial PS-1 mutations, as shown in many cell culture studies (36).

1.2.5 Targeting PS-1 and/or γ-secretase for inhibition

There are several approaches one can take in targeting PS-1 because of the complex nature of this protein and the entire γ-secretase complex. One could develop molecules that block the substrate binding site or catalytic site directly, or the molecule could bind to another area of PS-1 and allosterically modulate these sites. Also one could try to promote PS-1 to cleave substrates more specifically increasing the $A\beta_{40}$:$A\beta_{42}$ ratio through alterations of PS-1 or any of the other γ-secretase proteins.

1.2.5.1 Inhibition of PS-1 and/or γ-secretase in research

For research purposes there have been several γ-secretase inhibitors used. However, these compounds are not used clinically since high concentrations are needed for any antagonistic effect and/or they are non-specific protease inhibitors that are fatal if used in any whole biological system (41). In 2001, a class of small molecule inhibitors including one named DAPT was found. These inhibitors can specifically target γ-secretase so that only Aβ levels are reduced. As well, *in vitro* assays showed that DAPT was not toxic to the cell and *in vivo* there was a significant decreases in Aβ levels observed (41). More recently, there was another finding pertinent to our research because two compounds were found to be more selective in their antagonistic properties. Until now, all γ-secretase inhibitors including the small molecule inhibitors were not selective for PS-1 or PS-2 containing γ-secretase, but Zhao *et al* (22) were able to determine that the sulfonamide compounds, BMS299897 and ELN318463, were more selective for inhibiting PS-1 and only at much higher concentrations did they inhibit PS-2.

1.2.5.2 Inhibition of PS-1 and/or γ-secretase in AD

As already mentioned, most of the clinical PS-1 mutations increase the longer or more fibrillogenic form of Aβ. Due to this, initially pharmacological inhibition of γ-secretase was believed to be beneficial in AD. Yet it was found that since γ-secretase has other substrates critical for proper function and development such as Notch, its inhibition in animals caused many adverse effects. In the APP transgenic mouse model for AD, the mice were given the γ-secretase inhibitor, LY-411,575 (42). At the doses required for any significant reduction of Aβ, there were also serious effects on the differentiation and maturation of lymphocytes and intestinal cells (42). Therefore more selective and potent inhibitors of PS-1 and/or γ-secretase are needed for use in AD patients. These inhibitors would not only be more selective for APP processing, but would also reduce the more fibrillogenic $A\beta_{42}$ and increase the other less toxic and more soluble short forms of Aβ. Some problems which have been encountered so far in developing pharmacological PS-1 inhibitors are that the PS-1 knock-out is embryonic lethal, probably due to the fact that Notch is not cleaved and proper development is impeded (43). In addition, the γ-secretase complex has as yet to be crystallized so designing drugs based on its structure is not currently possible (43). Even with all of these obstacles there have been some inhibitors discovered with lots of promise. One example are the nonsteroidal anti-inflammatory drugs (NSAIDs). These drugs were discovered to be specific allosteric modulators of PS-1 and have been shown to maintain total Aβ levels, but to increase the short form of Aβ and decrease the $A\beta_{42}$ form independently of the NSAID's ability to inhibit cyclooxygenase (COX) (44). These inhibitors will likely help people with AD, but it is also important to remember that not all aspects of AD are related to the degree of Aβ plaque deposits, so looking at other roles for PS-1 and/or other proteins involved in AD are necessary for a complete treatment of the disease.

1.3 Monoamine Oxidase

Monoamine oxidase (MAO) was first discovered in 1928 by the graduate student Mary Hare, who observed that in liver extracts tyramine undergoes oxidation and deamination through an unknown enzyme, which she named tyramine oxidase (45). A decade later two other enzymes, aliphatic amine oxidase and adrenaline oxidase, were discovered and Blaschko *et al* (46) noticed that these two enzymes and tyramine oxidase were similar in their chemical reaction, pharmacological inhibition, animal distribution and substrates, so he concluded that these were actually one enzyme, which he labeled amine oxidase. This amine oxidase was later called monoamine oxidase by E.A. Zeller (47) and it's enzymatic substrates would subsequently include many other amines.

1.3.1 Gene and protein structure of MAO-A and MAO-B

There are two forms of MAO: monoamine oxidase-A (MAO-A) and monoamine oxidase-B (MAO-B). The first groups to determine the sequences of both of these enzymes were Bach *et al* (48) and Hsu *et al* (49). They found that the human MAO-B gene is 2498 nucleotides long (of which the first 78 and last 858 nucleotides are not translated) and the human MAO-A gene is 1937 nucleotides long (of which the first 73 and last 301 are not translated). The human MAO-A protein is 527 amino acids long with a molecular weight (MW) of 59.7 kDa, and the human MAO-B protein is 520 amino acids long with a MW of 58.8 kDa. Moreover the two amino acid sequences were found to be 70% identical, yet even with this high homology MAO-A and -B were hypothesized not to be splice variants or products of different post-translational processing, but rather that they were derived from two separate genes (48, 49). A year later, the bovine MAO-A protein sequence was elucidated and compared to the amino acid sequence of bovine MAO-B (50) and confirmed that both proteins derive from different genes.

Two research groups simultaneously found that the two genes of human MAO-A and MAO-B were linked to the X chromosome and their exact locations were neighboring each other on Xp11.23 (51, 52). On this chromosome, both MAO isoforms have a total of 15 exons with exactly the same order of exons and introns

(53). Also the highest conserved exon was exon 12, mostly likely because it codes for the protein area where MAO's co-factor, FAD, binds (53).

Concerning their 3-dimensional (3-D) structure, both MAO isoforms have four specific domains: three are hydrophyllic domains comprised of the ADP binding domain, the cofactor FAD binding domain and a substrate binding domain, and the third is the hydrophobic C-terminal domain (Figure 1.3 and 1.4). Specifically for human MAO-A, the beginning N-terminal amino acid residues make up an ADP binding domain (48, 49) and the subsequent amino acids 13-88, 220-294 and some C-terminal amino acids, 400-462, make up the FAD binding domain (the C-terminal amino acids Ser-Gly-Gly-Cys-Tyr are specific for covalent binding of FAD); the central residues of 89-219 and 295-399 make up the substrate binding domain; lastly, the end residues of 463-527 make up the transmembrane C-terminal domain (54). Human MAO-B, depicted in Figure 1.4, has the same initial N-terminal amino acids making an ADP binding domain (48, 49) and the next amino acids 4–79, 211–285 and some C-terminal amino acids, 391–453, make up the FAD domain; the central residues of 80–210, 286–390 and 454–488 make up substrate binding domain; lastly, the end residues 489-520 make up the transmembrane C-terminal domain (55). In their active folded conformation these isoforms are almost exactly identical. The only major difference in their 3-D shape is in their substrate cavities. The two cavities are made up of 20 amino acids but seven of the amino acids are different (54). These differences allow for MAO-B to have an extra cavity termed the entrance cavity. For all MAO-B substrates, they first must enter a smaller entrance cavity, then move into a larger substrate cavity by a concerted movement of four amino acids, Phe168, Leu171, Ile199 and Tyr326, that allow substrates to pass through (56). These two cavities may become a single cavity with specific substrates such as deprenyl (54, 55). In addition, they both have a cavity loop (in MAO-A it is comprised of amino acids 210-216 and in MAO-B it is comprised of amino acids 201-206), but the conformation of the MAO-B loop is more condensed and folded due in part to the seven dissimilar amino acids (54). Taken together, these two variations make the MAO-B cavity longer and narrower

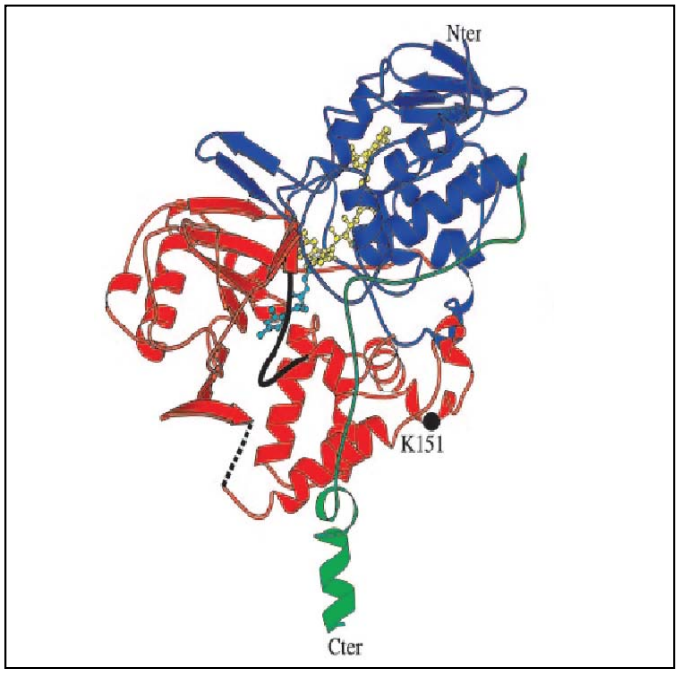

Figure 1.3: 3-Dimentional structure of human MAO-A. The MAO-A protein is depicted using the "ribbon" format. The red color denotes the substrate binding domain, the blue denotes the FAD binding domain and the green denotes the C-terminal domain (ADP binding domain is not shown) (image from De Colibus *et al* (54); copyright (2005) National Academy of Sciences, U.S.A).

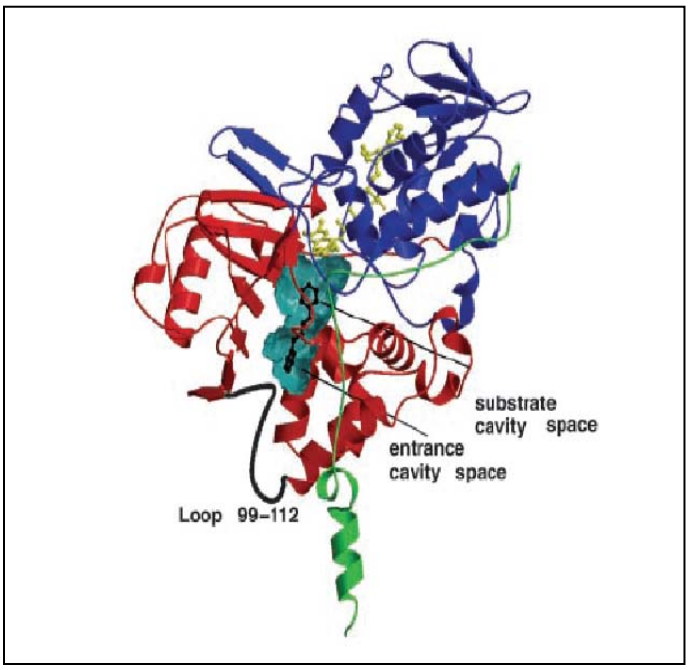

Figure 1.4: 3-Dimentional structure of human MAO-B. The MAO-B protein is depicted using the "ribbon" format. The red color denotes the substrate binding domain, the blue denotes the FAD binding domain and the green denotes the C-terminal domain (ADP binding domain is not shown) (image from Binda *et al* (55); copyright (2003) National Academy of Sciences, U.S.A).

than the MAO-A cavity, thereby accounting for differences in substrate type and affinity.

1.3.2 Location of MAO-A and MAO-B

MAO has been found in mostly all eukaryotic organisms from parasitic worms to sea urchins to primates, and in vertebrates it is also found in all tissues (46), although some tissues such as the human placenta and skin fibroblasts express only MAO-A, and platelets and lymphocytes express only MAO-B (57). In rat and non-human primate brains, immunohistochemical studies have found that MAO-B is mostly in astrocytes (and not oligodendrocytes), and in serotonergic neurons of the nucleus centralis superior and dorsal raphe nucleus, while MAO-A is mostly in catecholaminergic neurons in the locus coeruleus, substantia nigra and the periventricular region of the hypothalamus (58, 59). Later studies on MAO-A and -B in human brains confirmed these findings (60).

For MAO's subcellular localization, it was generally believed, because of its specific enzymatic reaction, that MAO was located specifically at the mitochondria. This was first demonstrated by Cotzias and Dole (61), and then substantiated by several others, including Rodriguez De Lores Arnaiz and De Robertis (62), Oswald and Strittmatter (63), and Gorkin (64). Whether or not MAO was located on the outer or inner mitochondrial membrane was harder to establish because of possible contamination when separating the mitochondrial membranes and mitochondrial compartments. Even with these difficulties, MAO was ultimately shown to reside on the outer mitochondrial membrane (65, 66).

1.3.3 Functions of MAO-A and MAO-B

MAO is an enzyme that catalyzes the oxidative de-amination of endogenous and exogenous primary, secondary and tertiary amines. In order for this enzyme reaction to occur the cofactor, FAD, must be covalently bound to MAO. Therefore MAO is classified as part of the flavoproteins. The exact reaction, reviewed in Binda *et al* (56), begins with the MAO-FAD complex (FAD is in its oxidized form) binding and oxidizing its substrate (an amine), thereby reducing FAD. The reduced

FAD then binds oxygen, allowing it to be re-oxidized and this leads to the production of hydrogen peroxide. As a result of the FAD re-oxidization, the bound imine (the oxidized amine substrate) is released from the MAO-FAD complex and is spontaneously hydrolyzed (*ie.* without the use of an enzyme) to an aldehyde, releasing ammonia as a by-product (56).

The substrates for MAO-A and MAO-B are numerous and since these two enzymes have similar amino acid sequences, they also have equal affinities for substrates such as dopamine and adrenaline (67). On the other hand, the slight differences in their respective sequences allow both isoforms to have different affinities for particular substrates too. So far, it is known that MAO-A is more selective in its substrates than is MAO-B and only the neurotransmitter serotonin or 5-hydroxytryptamine (5-HT) has a high affinity for MAO-A (68). In contrast, the compounds phenylethylamine (PEA), benzylamine and 1-methyl-4-phenyl-1, 2, 3, 6-tetrahydropyridine (MPTP) all have a high affinity for MAO-B (56).

In the peripheral nervous system, one major physiological role for both MAO isoforms is the oxidative deamination of tyramine from tyramine-rich foods such as cheese and beer (67). When these foods or drinks are ingested then both enzymes in the intestine and liver break down tyramine, thereby blocking its uptake into the blood and its subsequent uptake into adrenergic neurons and stimulate noradrenaline release. If enough noradrenaline is released, then a sympathetic response is initiated resulting in hypertension (67). MAO is essential in the regulation of all sympathomimetic amines in food.

In the central nervous system, the metabolism of neurotransmitters such as dopamine, serotonin and noradrenaline by MAO is critical. These neurotransmitters are routinely released, and in large amounts, into the synapse, so specific proteins such as MAO are involved in their degradation and clearance. If not properly cleared, then chronic stimulation of the neurotransmitter's post-synaptic receptor can occur, which can lead to receptor down-regulation. In contrast, disease due to excessive MAO protein expression and/or activity usually is a consequence of receptor under stimulation. Many related therapies therefore target inhibition of MAO activity. For example it is known that the release of the neurotransmitters

dopamine and noradrenaline are involved in generating the stress response. As these neurotransmitters are MAO substrates it is not surprising that MAO-A (69) and MAO-B (70) knockout mice submitted to a forced swim test exhibit an increased stress response. In keeping with this, some MAO inhibitors have been found to be beneficial in people with posttraumatic stress disorder, anxiety and panic disorders (71).

From a research perspective, MAO-B has an extremely important role when studying Parkinson's disease. As mentioned above, MAO-B can metabolize the synthetic compound MPTP. MPTP is a great research tool for scientists because MAO-B-mediated oxidative de-amination of MPTP leads to the neurotoxic metabolite 1-methyl-4-phenylpyridinium (MPP^+) (72), which specifically targets the neuronal pathways associated with Parkinson's disease. This was first demonstrated in rhesus monkeys whose brains were found to have a selective degeneration of neurons in the substantia nigra *pars compacta* (an area that is implicated in Parkinson's disease) following administration of MPTP/MPP^+ (73).

1.3.4 MAO as a therapeutic target in disease

Prior to the 1950s, MAO was not implicated in any disease and much of the research still focused on its cellular characterization. However, the use of a new drug, iproniazid, for the treatment of tuberculosis (TB), was not only effective in treating tuberculosis, but it also increased patient's mood (47). As a result numerous investigations started for the use of iproniazid in depression, and this lead to the finding that iproniazid was actually an MAO inhibitor (47). Very quickly thereafter, many MAO inhibitor drugs were produced and tested in patients with depression; however, scientists observed that the MAO inhibitors brought about serious hypertensive effects in patients (74). This effect was speculated to be due to the previously described excessive dietary intake of tyramine-rich foods, such as cheese, and consequently became known as the 'cheese effect' (74). Because of the side effects, MAO inhibitors were quickly pulled from the clinical trials until reversible and/or more selective inhibitors of MAO were found.

1.3.4.1 MAO-B as a target in disease

In 1965, a new irreversible MAO antagonist was developed called deprenyl or selegiline (75). This compound was clearly more beneficial than the original MAO inhibitors in two ways; (i) it did not produce any cheese effect in patients because it inhibits catecholamine release in vascular smooth muscle and (ii) it specifically inhibits only the B isoform of MAO (75). Additionally, it was noticed in a clinical study of 223 patients, that co-administration of deprenyl with an inhibitor of peripheral decarboxylase, benserazide, and levodopa improved the motor symptoms of the majority of Parkinson's patients (76). Subsequent work from this same group showed that deprenyl was also neuroprotective in that it delayed the degeneration of dopamine neurons in the striatum allowing people with Parkinson's to live longer (77). Recently a similar irreversible MAO-B antagonist called rasagiline, which does not have deprenyl's amphetamine-like structure, was created and *in vivo* experiments have shown that it also increased dopamine levels in the striatum (78) and mediated neuroprotection *in vitro* (79).

MAO-B has been linked to the addiction seen in many cigarette smokers. By using specific radiotracers and positron emission tomography (PET), the brains of smokers were found to have a reduced level of MAO-B, compared to non-smokers, in all brain regions including the frontal cortex, cerebellum, thalamus and basal ganglia (80). This reduced MAO-B concentration was believed to happen through some chemical in cigarette smoke, but it has never been identified (80). The decreased MAO-B is important because it allows for one of its substrates, dopamine, to avoid degradation and prolongs the dopamine reinforcing effects that are believed to contribute to the addictive behavior.

1.3.4.2 MAO-A as a target in disease

J.P. Johnston (68) synthesized clorgyline or N-methyl-N-propargyl-3(2,4-dichlorophenoxy) propylamine hydrochloride. When characterizing this substance he found that there were actually two concentration-response curves that lead to his surmise that MAO was actually two enzymes, which he named MAO-A and MAO-B, with different affinities for different substrates. In this case, MAO-A was shown

to have an extremely higher affinity for clorgyline, making it the first recognized selective irreversible inhibitor of MAO-A (68). Unfortunately because clorgyline is an irreversible MAO-A antagonist (MAO-A is the main culprit in producing the cheese effect) and in light of the successes with MAO-B antagonists, very little research focused on the therapeutic effects of inhibiting MAO-A. Not until reversible MAO-A inhibitors such as moclobemide were discovered was its therapeutic potential revealed. Moclobemide does not lead to the cheese effect and can increase the levels of neurotransmitters noradrenaline, serotonin and dopamine (81). Its use as an anti-Parkinson drug is doubtful given the mild improvement in symptomatology (82), but its role as an anti-depressant has more potential because of its ability to increase the availability of serotonin, which has an important role in depression. Bonnet *et al* (83) found that this drug was as effective as some tricyclic antidepressants and selective serotonin reuptake inhibitors, and there were no decreases in cognitive or psychomotor functions as with other antidepressants. As such, this MAO-A inhibitor may be useful in treating the elderly.

Concerning MAO-A's interaction in cigarette smokers, it too was found to be decreased in all brain regions looked at in people who smoked compared to non-smokers but the decrease was by only 28% (84) while MAO-B was decreased by 40% (80).

1.4 Presenilin-1 and monoamine oxidase in AD

Even though PS-1 and MAO have distinct physiological roles, there is evidence that both proteins may contribute to AD-related pathology and that a potential association between PS-1 and MAO is not an unreasonable hypothesis.

1.4.1 Depression in AD

MAO is implicated in depression because the neurotransmitters which are altered in depression are substrates of MAO. This is now corroborated by the observation that MAO inhibition has been effective in treating this disorder.

Depressive episodes or symptoms are also associated with AD in both the later stages (85) and, perhaps more importantly, the earlier preclinical stages of AD (86-89). Because the destructive cellular changes in AD occur many years before any clinical presentation of symptoms (90), it is quite possible that MAO-mediated effects contribute to the onset of AD symptoms. In one study non-demented females in Mexico whose families had a history of familial AD were assessed for depressive symptoms (89). Even though none of the women knew if they were carrying a PS-1 gene mutation, the women who were carriers were found to be significantly more depressed than the comparable non-carriers (89). Another study found that AD patients with the PS-1 E280A mutation (this mutation is associated with a broad range of onset for AD, *i.e.* between 36- 62 years) who developed the disease the earliest, *i.e.* before 46 years old, were four times more likely to have a history of depressive symptoms (91). These studies implicate that MAO changes, manifested as depression, are part of the early neurochemical changes occurring in AD.

1.4.2 Regional co-localization

It is well-known that post-mortem Alzheimer brains have significant cortical shrinkage and enlargement of ventricles including ventricles around the hippocampus. Thus general brain atrophy is one of the final outcomes of AD but before this specific neuron systems degenerate including the cholinergic, noradrenergic and serotonergic systems (92). These neuron systems all project extensively to the cortex and hippocampus, and the noradrenergic and serotonergic systems also project to the cerebellum (92). Furthermore, it is of great importance to recall that noradrenergic and serotonergic systems are where MAO-A and MAO-B, respectively, exist abundantly in the brain (58, 59). In addition, an examination of 246 cortical brain samples showed that the frontal cortex from people with AD had a drastic increase in MAO mRNA compared to controls (93) and concerning this and other cortical regions, another group found that, in AD patients, there was an increase in MAO-A protein activity in the frontal cortex and MAO-B activity was increased in the temporal cortex (94).

It has already been shown, for example by Smith *et al* (95) and Sayre *et al* (96), that part of the neuronal death seen in AD brains results from oxidative stress. The chief molecule associated with oxidative stress is the hydroxyl radical. As already discussed above, MAO catalyzes the oxidative deamination of its substrate amines, generating hydrogen peroxide as a by-product of the reaction. Through the Fenton reaction hydrogen peroxide can combine with the ferrous ion, Fe (II), producing the ferric ion, Fe (III), and the hydroxyl radical, which is toxic to DNA, lipids and proteins (20). It is likely that this reaction contributes to AD neurodegeneration because Fe (II) and Fe (III) were found to specifically accumulate in the same areas as neurofibrillary tangles and amyloid plaques (97). As well, a recent drug named M30 was developed which has the interesting characteristics of being both a selective brain MAO inhibitor and iron chelator (98). Initial studies of this drug have already found its neuroprotective properties in *in vitro* models of cell death, although its effectiveness in treating AD is still being determined (98). These combined data suggest that similarly to PS-1, MAO may play a role in the pathogenesis of AD, although this role for MAO is not necessarily independent of PS-1.

Subcellular localization studies have clearly demonstrated that MAO resides in the mitochondria, but it is only recently that PS-1 (but not PS-2) and all of the other γ-secretase-associated proteins have also been found in this same fraction (13, 14). The function of PS-1 and/or γ-secretase at the mitochondria is still unknown but what is clear is that these enzymes are not involved in processing APP to the toxic Aβ peptide, since in the mitochondria APP has a different orientation, than at the plasma membrane, *i.e.* its C-terminal is cytosolic and inaccessible for cleavage by γ-secretase (99). Other areas where both PS-1 and MAO could interact include the ER and golgi apparatus because PS-1 is most abundantly expressed in these locations and MAO needs to pass through these membrane systems in order to get processed for targeting to the mitochondria. Thus, the potential for these two proteins to interact is suggested first by their association with depression and second because of their neuronal and subcellular co-localization.

1.4.3 Ca^{2+} as the intermediate ion between PS-1 and MAO

The interaction between PS-1 and MAO may not be a direct one, but rather could rely on an intermediate molecule, the Ca^{2+} ion. At normal concentrations, Ca^{2+} is needed for proper physiological functioning. However, in AD cytosolic Ca^{2+} levels are highly dysregulated, and PS-1 has been implicated in this dysregulation. Wild-type PS-1 and mutant PS-1 proteins are able to form passive Ca^{2+}-leak channels in the ER membrane (the degree of effect of the mutant proteins is dependent on the mutation) (32). In addition, cells expressing PS-1 mutant proteins (100-102) and PS-1 transgenic mice (standard and knock-in) (103-106) have an increased cytosolic Ca^{2+} level, compared to WT PS-1, that is believed to be mainly due to the alterations in the ER's Ca^{2+} store and/or buffering ability. For example, the ER Ca^{2+} release agonists carbachol and bradykinin and the ER Ca^{2+}-ATPase inhibitor, thapsigargin, caused a significant increase in intracellular Ca^{2+} in PC12 cells expressing a PS-1 mutant when compared to those expressing WT PS-1 (101). Moreover, mitochondria become less efficient in the production of ATP in the aging brain (107) and Aβ, cleaved via PS-1 mediated proteolysis of APP, can drastically reduce ATP levels in neurons and astrocytes (108). This is important because in neurons, the mitochondria acts as stores for Ca^{2+} (taken up through its Ca^{2+} ATPase) when cells have an excessive amount of Ca^{2+}, whereas in cortical astrocytes the mitochondria play a key role in storing Ca^{2+} at normal physiological levels (109). As such, a significant reduction in ATP levels would not only cause mitochondrial dysfunction, but it would also result in a significant increase in intracellular Ca^{2+}. The ability of PS-1 to alter cytosolic Ca^{2+} levels is important because the level of MAO activity has been positively linked to Ca^{2+} concentrations. Kosenko *et al* (110) and Cao *et al* (111) have demonstrated, *in vitro*, that the activity of mitochondrial MAO-A can be increased when Ca^{2+} availability increase. Additionally, in the hippocampus, an area that is greatly affected in AD, there is an increase in basal free Ca^{2+} levels compared with other regions of the aging brain (112). The mechanism behind this regionally-specific increase is not clear, but it might rely on the loss of expression of Ca^{2+} buffering proteins, such as calbindin (a cytosolic Ca^{2+}-binding protein) and calreticulin (a Ca^{2+}-binding protein in the ER lumen), as observed in the

hippocampus of 30 month-old rats (112). These data could explain why the AD hippocampus is more susceptible to the PS-1- and MAO-generated hydroxyl radicals.

The dysregulation of cytosolic Ca^{2+} is a significant pathological mediator in AD as shown in patients taking Ca^{2+}-related pharmacological interventions such as nimodipine and memantine. Nimodipine, an L-type voltage-gated Ca^{2+} channel antagonist developed for high blood pressure, slowed the progression of AD in 227 patients compared to those receiving the placebo (113). Likewise, the NMDA (Ca^{2+} ion channel receptor) antagonist, memantine, has proven effect for moderate to severe AD cases (114).

1.5 Research project

Research in the Cell Signalling Laboratory focuses on mechanisms of cell death in the CNS. This thesis is aimed at examining the role of PS-1 in MAO-A function in models of Alzheimer disease.

The specific hypothesis is that PS-1 regulates basal and Ca^{2+}-sensitive MAO-A activities and that this contributes to the oxidative stress seen in AD.

For this work three common FAD mutations, PS-1 Exon 9 deletion (ΔEx9), Y115H, and M146V were used and compared to PS-1 WT and the PS-1 D257A dominant negative mutant.

1.5.1 Presenilin-1 constructs

1.5.1.1 Exon 9 deletion

The PS-1 Exon 9 deletion (ΔEx9) genotype was first found in a British family with EOFAD (115). Several other families with the ΔEx9 mutation were subsequently discovered and the mean age of onset was determined to be between 45-55 (40). Exon 9 comprises the amino acids (a.a.) 290-319 and these a.a. are deleted, in these families, by a missense mutation (a G to T nucleotide change)

occurring at the Intron and Exon 9 boundary that removes the splice recognition site. Moreover because this is an in-frame deletion, there is no change to the translated PS-1 protein except for a serine290cysteine substitution, which is at the junction of Exon 8 and 10 (115). As discussed previously, it was found that PS-1 undergoes some post-translational processing, which includes endoproteolytic processing to an active heterodimer, and this processing is disturbed if Exon 9 is deleted because the cut site overlaps with the Exon 9 region (26). As a result the PS-1 ΔEx9 mutant maintains its full length form and since it is not processed to the commonly found active heterodimer, then one would assume that its APP cleavage role would be reduced; however, this is not the case as two groups have found that in comparison to other mutations the PS-1 ΔEx9 mutant actually generates more fibrillogenic $A\beta_{42}$ (36, 116). Steiner *et al* (117) have proposed that this gain-of-function mutation is actually a result of the serine to cyteine mutation at the Exon 8/10 junction and not the ΔEx9.

This mutation has been used by various groups such as Smith *et al* (118) and Cedazo-Minguez *et al* (102) to show that Ca^{2+} store concentrations are increased in experimental models expressing PS-1 ΔEx9, compared to WT and the former group also showed that CCE was suppressed (102, 118).

1.5.1.2 Y115H mutant

The PS-1 Y115H mutant was first found by Campion *et al* (119) who were screening for PS-1 gene mutations in 12 different French families with EOAD. PS-1 Y115H is a missense mutation that changes the codon TAT to CAT producing a histidine instead of a tyrosine amino acid during translation. This mutation is very aggressive as the age of onset, at 35-37 years of age, was the earliest of all families screened (119). This same group found the Y115H missense mutation in another EOAD family with an age of onset of 36-47 years (120).

Not much work has been done with the PS-1 Y115H mutant, but three studies that revealed much about PS-1 function, Aβ production and AD will be described. First, it was commonly thought that when PS-1 WT proteins are mutated their activity would decrease, but in the case of PS-1 Y115H it actually was more

active. This increased function was discovered when it was observed that N-terminal truncated Y115H and C-terminal truncated PS-1 WT are still able to form active heterodimers (121). This fact led to the notion that PS-1 mutations could cause an increase, and not necessarily a decrease, in function. It was then found in 13 different cell lines and six FAD PS-1 mutations (Y115H, ΔEx9, L392V, H163R, M146L and L286V) that the ratio of $A\beta_{42}$ to total Aβ was the highest for PS-1 ΔEx9 (age of onset 45-55 years) and third lowest for PS-1 Y115H (age of onset 35-37 years) (116). This work illustrated that more Aβ production might not necessarily lead to an earlier onset of AD. Lastly, over-expression of either of the PS-1 mutants Y115H, M146V or D257A in a mouse embryonic fibroblast (MEF) cell line that had both endogenous PS-1 and PS-2 knocked-out, Kim *et al* (28) showed that each of these mutants could generate different levels of the Notch intracellular domain (NICD). PS-1 M146V produced the highest amount, even higher than WT, and PS-1 Y115H produced less than WT (28). The D257A mutant did not generate any NICD (28). These data provided evidence for different PS-1 missense mutations having different cellular effects even though they all lead to familial AD.

1.5.1.3 M146V mutant

In contrast to PS-1 Y115H, the PS-1 M146V mutation is used in numerous experimental research studies probably because of the former's lack of clinical features and the latter's abundance. The PS-1 M146V missense mutation was found in families from Finland and Sweden, and the mean age of onset is around 36-40 years of age (40). Some of the clinical signs that have a higher incidence in people with this mutation compared to sporadic AD are myoclonus, seizures, extrapyramidal signs and apraxia (40).

Very recently the specific M146V mutation was found to be responsible for a significant increase in p75 neurotrophin receptor proteolysis compared to WT PS-1 (122). In contrast, the PS-1 ΔEx9 mutant produced a lower amount of p75 neurotrophin receptor fragments, when compared to WT PS-1. As this receptor is involved in promoting neuronal death and is expressed on basal forebrain cholinergic neurons (which very susceptible during AD), then the p75 peptide

fragments formed by PS-1 M146V could initiate cell signaling events leading to apoptosis (122). Other reports have found that this mutation does not stimulate neurite growth and that it decreases the nuclear translocation of the Notch1 NICD (123). Overexpression of the PS-1 M146V mutant in cells results in an increased amount of free Ca^{2+} (100, 124), but the mechanism involved is not dependent on the formation of passive cation channels in the ER as seen with PS-1 WT, D257A and ΔEx9 proteins (32). Also in transgenic PS-1 M146V knock-in mice, there are increases in oxidative stress (125) and increases in cytosolic Ca^{2+} levels compared to controls (103, 104, 126).

1.5.1.4 D257A mutant

As discussed earlier, PS-1 contains the catalytic core of γ-secretase and this catalytic area is an aspartyl protease centered on the amino acids Asp 257 and 385 (29). The PS-1 aspartic acid 257 to alanine 257 (D257A) mutant is an artificial mutation, on the NTF of PS-1 that, for experimental reasons, is used when a theoretically inactive PS-1 is needed.

The manner in which the two key aspartic acids of PS-1 interact with each other and its substrate(s) is still subject to theory, but one group has provided some evidence that aspartic acid 385 is sterically blocked inside and aspartic acid 257 is more accessible by facing the outside (28). First it was observed that when PS-1 D257A and WT PS-1 NTF were co-expressed in PS-1/2 double knockout MEFs, Notch could still not be cleaved; however, when PS-1 WT and the D385A counterpart, PS-1 CTF, were co-expressed in the same cell line, Notch cleavage was reestablished (28). Furthermore WT PS-1 CTF with PS-1 D385A co-immunoprecipitated, but WT PS-1 NTF and PS-1 D257A did not (28). Altogether, their data suggested that unlike the D385A mutant, which cannot freely associate with proteins because of its orientation inward, the D257A mutant can easily associate with proteins because it faces outward.

Concerning PS-1 D257A's involvement in γ-secretase activity, most people uphold Wolfe *et al*'s (29) idea that this is a dominant negative mutant, even though some reports have shown that expression of PS-1 D257A does not reduce the

production of Aβ (although Notch cleavage to the NICD is almost always affected) (127, 128).

1.5.2 Research objectives

All of the just described PS-1 constructs will be used to examine our hypothesis that proposes a tri-partite relation between PS-1, MAO-A and Ca^{2+} in AD. The specific aims are:

1) To determine if familial AD-associated PS-1 mutations affect intracellular Ca^{2+}.

2) To determine if over-expression of PS-1 proteins in cells can affect basal and Ca^{2+}-sensitive MAO activities.

3) To determine if basal and Ca^{2+}-sensitive MAO activities are altered in brain tissue homogenates from PS-1 transgenic mice.

4) To identify if any change in MAO activity are a result of altered protein levels.

2 MATERIALS AND METHODS

2.1 Materials

All of the materials and reagents discussed below and in the methods section were obtained from each company identified (in brackets) immediately following the product or reagent, and the company addresses are listed in Table 2.1.

2.1.1 Vectors

Three vectors were used during the course of these experiments; namely pcDNA3.1(+), for simple expression (Invitrogen), pCMV/myc/mito, for targeting of proteins to the mitochondria (Invitrogen), and pREP, for expressing CB-28K (kindly provided by Dr. Allan Pollock, University of California, San Francisco, USA).

The pcDNA3.1(+) vector enables a high level of protein expression in mammalian cells through its Human cytomegalovirus immediate-early (CMV) promoter. It also has a forward (+) direction Multiple Cloning Site (MCS) to allow insertion of the cDNA as well as an Ampicillin resistance gene which facilitates the selection of pcDNA3.1(+) positive bacterial colonies during transformations of bacterial plasmids and for selection of stable transformants, if needed. The pREP and pCMV/myc/mito vectors also have a specific MCS and allow for Ampicillin resistance.

2.1.2 Plasmids

The cDNAs for PS-1 WT, D257A, Y115H, and Exon 9 deletion (ΔEx9) are all subcloned in the pcDNA3.1 vector and were kindly provided by Dr. Georges

Table 2.1: Company name and address

Company	Address
American type culture collection	Manassas, VA, USA
Amersham Biosciences	Piscataway, NJ, USA
BD Biosciences	Mississauga, ON, Canada
BDH Inc.	Toronto, ON, Canada
Bio-Rad	Hercules, CA, USA
Cell Signaling Technology, Inc.	Danvers, MA, USA
CHEMICON International	Temecula, CA, USA
EM Science Inc	Gibbstown, NJ, USA
EMD Biosciences Inc.	San Diego, CA, USA
EMD Chemicals Inc	Gibbstown, NJ,USA
Fermentas Inc	Burlington ON, Canada
GE Healthcare	Uppsala, Sweden
GIBCO-BRL	Gaithersburg, MD, USA
Hyclone	Logan, UT, USA
ICN Biomedicals	Aurora, OH, USA
Invitrogen	Carlsbad, CA, USA
J.T. Baker	Phillipsburg, NJ, USA
MP Biomedicals	Solon, OH, USA
PerkinElmer	Waltham, MA, USA
Pierce	Rockford, IL, USA
Santa Cruz Biotechnology, Inc	Santa Cruz, CA, USA
Sigma-Aldrich	St. Louis, MO, USA
Stratagene	La Jolla, CA, USA
The Jackson Laboratory	Bar Harbor, ME, USA
VWR	West Chester, PA, USA

Lévesque at Laval University, Quebec. WT PS-1 cDNA was used to generate the PS-1 M146V mutation.

2.1.3 Competent bacterial cells used for transformation

The DH5α *E. coli* bacterial strain was obtained from American type culture collection (ATCC) and was used to make competent cells for plasmid transformation.

2.1.4 Cell lines

Cell lines included mouse hippocampal-derived HT-22 cells (kindly provided by Dr. P. Maher, The Scripps Research Institute, La Jolla, CA), human embryonic kidney (HEK) 293A cells (ATCC) and rat phaeochromocytoma (PC12) cells (ATCC). Both the HT-22 and PC12 cells are neuronal cell lines, and have a high MAO-A activity and low MAO-A protein expression; in contrast, HEK 293A cells are non-neuronal and have a high MAO-A protein expression but low MAO-A activity. HT-22 and HEK 293A cells are immortalized cell lines while the PC12 cell line is derived from a neuroendocrine tumor cell. Therefore, each cell line was applied for a specific use in each experiment.

2.1.5 Antibodies

The PS-1 protein was detected using a mouse monoclonal anti-PS-1 loop antibody (CHEMICON International). This antibody recognizes the PS-1 loop near the C-terminal of the protein, which spans amino acids 263 to 378, and detects an 18-20 kDa band on Western blot. The dilution ratio used, for all membranes, was 1: 1000.

The three MAO antibodies, MAO-A (H-70), MAO-A (T-19) and MAO-B (C-17) are from Santa Cruz Biotechnology, Inc. MAO-A (H-70) binds to C-terminal amino acid residues 458-527 and is a rabbit polyclonal antibody. MAO-A (T-19) binds to N-terminal amino acid residues and is a goat polyclonal antibody. On Western blots, both of these antibodies detect a 61 kDa band. The MAO-B (C-17) goat polyclonal antibody recognizes C-terminal amino acid residues on the MAO-B protein and detects a 60 kDa band on Western blot. The antibody MAO-A

(H-70) was diluted in a ratio of 1: 250-1000, MAO-A (T-19) was diluted in a ratio of 1: 1000 and MAO-B (C-17) was diluted in a ratio of 1: 500-1000.

A rabbit polyclonal anti-Calbindin D28K (H-50) (Santa Cruz Biotechnology, Inc.) binds to N-terminal amino acids 35-84 on the calbindin protein and detects a 29 kDa band on Western blot. The dilution ratio used, for all membranes, ranged from 1: 50-250.

For detecting activated (phosphorylated) p38 the rabbit polyclonal phospho-p38 MAP kinase antibody from Cell Signaling Technology, Inc. was used. This antibody recognizes p38 MAP kinase when it is phosphorylated on threonine180 and tyrosine182. On Western blots, the phospho-p38 protein migrates as a 43 kDa band (presumable due to additional post-translational modification). Phospho-p38 MAP kinase antibody was diluted in a ratio of 1: 100.

In all Western blots β-actin protein levels were examined to demonstrate equal protein loading across lanes (as an internal standard, loading control). The primary mouse monoclonal anti-β-Actin antibody was used (Sigma-Aldrich). This antibody will recognize N-terminal amino acids on the β-actin protein and present as a 49 kDa band on Western blot. The dilution we used for all immunoblots was 1:3000.

When needed, all of the antibodies discussed above were diluted using 5% milk in TBS-Tween 20 except the phospho-p38 MAP kinase which was diluted using 5% BSA (EMD Chemicals Inc) in TBS-Tween 20. All primary antibodies are stored at -20°C except for the MAO antibodies and the Calbindin D28K antibody, which are stored at 4°C.

2.1.6 Radioactivity

The protocols, radioactive work areas and equipment involved in the use of radioactive substances followed the University of Saskatchewan's Radiation Safety Code and were approved by Radiation Safety Advisory Committee. The nuclear substance permit (NPR-05-U) was obtained from the Radiation Safety Protocol Approval Committee. For this project all [^{14}C]-radiolabelled substances were obtained from PerkinElmer.

2.1.7 Mice

All of the handling, care, housing and experiments involving mice followed the guidelines from the Canadian government's Canadian Council on Animal Care. In addition each procedure was approved by the University of Saskatchewan's Committee on Animal Care and Supply. Mice were purchased from Jackson Labs (The Jackson Laboratory).

2.2 Methods

2.2.1 Competent cell preparation

a. Incubate one colony of DH5α *E. coli* bacteria (ATCC) with 5 ml Double Yeast Tryptone (DYT) solution (16 g Bacto^{TM} Tryptone, BD Biosciences; 10 g Bacto^{TM} Yeast extract, BD Biosciences; 5 g NaCl, EMD Chemicals Inc; 1000 ml ddH_2O, pH 7.0, autoclaved) overnight at 37°C in a bacteria shaker.
b. Combine 2 ml of above solution with 100 ml SOB (950 ml ddH_2O, 20 g Bacto^{TM} Tryptone, BD Biosciences; 5 g Bacto^{TM} Yeast extract, BD Biosciences; 0.5 g NaCl, EMD Chemicals Inc) and incubate at 37°C while shaking until the optical density (OD) of 0.45 is achieved.
c. Equally separate the solution into four 50 ml autoclaved centrifuge tubes and store on ice for 10 min.
d. Centrifuge the tubes at 2500 rcf for 10 min at 4°C and remove the supernatant carefully.
e. Add 8 ml of pre-chilled transformation buffer (15 mM $CaCl_2$, BDH Inc.; 250 mM KCl, BDH Inc; 10 mM 1,4-Piperazine Diethane Sulfonic Acid, Sodium Salt (PIPES), EMD Chemicals Inc; 55 mM $MnCl_2$, EMD Chemicals Inc; pH 6.7) to each tube to resuspend the cells and store on ice for 10 min.
f. Centrifuge the tubes at 2500 rcf for 10 min at 4°C and remove the supernatant carefully.

g. Add 2 ml of pre-chilled transformation buffer to each tube to resuspend the cells.
h. To each tube slowly add enough DMSO (EM Science Inc) to have a total of 7% DMSO and store on ice for 10 min.
i. On dry ice, aliquot 50-100 µl into pre-chilled and autoclaved microcentrifuge tubes. Store at -70°C.

2.2.2 Transformation

Amplification of plasmid DNA is carried out using bacterial competent cells. This method involves taking a plasmid or vector which contains a specific DNA construct and inserting it into a bacterial cell through its membrane pores. The bacteria cell will then duplicate this plasmid when it undergoes replication. The transformation protocol is as follows:

a. Pre-chill all Falcon® polypropylene tubes (BD Biosciences) on ice.
b. Remove the bacterial cells (DH5α competent *E.coli* cells) from the -70°C freezer and thaw on ice.
c. Once thawed, combine 1-2 µl of DNA and a 50 µl aliquot of DH5α cells in the Falcon® tube.
d. Keep mixture on ice for 30 min.
e. Place the Falcon® tube with the mixture in a 42°C water bath for 30 sec to heat shock the bacterial cell membrane.
f. Place the tube on ice for 2 min again to help the bacterial cell membrane recover.
g. Add 250 µl of SOC medium to the Falcon® tube.
    a) For 1 ml SOC Medium:
        i. Work at all times near an open flame.
        ii. Add 975 µl SOB (950 ml ddH_2O, 20 g Bacto™ Tryptone, BD Biosciences; 5 g Bacto™ Yeast extract, BD Biosciences; 0.5 g NaCl, EMD Chemicals) to a microcentrifuge tube.
        iii. Add to the tube 5 µl of 2 M $MgCl_2$ (EM Science Inc) and 20 µl 1 M glucose (BDH Inc).

h. Shake the tube for 30 min at 37°C to help the bacteria grow.

i. While waiting for 30 min remove agar plates from 4°C fridge and place in incubator to warm up the agar. This helps the DNA/bacteria solution to absorb.

   a) Preparation of agar plates:

      i. Combine DYT solution (16 g Bacto™ Tryptone, 10 g Bacto™ Yeast extract, 5 g NaCl, 1000 ml ddH_2O, pH 7.0, autoclaved) with 15 g of Bacto™ Agar (BD Biosciences).

      ii. Depending on the selection gene expressed in the plasmid, add either the ampicillin (EMD Biosciences Inc.) or kanamycin (Sigma-Aldrich) antibiotic in a 1: 1000 ratio of antibiotic to DYT/agar solution.

      iii. Working near a flame, pour the solution into Petri dishes and flame the top of the solution for a couple seconds to get rid of the air bubbles.

      iv. Keep at room temperature for a couple hours for the agar to solidify.

      v. Store agar plates upside down in a 4°C fridge.

j. Using all ethanol (EMD Chemicals Inc) sterilized tools and near an open flame plate 4 µl, 20 µl and 100 µl of the DNA/bacteria solution on three separate agar plates.

k. Place the plates in a 37°C incubator for16-20 hours.

l. Agar plates with antibiotic can be stored at 4°C for approximately one month.

2.2.3 Mutagenesis

The PS-1 plasmids were obtained from Dr. Georges Lévesque at Laval University. Only the PS-1 M146V mutant had to be generated. This was done using the QuikChange® Site-Directed Mutagenesis Kit from Stratagene.

Two primers (forward and reverse) were designed according to the manufacturer's suggestions. The PS-1 wild-type sequence from the National Center for Biotechnology Information (NCBI) GenBank, was analyzed and the forward primer was chosen to be 5′-C ATG ATC AGT GTG ATT GTT GTC GTG ACT ATC CTC CTG GTG GTT C-3′. Consequently the reverse primer was then: 5′-G AAC CAC CAG GAG GAT AGT CAC GAC AAC AAT CAC ACT GAT CAT G-3′. These primers are 44 base pairs long, have a Tm (melting temperature) of 81.2°C,

a %GC of 48 and the single point mutation is in the middle, which follows the primer criteria in the Stratagene manual. Once the sequence was chosen, the primers (Invitrogen) were diluted with ultrapure H_2O and stored at -20°C. The following specific polymerase chain reaction (PCR) procedure was carried out:

a. To an autoclaved PCR tube add the reagents below in the amounts specified:

5 µl	10X Reaction buffer
2 µl	DNA template (50 ng)
1 µl	Forward primer (125 ng/µl)
1 µl	Reverse primer (125 ng/µl)
1 µl	dNTP mix
40 µl	ddH_2O

(All above reagents, with the exception of the primers, are from Stratagene and all are stored at -20°C)

b. Vortex the tube, then add 1 µl of 2.5 U/µl PfuTurbo® DNA polymerase (Stratagene).

c. Vortex again and briefly tap the tube so all solution is at the bottom.

d. Place the samples in a thermal cycler and use the following program:

First stage: 1 cycle at 95°C for 30 sec.
Second stage: 16 cycles of: 1) Denature step: 95°C for 30 sec
2) Anneal step: 55°C for 60 sec
3) Extension step: 68°C for 7 min

e. Immediately place the tubes on ice for 2 min.

f. To each tube add 1 µl of 10 U/µl *Dpn* I (Stratagene) and mix with the pipet tip. (The *Dpn* I enzyme will digest all parental *methylated* DNA).

g. Briefly spin down the tube and incubate each tube for 1 hour at 37°C.

h. Pre-chill all Falcon® polypropylene tubes (BD Biosciences) on ice.

i. Remove the bacterial cells (use XL1-Blue supercompetent cells (Stratagene)) from the -70°C freezer and thaw on ice.

j. Once thawed, combine exactly 1 µl of DNA to each 50 µl aliquot of XL1-Blue supercompetent cells in the Falcon® tube.

k. Keep mixture on ice for 30 min.

l. Place the Falcon® tube with the mixture in a 42°C water bath for 45 sec to heat shock the bacterial cell membrane.

m. For 2 min place the tube on ice again to help the bacterial cell membrane recover.

n. Add 500 µl of preheated (42°C) NZY+ medium (10 g NZ amine casein hydrolysate, Sigma-Aldrich; 5 g Bacto™ Yeast extract, BD Biosciences; 85.5 mM NaCl, EMD Chemicals Inc; 12.5 mM $MgCl_2$, EMD Chemicals Inc; 12.5 mM $MgSO_4$, EMD Chemicals Inc; 20 mM glucose, BDH Inc.; pH 7.5).

o. Shake the tube for 1 hour at 37°C to help the bacteria grow.

p. To plate the bacteria, complete steps i-l from the transformation protocol in section 2.2.2. The only exception is in step 2.2.2.j. it is necessary to plate 100 µl and 250 µl of the DNA/bacteria solution.

2.2.4 Maxi-prep

A maxi-prep is the process of amplifying and purifying plasmid DNA on a large scale. The general procedure involves growing a bacterial culture, then harvesting and lysing the bacteria, and finally purifying the plasmid DNA. The method is as follows:

a. Growing the bacteria:

a) To a 14 ml round-bottom polypropylene test tube add 4.5 ml of Terrific broth (TB) (12 g Bacto™ Tryptone, BD Biosciences; 24 g Bacto™ Yeast extract, BD Biosciences; 4 ml glycerol, MP Biomedicals; 900 ml ddH_2O; autoclaved) and 0.5 ml of 0.17 M Potassium Phosphate Monobasic (KH_2PO_4) (J.T. Baker) /0.72 M Potassium Phosphate Dibasic (K_2HPO_4) (J.T. Baker).

b) Add the appropriate antibiotic in a 1: 1000 (antibiotic: solution) ratio.

c) Near a Bunsen burner flame use an autoclaved pipette tip to pick up a single freshly isolated transformed bacteria colony from the agar plate.

d) Incubate the test tube in a shaker/incubator for 6 hours at 37°C.

e) After 6 hours, combine the bacteria solution with 270 ml of TB and 30 ml 0.17 M KH_2PO_4 / 0.72 M K_2HPO_4 to a 1 L conical flask near an open flame.

f) Add the proper antibiotic in a 1: 1000 (antibiotic:solution) ratio to the conical flask.

g) Shake the conical flask in a bacteria shaker for 16-20 hours at 37°C.

b. Harvesting and lysing the bacteria:

a) The next day take out and mix 850 µl of bacteria culture and 150 µl sterile glycerol (autoclaved) in a 1 ml cryogenic vial. Store this in a -70°C freezer for future use.

b) Split the rest of the 300 ml bacteria culture into two 250 ml centrifuge bottles.

c) In a centrifuge, spin at 4000 rpm for 15 min at room temperature (20°C).

d) Take out the supernatant and re-suspend the two pellets with 50 ml of cold STE (0.1 M NaCl, EMD Chemicals Inc; 10 mM Tris (base), pH 8.0, J.T. Baker; 1 mM EDTA, pH 8.0, EMD Chemicals Inc; store at 4°C).

e) Spin the centrifuge bottles again at 4000 rpm for 15 min at room temperature (RT) (20°C).

f) Remove the supernatant and add 10 ml solution I (50 mM Glucose, BDH Inc; 10 mM EDTA, pH 8.0; 25 mM Tris (base), pH 8.0) to each bottle to re-suspend the pellet.

g) Combine the two bottles and gently mix in 40 ml solution II (0.2 N NaOH, VWR; 1% sodium dodecyl sulfate (SDS), ICN Biomedicals). Keep at RT (20°C) for 5-10 min.

h) Then add to the bottle 20 ml of the acidic solution, solution III (300 ml 5 M Potassium Acetate, EMD Chemicals Inc; 57.5 ml Glacial Acetic Acid, BDH Inc; 142.5 ml ddH_20) and mix well. Keep on ice for 5 min.

i) Centrifuge for 15 min at 4000 rpm at RT.

j) Filter the supernatant through 4 layers of cheese-cloth into a clean 250 ml centrifuge bottle.

k) Add isopropanol (EMD Chemicals Inc) in the amount equal to 60% of the total filtered supernatant volume. Keep at RT for 10-30 min.

l) Centrifuge for 15-30 min at 5000 rpm at RT.

m) Take out the supernatant and carefully add some 85% ethanol (EMD Chemicals Inc) to the pellet to wash it.

n) Remove ethanol (let air dry) and liquefy the pellet with 3 ml T.E. (10 mM Tris (base), pH 8.0; 1 mM EDTA, pH 8.0).

c. Purification of the plasmid DNA:

a) Pour the dissolved pellet into a 50 ml polypropylene test tube and mix in 4.8 ml of ice-cold 5 M lithium chloride (J.T. Baker, store at 4°C).
b) Centrifuge the tube for 10 min at 10000 rpm at RT.
c) Transfer the supernatant to another 50 ml polypropylene test tube and add to it the same volume of ispropanol. Vortex and keep at RT for 5 min.
d) Centrifuge the tube again for 10-20 min at 10000 rpm at RT.
e) Take out the supernatant and add 85% ethanol to rinse the pellet.
f) Remove all ethanol and add 500 µl T.E to dissolve the pellet. Then add 5 µl Ribonuclease A (10 mg/ml, Fermentas Inc). Keep at RT for 30 min.
g) After 30 min, mix in 400 µl of 1.6 M NaCl/13% (w/v) polyethlyene glycol (PEG) (EM Science Inc) (100 ml 1.6 M NaCl, 13 g PEG) and transfer the solution to a microcentrifuge tube.
h) Vortex and then centrifuge for 2 min at 12000 rcf at 4°C.
i) Discard the supernatant and resuspend the pellet in 500 µl T.E to dissolve.
j) In a fumehood, add 500 µl phenol (EMD Chemicals Inc). Then vortex and centrifuge at 5000 rpm for 5 min at RT.
k) Remove the top aqueous layer to another microcentrifuge tube.
l) Repeat the above 2 steps.
m) In a fumehood, add 500 µl chloroform (BDH Inc). Then vortex and centrifuge at 5000 rpm for 5 min at RT.
n) Remove the top aqueous layer to another eppendorf tube.
o) Add enough 5 M NaCl for a final concentration of approximately 125 mM.
p) Mix in two volumes of 400 µl cold 100% ethanol and incubate on ice for 10-30 min.
q) Centrifuge for 5 min at 12000 rcf at 4°C.
r) Discard the supernatant and add 200 µl of 85% ethanol. Vortex and centrifuge for 2 min at 12000 g at 4°C.
s) Remove all ethanol and dissolve the pellet in 300-1000 µl ultrapure H_2O.

t) Store DNA in 1 µg/µl concentrations at -20°C.

2.2.5 Transfection of cells

Transfection of DNA into a mammalian cell allows the cells to transiently over-express the corresponding protein. Transfection is performed as follows:

a. 24 hours before transfection, plate $3x10^6$ cells in each 100 mm cell culture dish in 7.5 ml of the appropriate cell growth medium – for HT22 cells, this would be a medium of 10% Fetal Bovine Serum (FBS) (GIBCO-BRL) in Dulbecco's Modified Eagle's Medium (DMEM)/Low glucose (Hyclone).
b. At the time of transfection, add the plasmid DNA (the DNA: LipofectamineTM 2000 ratio should be 1.5 µg: 2.5 µl) and 60 µl Lipofectamine™ 2000 (Invitrogen) to separate autoclaved microcentrifuge tubes containing 1500 µl of DMEM/Low glucose. Vortex gently.
c. Incubate at RT (20°C) for 4-5 min.
d. Combine the plasmid DNA solution with the Lipofectamine™ 2000 solution and vortex gently.
e. Incubate at RT for 20 min.
f. After 20 min, add the solution to side of each cell culture dish containing the medium and adhered cells. Rock the dish back and forth to distribute the solution evenly.
g. After 4-6 hours replace the medium with new growth medium.
h. Incubate the cells for 24-48 hours in a cell culture incubator (37°C, 5% CO_2).

In order to use these transfected cells for various assays, the cells from each cell culture dish are first harvested by removing the growth medium and adding Trypsin-EDTA solution (Sigma-Aldrich) (1 ml/100 mm cell culture dish) for 1 min at 37°C and then collected with cell growth medium and 1X PBS (Phosphate buffered saline) (8 g NaCl, EMD Chemicals Inc; 0.2 g KCl, BDH Inc; 1.44 g Na_2HPO_4, EMD Chemicals Inc; 0.24 g KH_2PO_4, J.T. Baker; 1000 ml ddH_20; pH 7.4). After collecting the cells they are centrifuged at 1000 g for 5 min at 4°C, and the supernatant is removed. The pellet is washed 3 times by first re-suspending with

1X PBS and centrifuging at 1000 g for 5 min at 4°C, then aspirating the 1X PBS. The resulting cell pellet can be used immediately for experiments.

2.2.6 Immunoprecipitation

Immunoprecipitation is used to determine if a protein physically interacts with other proteins. Either protein A or protein G sepharose bead solutions are used to pull down the protein of interest, and any associated protein(s). Western Blot technique (discussed in the next section) is used to detect the associated proteins. The general procedure for immunoprecipitation is as follows:

a. Freshly harvest cells (harvesting protocol is described in the final paragraph of section 2.2.5) from, at minimum, one 90% confluent 100 mm cell culture dish per sample.
b. Re-suspend the entire cell pellet with a proper amount (first try a total volume of 100 µl) of Lysis buffer (1% Triton®- X 100, Sigma-Aldrich; 20 mM Tris, ICN Biomedicals, pH 7.5; 10% glycerol, MP Biomedicals; 1 mM EDTA, EMD Chemicals Inc) and 100X protease inhibitor cocktail (Sigma-Aldrich). Incubate on ice for 30 min.
c. Centrifuge for 10-20 min at 16000 g at 4°C.
d. Determine the total protein concentration for each cell lysate with the BCA™ protein assay kit (Pierce). The standards used were bovine serum albumin (BSA) protein standards which are included in the kit.
e. For obtaining a total cell lysate (TCL) sample:
    a) Aliquot out enough supernatant to obtain at least 40 µg protein per sample and prepare a 1 µg/µl TCL sample using 4X Loading buffer (2 ml 1 M Tris, pH 6.8; 4 ml glycerol; 2 ml 2-mercaptoethanol, EM Science Inc; 30 mg bromphenol blue, Sigma-Aldrich; 800 mg SDS, ICN Biomedicals; 10 ml ddH_20) and Lysis buffer.
    b) Boil all samples for 5 min at 95°C and store at -20°C.
f. With the rest of the cell lysate supernatant (a minimum of 300 µg of protein is needed for each immunoprecipitation), add the specific amount of primary

antibody in the ratio recommended (if no ratio is specified then try 1 µg antibody: 100 µg protein).

g. Rock the microcentrifuge tubes on their side overnight at 4°C.
h. The next morning, add 50 µl protein sepharose A (GE Healthcare) (generally used for polyclonal antibodies) or protein sepharose G (GE Healthcare) (generally used for monoclonal antibodies) to the microcentrifuge tubes.
i. Rock the tubes, on their side, for 1 hour at 4°C.
j. Centrifuge the tubes at 10 000 g for 5 min at 4°C.
k. Check if all pellets are equal in size. If not equal, add more of the protein sepharose A or G used in step h and repeat steps i and j.
l. If all pellets are equal, to obtain a supernatant sample repeat all directions under step e.
m. If a supernatant sample is not required, carefully aspirate all of the supernatant without touching the pellet.
n. Re-suspend the pellet in 500 µl of lysis buffer and briefly vortex.
o. Centrifuge all tubes at 10 000 g for 5 min at 4°C.
p. Carefully, aspirate all of the supernatant without touching the pellet.
q. Repeat steps n through p two more times.
r. Add 20-25 µl of 1X loading buffer to each tube and mix by tapping the tube gently.
s. Boil all tubes for 5 min at 95-100°C and store at -20°C.
t. When ready to use the sample, centrifuge all tubes at 10 000 g for 5 min at room temperature.

To determine if proteins interact, then the Western blot protocol, explained in the next section, is used (simply begin at step b). The only exception is at the time of loading the sample into the stacking gel well, load only the supernatant and not any of the sepharose beads. Also when running the gel (step 2.2.7.b.d: transferring proteins to a gel), it may be necessary to run for approximately 30 min – 45 min longer than the usual Western blot time if the molecular weight of the protein of interest is similar to the antibody heavy chain molecular weight that is around 50 kDa. This will allow for better resolution of the two bands.

2.2.7 Western blot (Immunoblot)

The Western blot or immunoblot assay is used for the qualitative comparison of protein levels. Equal amounts of total protein extracts from tissue or cell samples are loaded onto a gel and they migrate according to molecular weight (MW); the smaller the protein is the smaller the MW, so it will migrate faster. Similarly, the larger the protein, the slower it will migrate. The specific proteins are detected by specific antibodies, which are, in turn, detected by secondary antibodies conjugated with horseradish peroxidase. Incubation with a chemiluminescent substrate allows for an image of the protein band to be detected on a film.

There are four main parts to Western Blot assay: Denaturing the three-dimensional proteins to linear proteins, loading the proteins onto a gel, transferring them to a membrane and then visualizing the proteins on film.

a. Denaturing proteins to linear proteins:

a) Take harvested cells (harvesting protocol is found in the end paragraph of section 2.2.5) or tissue, and lyse – tissue should be homogenized then lysed - with the appropriate amount of Lysis buffer (1% Triton®- X 100, Sigma-Aldrich; 20 mM Tris, ICN Biomedicals, pH 7.5; 10% glycerol, MP Biomedicals; 1 mM EDTA, EMD Chemicals Inc) and 100X protease inhibitor cocktail (Sigma-Aldrich). Incubate on ice for 30 min.

b) Centrifuge for 10-20 min at 16000 rcf at 4°C.

c) Determine the total protein concentration for each cell lysate with the BCA™ protein assay kit (Pierce).

d) Prepare equal protein concentrations of 1-2 µg/µl using 4X Loading buffer (2 ml 1 M Tris, pH 6.8; 4 ml glycerol; 2 ml 2-mercaptoethanol, EM Science Inc; 30 mg bromphenol blue, Sigma-Aldrich; 800 mg SDS, ICN Biomedicals; 10 ml ddH_20) and Lysis buffer.

e) Boil all samples for 5 min at 95°C and store at -20°C.

b. Transferring proteins to a gel:

a) Following the amounts shown below prepare an SDS-PAGE gel, which has a 10% resolving gel (bottom layer of the gel) and 4% stacking gel (top layer of the gel). (NB: The amounts listed below are for a 1 mm thick gel.)

10% Resolving gel (10 ml)		4% Stacking gel (5 ml)	
ddH_2O	4.01 ml	ddH_2O	3.00 ml
Buffer A	2.50 ml	Buffer C	1.25 ml
Acrylamide	3.33 ml	Acrylamide	0.67 ml
10% APS	50 µl	10% APS	25 µl
10% SDS	100 µl	10% SDS	50 µl
TEMED	10 µl	TEMED	5 µl

Buffer A: 18.45 g Tris-HCL, ICN Biomedicals; 77 g Tris (base), J.T. Baker; 2 g SDS; 50 0ml H_2O; pH 8.8

Buffer C: 30 g Tris (base), 2 g SDS, 500 ml H_2O, pH 6.8

10% Ammonium persulfate (APS): 1 g APS, Invitrogen, 10 ml H_2O

10% Sodium dodecyl sulfate (SDS): 1 g SDS, 10 ml H_2O

(TEMED and Acrylamide are from Bio-Rad and are stored at 4°C, 10% APS is stored at -20°C, and Buffer A, Buffer C and 10% SDS are stored at RT)

b) To the gel apparatus, add 1X Running buffer from a 10X Running buffer stock (30.3 g Tris (base); 144 g glycine, MP Biomedicals; 10 g SDS, 1000 ml H_2O).

c) In the first well load a broad range protein ladder (3 µl in 1X Loading buffer) (PageRuler™ Prestained Protein Ladder Plus, Fermentas Inc), then load each well with an equal volume of sample (sample preparation was discussed in section 2.2.7.a) ranging from 10 µl – 40 µl of sample per well.

d) Set apparatus to a constant voltage of 100 - 115 Volts (V) and run for the suitable amount of time.

c. Transferring proteins from a gel to a membrane:

a) First sandwich the gel and a pure Nitrocellulose membrane (Bio-Rad) between two filter papers (Bio-Rad) and roll out the bubbles. Then place everything between two filter pads and put in the appropriate holder.

b) Pour in 1X Transfer buffer (3 g Tris (base), 14.4 g glycine, 37.5 mg SDS; 200 ml methanol, EMD Chemicals Inc; 800 ml H_2O) and set the apparatus

to 230 mA. Transfer for the suitable amount of time and make sure to add an ice pack inside the apparatus and constantly stir the 1X Transfer buffer.

d. Visualization of protein bands:

a) Prepare 15-20 ml of 5% milk (instant skim milk powder) in 1X TBS solution (from a 10X TBS stock solution: 30 g Tris (base); 80 g NaCl, EMD Chemicals Inc; 1000 ml H_2O, pH 7.4) and rock the membrane in this solution for 1 hour at RT to block it.

b) Prepare 5 ml of 5% milk in TBS- Tween® 20(T) solution (500 µl Tween® 20, EM Science Inc per 1000 ml TBS). Add the primary antibody to this solution in the recommended ratio.

c) Put the membrane with antibody solution in a sealed bag with no air bubbles and place between two glass plates.

d) Rock overnight at 4°C.

e) The next morning remove the primary antibody (antibody solution can be re-used, for up to one month, by adding 10% sodium azzide and storing at 4°C) and wash the membrane with TBS-T for 10 min on a rocker.

f) Repeat the wash 2 more times.

g) Prepare 15 – 20 ml of 5% milk in TBS-T and add the secondary antibody in the recommended ratio.

h) Add the secondary antibody solution to the membrane and rock for 1 - 2 hours at RT.

i) Discard the secondary antibody and wash with TBS-T for 10 min on a rocker.

j) Repeat the wash 2 more times.

k) Combine enhanced chemiluminescent ECL Detection reagent 1 and Detection reagent 2 (Amersham Biosciences) in equal volumes and vortex.

l) Incubate the membrane for 1 min in ECL and then immediately place the membrane in a light-proof cassette.

m) In a dark room, place Hyperfilm™ (High performance chemiluminescence film, Amersham Biosciences) on top of the membrane (membrane is

covered by a thin transparent plastic cover), in the cassette, and wait for the necessary amount of time.

n) Develop the film using a developer machine.

2.2.8 Monoamine oxidase activity assay

The Monoamine Oxidase (MAO) activity assay estimates the enzymatic rate of conversion of monoamines to aldehydes by MAO. This assay specifically uses the [^{14}C]-radiolabelled monoamine substrates serotonin (5-HT) and phenylethylamine (PEA) to measure the activity of MAO-A and MAO-B, respectively. Generally, the protocol is as follows:

a. Bubble oxygen through potassium phosphate buffer (181.6 ml 1 M K_2HPO_4, 18.4 ml 1 M KH_2PO_4, 1000 ml H_2O, pH 7.85, both compounds are from J.T. Baker) for 30-45 min at RT.
b. After the buffer is saturated with oxygen, add 1000 µl- 15000 µl of potassium phosphate buffer to the cells and break the cells – or in the case of brain tissue, homogenize then break the cell tissue - with 10 plunges of a 1 ml syringe (22 gauge needle).
c. Determine the total protein concentration for each sample with the BCA^{TM} protein assay kit (Pierce).
d. Make each sample have the same protein concentration of 1-2 µg/µl using the oxygen saturated potassium phosphate buffer to dilute the more concentrated samples.
e. Add 50 µl of cell or tissue homogenate to each 1.5 ml microcentrifuge tube and keep on ice. (NB: each sample has at least one blank and one test sample done in triplicates).
f. Prepare all solutions below if required for the particular experiment:
    a) If measuring MAO-A activity, radiolabeled serotonin substrate is made as follows (in an authorized radioactive work area):
        i. To make, for example, 3500 µl of 1X total serotonin (5-HT) substrate, combine 17.5 µl Hydroxytryptamine binoxalate, 5-[2-^{14}C]- (hot 5-HT stock) from PerkinElmer at a specific activity of 48.9 mCi/mmol with

17.5 µl of 98.0 mM 5-Hydroxytryptamine hydrochloride (cold 5-HT stock) from Sigma-Aldrich (hot to cold stock is in a 1: 1 ratio as determined by the specific activity) and 3465 µl oxygen saturated potassium phosphate buffer.

b) If measuring MAO-B activity, radiolabeled PEA substrate is made as follows (in an authorized radioactive work area):
   i. To make, for example, 3500 µl of 1X total PEA substrate, combine 3.5 µl PEA hydrochloride, β-[ethyl-1-^{14}C]- (hot PEA stock) from PerkinElmer at a specific activity of 43.8 mCi/mmol with 31.5 µl of 10.9 mM phenethylamine hydrochloride from Sigma-Aldrich (hot to cold stock is in a 1: 9 ratio as determined by the specific activity) and 3465 µl of oxygen saturated potassium phosphate buffer.

c) For 1 mM Ca^{2+} and lesser concentrated Ca^{2+} solutions:
   i. First make a 100 mM Ca^{2+} solution (100X Ca^{2+} working stock) by adding 3.68 mg Ca^{2+} chloride dehydrate (BDH Inc) to 250 µl ddH_2O.
   ii. For all subsequent 100X Ca^{2+} working solutions dilute the 100 mM Ca^{2+} stock by half to get the required concentration.

d) For 1 mM DAPT and lesser concentrated DAPT solutions:
   i. First make a 10 mM DAPT (10X working stock solution) by adding 0.35 mg DAPT (Sigma-Aldrich) to 80 µl DMSO (EM Science Inc).
   ii. For all subsequent 10X Ca^{2+} working solutions dilute the 10 mM DAPT by the appropriate amount to get the required concentration.

g. Working in an authorized radioactive work area and with designated equipment, incubate the first sample (at least 3 sample tubes) with either Ca^{2+} or DAPT for 20 min at RT.

h. After 10 min, incubate the second sample (at least 3 sample tubes) with either Ca^{2+} or DAPT for 20 min.

i. At the end of 20 min for the first sample, add 10 µl of HCL (hydrochloric acid, BDH Inc) to at least 3 other sample tubes, from the first sample, selected to be the blank.

j. Place all of the first sample's tubes in a 37°C water bath and add 50 µl of radiolabelled substrate, either 5-HT or PEA, to each tube in a consecutive manner. Keep in the water bath for 10 min.

k. After 10 min, add 10 µl of HCL to all tubes except for the blank tubes in the exact order the radiolabelled substrate was added.

l. Immediately after, take the first sample's tubes out of the water bath and in a fume hood, add 1000 µl of H_20 saturated ethyl acetate (BDH Inc)/ toluene (EMD Chemicals Inc) (1: 1) solution.

m. Right after, repeat step i and j for the second sample.

n. While the second sample is incubating in the water bath, vortex all of the first samples for a couple seconds and centrifuge at the highest speed for 30 sec at RT.

o. Take out 700 µl of the top layer of each sample tube and put into a liquid scintillation vial.

p. To each vial, add 4 ml of liquid scintillation fluid (ACS Scintillation Cocktail, Amersham Biosciences), cap the vial and put in a vial holder.

q. Once 10 min have passed for the second sample then repeat steps k-l and then n-p for the second sample.

r. Repeat the entire procedure from steps g-q, if there are more than 2 different samples.

s. Once all samples have been placed in the vials and into the vial holder, add 50 µl of radiolabelled substrate and 4 ml of liquid scintillation fluid, to be able to measure total activity.

t. Also wipe test at least 3 different areas, with swipe pads, and place in a vial with 4 ml of liquid scintillation fluid.

u. Measure the activity in a liquid scintillation counter machine.

2.2.9 Fluorescent measurements using Fluo-3AM or DCFDA

Fluo-3AM allows for the detection of free intracellular Ca^{2+} levels and DCF detects reactive oxygen species. Both Fluo-3AM and DCFDA are able to pass into

the cell where either it binds to Ca^{2+} or undergoes oxidation, respectively, and fluoresces.

All of the necessary PS-1 plasmids discussed in section 2.1.2 were transfected into HT-22 cells, following the protocol in section 2.2.5, and the level of fluorescence was observed by a confocal laser fluorescent microscope. The only exception to the transfection protocol was that a 12-well cell culture dish , instead of a 100 mm cell culture dish, was used and the cells were seeded and grown on a circular coverslip. After, the next steps were carried out:

a. Remove the cell growth medium and wash cells once with 1X PBS (8 g NaCl, EMD Chemicals Inc; 0.2 g KCl, BDH Inc; 1.44 g Na_2HPO_4, EMD Chemicals Inc; 0.24 g KH_2PO_4, J.T. Baker; 1000 ml ddH_20; pH 7.4).
b. Carefully cover the cells with about 150-200 µl of the Fluo-3AM or DCFDA solution.
    a) The Fluo-3AM solution is prepared by combining equal volumes of Fluo-3AM (Invitrogen) and pluronic F-127 (Invitrogen), and then adding this solution to 1X Hanks balanced salt solution for neurons (GIBCO-BRL) to make a final working concentration of 4 µM of Fluo-3AM/pluronic F-127 solution.
    b) The DCFDA solution is prepared by combining a 100 µM DCFDA stock solution (250 mg DCFDA (Invitrogen) in 10% H_20 and 90% DMSO (EM Science Inc)) with 1X Hanks balanced salt solution for neurons to make a final working concentration of 10 µM DCFDA.
c. Cover the cell culture dish with tin foil and incubate the cells for 30 min at 37°C and 5% CO_2.
d. Once 30 min has passed, gently wash the cells two times with 1X PBS.
e. Add 1-2 drops of 1XPBS on a rectangular coverslip and place the cell side of the circular coverslip on top of the 1XPBS.
f. Immediately observe the fluorescence with a confocal microscope set at an excitation wavelength of approximately 488 nm (Fluo-3AM) or 493 nm (DCFDA) and emission wavelength at 530 nm (Fluo-3AM) or 522 nm (DCFDA).

2.2.10 Genotyping of transgenic mice

There are two steps of genotyping transgenic mice. A "tail snip" is first digested, allowing for the extraction of genomic DNA, and then subjected to PCR.

a. Tail snip or tissue digestion:

a) Heat a water bath to 55°C and a heat block to 100°C.
b) If the tail snip or tissue was stored at -20°C then leave them at RT for at least 30 min.
c) In an autoclaved microcentrifuge tube add 2 µl/sample of Proteinase K (20 mg/ml, Fermentas Inc) and 20 µl/sample of Extraction buffer (50 mM Tris-HCL, pH 8.0, ICN Biomedicals; 20 mM NaCl, EMD Chemicals Inc; store at RT). Vortex and centrifuge briefly.
d) Add 22 µl of the solution above into each autoclaved microcentrifuge tube containing the thawed tail snip or tissue section.
e) Vortex for 2 sec and centrifuge for 3 sec at 12,000 rpm.
f) Digest the tissue in the 55°C water bath for 15 min.
g) Vortex for 2 sec and centrifuge for 3 sec at 12,000 rpm.
h) For a second time, digest the tissue in the 55°C water bath for 15 min.
i) If the tissue is not completely digested then repeat steps g and h.
j) Add 70-178 ml of ddH_20 to each tube. Vortex for 2 sec and centrifuge for 3 sec at 12,000 rpm.
k) Boil the tubes for 5 min in a 100°C heat block to inactivate the Proteinase K.
l) Cool the tubes for 1-2 min before using for PCR or store at -20°C for later use.

b. PCR and PCR gel formation, loading and visualization:

The below procedure is a general procedure and all reagents, solution amounts, PCR reaction times and primers had to be customized depending on which gene was being genotyped. The different primers used were:

hAPP forward primer :GCC GTT GAC AAG TAT CTC GAG ACA CCT GG

hAPP reverse primer: GTG TCT CCA CCA GCT GCT GTC TCT CGT TGG C

PS-1 forward primer: GAC AAC CAC CTG AGC AAT AC

PS-1 reverse primer: CAT CTT GCT CCA CCA CCT GCC

The general PCR procedure is as a follows:

a) To an autoclaved microcentrifuge tube add the reagents below in the amounts specified for 16 PCR samples:

40 µl	Hot start 10X Reaction buffer
24 µl	25 mM $MgCl_2$
3.2 µl	Forward primer (20 µM)
3.2 µl	Reverse primer (20 µM)
8 µl	10 mM dNTP mix
301.6 µl	ddH_2O
4 µl	Hot start Taq DNA polymerase

(All above reagents, with the exception of the primers and dNTP (both are from Invitrogen) are from Fermentas Inc. and are stored at -20°C)

b) Aliquot out 24 µl of the above master mix to autoclaved PCR tubes.

c) Add to each tube 1 µl of digested tissue sample.

d) Vortex and briefly tap the tube so all solution is at the bottom.

e) Place the samples in a thermal cycler and set the machine to the parameters below:

For PS-1 genotyping with Hot start *Taq*:

First stage:	1 cycle at 95°C for 4 min
Second stage:	35 cycles of: 1) Denature step: 94°C for 30 sec
	2) Anneal step: 52°C for 30 sec
	3) Extension step: 72°C for 1 min
Third stage:	1cylcle of 72°C for 10 min

For APP genotyping with Hot start *Taq*:

First stage:	1 cycle at 95°C for 4 min.
Second stage:	28 cycles of: 1) Denature step: 94°C for 1 min
	2) Anneal step: 55°C for 1 min
	3) Extension step: 72°C for 2 min 35 sec

f) Pour a 1% agarose gel (1 g ultra pure agarose, Invitrogen; 100 ml 0.5X TBE; 5 µl ethidium bromide, Sigma-Aldrich) into the proper PCR gel apparatus. NB: 0.5X TBE is from a 1X TBE stock (10.8 g Tris Base, J.T. Baker; 5.5 g boric acid, EM Science Inc; 4 ml 0.5 M EDTA, pH 8.0, EMD Chemicals Inc; 1000 ml ddH_2O).

g) Wait at least 30 min for the gel to solidify and then add 0.5X TBE buffer.

h) Load 2.5 µl of protein ladder (Fermentas Inc) into the first well.

i) In each of the next wells load 2 µl of 6XLB (30% glycerol in water, MP Biomedicals; 0.25% bromophenol blue, Sigma-Aldrich; 0.25% xylene cyanol FF, Sigma-Aldrich) and 10 µl of the PCR sample.
j) Set apparatus to a constant voltage of 100 V and run for the suitable amount of time (approximately 20-30 min for PS-1 and APP, respectively).
k) Visualize the PCR bands under UV light.

2.2.11 HPLC

Six month old mice (The Jackson Laboratory) were euthanized by injection of sodium pentobarbital and the cortex, cerebellum and hippocampus were removed and stored at -70°C. A sample section from these brain regions were then measured for specific biogenic amines through HPLC with electrochemical detection. This measurement was carried out in collaboration with Dr. Glen Baker at the University of Alberta and the exact method is explained in Baker *et al* (129).

2.2.12 Water maze

For two straight days, 6 month old mice (The Jackson Laboratory) were subjected to a water maze test. This is a behavioural test which measures short-term memory by allowing the mouse to recognize and remember visual markers placed on the walls of the pool. On the first day, each mouse is placed, at a designated direction, into a pool of water at 22°C for 1 min or until they find the hidden platform in the northwest quadrant. This is done for a total of 20 randomly ordered directions. On the second day the platform is removed and each mouse is placed in the pool only at the South direction and the swimming pattern is recorded for 1 min. Analysis of the swimming pattern was done through the EthoVision program from Noldus Information Technology Inc (Leesburg, VA, USA).

2.2.13 Statistical analysis

Data were analyzed by unpaired Students *t*-test (two groups) or analysis of variance (ANOVA) (more than two groups) with significance set at $P<0.05$. Post-hoc analysis relied on the Bonferroni multiple comparisons' test (GraphPad

Software, Inc., San Diego, CA, USA). Data are shown as mean ± standard error of the mean.

3 RESULTS

3.1 PS-1 is expressed in the mitochondrial fraction

The major objective of this work is to examine the possible functional interaction between PS-1 and MAO. As such, the distribution of PS-1 in the cell had to be examined to determine if it might be expressed in the mitochondria, where MAO is located and functions. It is well established that PS-1 exists in the membranes of the ER and golgi body but several groups have shown, through immunoelectron microscopy, that PS-1 and other components of the γ-secretase complex are also found in the mitochondrial membrane (13, 14). Subcellular fractionation of HT-22 and HEK 293A cells, followed by Western Blot analysis confirms that PS-1 can be found in the mitochondrial-enriched fraction of both cell lines (Figure 3.1).

3.2 Chromatogram sequences of PS-1 WT, D257A, Y115H, ΔEx9 and M146V

The PS-1 plasmid constructs obtained from Dr. G. Levesque were sequenced and confirmed against NCBI GenBank sequences. The complete PS-1 WT construct was sequenced with the T7, D257AF2 and PS1END primers (Figure 3.2a - Figure 3.2c). The PS-1 M146V construct was created by mutating the PS-1 wild-type DNA with Stratagene's QuikChange® Site-Directed Mutagenesis Kit (see section 2.2.3 for the exact protocol).

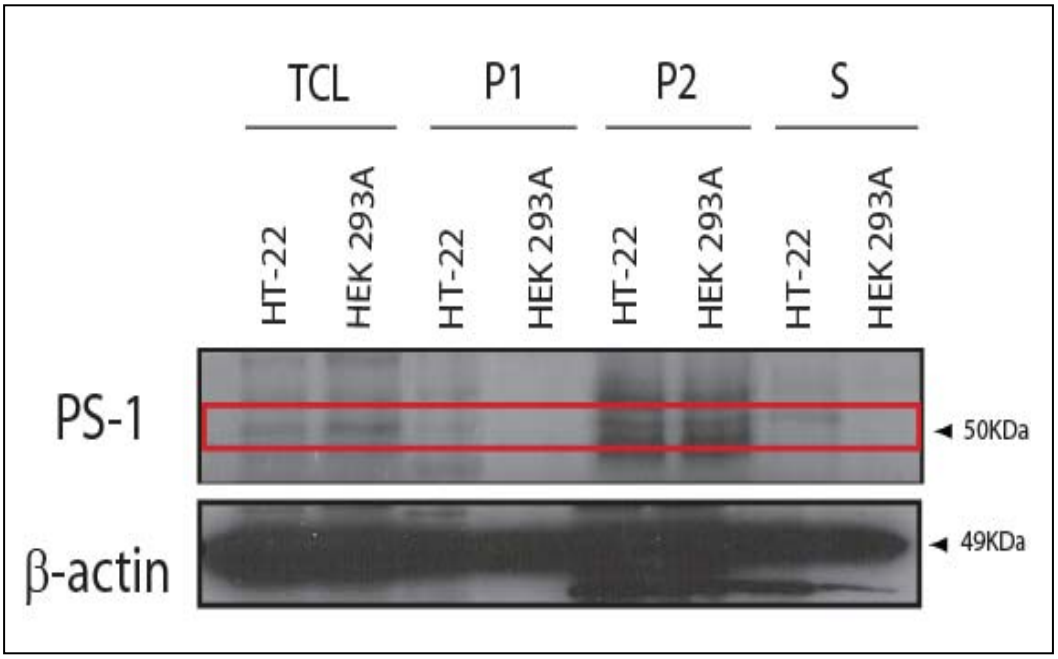

Figure 3.1: Western blot analysis of the subcellular distribution of PS-1. Subcellular fractionation was performed on HT-22 and HEK 293A cells and then each fraction (TCL: total cell lysate, P1: nuclear/ER/cell debris, P2: mitochondria-enriched, S: soluble/cytosol) was resolved by SDS-PAGE, transferred to membrane and probed with the primary antibody PS-1. There is a detectable amount of PS-1 in the mitochondrial fraction of both HT-22 and HEK 293A cells. (n=1)

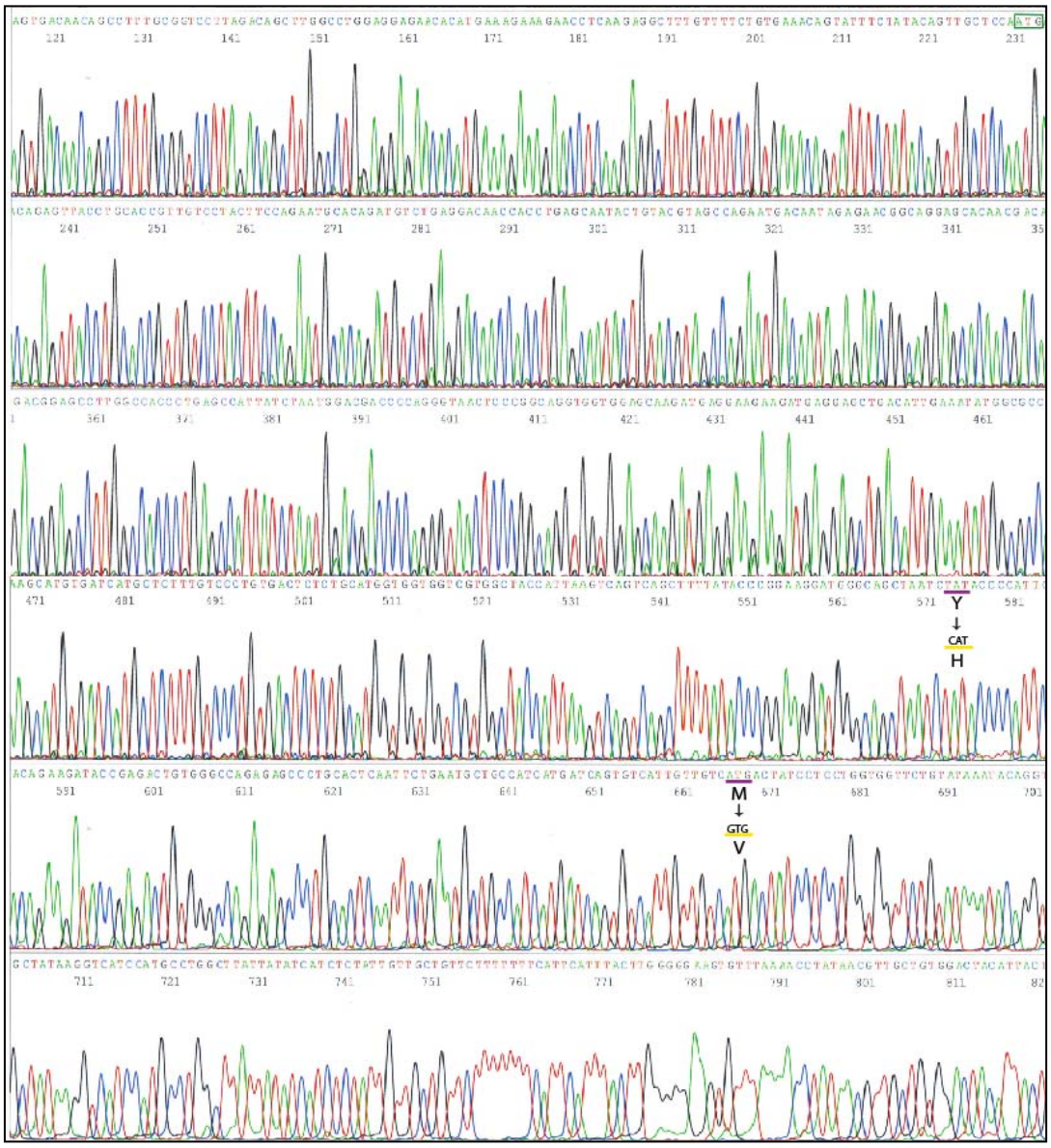

Figure 3.2a: Chromatogram of PS-1 wild-type (WT) nucleotides 1-590. Nucleotide 1 of the PS-1 cDNA sequence is at position 231 of the chromatogram, with the "ATG" start codon boxed in green). The wildtype codons (underlined in purple) and the corresponding amino acid, and the mutated codon (underlined in yellow) and corresponding amino acid substitution are shown.

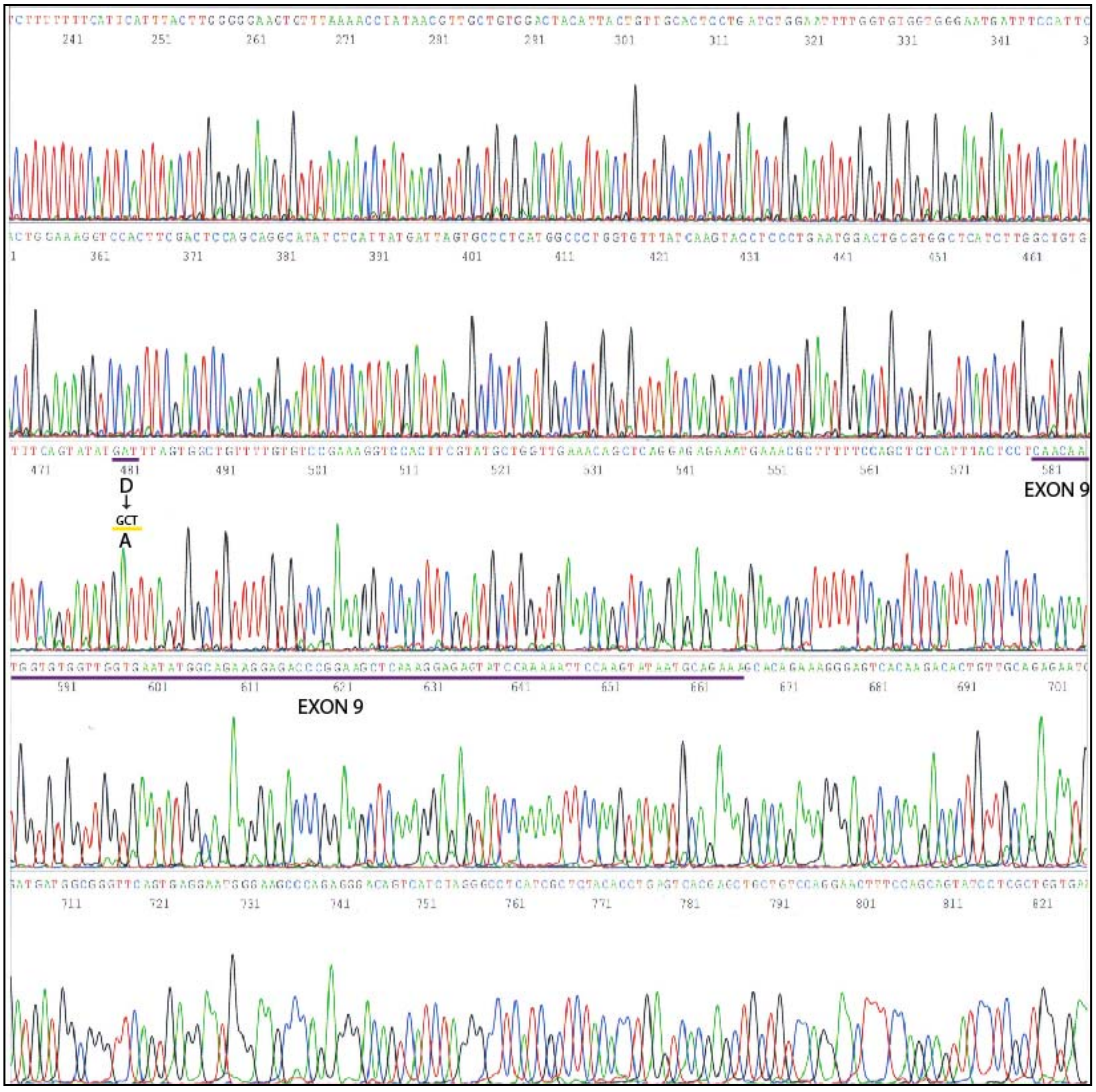

Figure 3.2b: Chromatogram of PS-1 wild-type (WT) nucleotides 590-1110. Nucleotide 590 of the PS-1 cDNA sequence is at position 301 of the chromatogram and nucleotide 1110 is at position 821 of the chromatogram. The wildtype codons (underlined in purple) and the corresponding amino acid, and the mutated codon (underlined in yellow) and corresponding amino acid substitution are shown (the Exon 9 amino acids, underlined in purple, are deleted in the PS-1 ΔEx9 mutant).

Figure 3.2c: Chromatogram of PS-1 wild-type (WT) nucleotides 1110-1400. Nucleotide 1110 of the PS-1 cDNA sequence is at position 191 of the chromatogram and nucleotide 1400 is at position 481 of the chromatogram. The "TAG" stop codon is boxed in red.

3.3 PS-1 mutant proteins affect basal and Ca^{2+}-sensitive MAO-A activity

Wildtype (WT) and mutant (PS-1 D257A, Y115H, ΔEx9 and M146V) PS-1 proteins were overexpressed in HT-22 cells for 24 hours (Figure 3.3). The corresponding homogenates were incubated in the absence or presence of 1 mM Ca^{2+} and assayed for MAO enzymatic activity. Endogenous MAO-A activity is altered differently by the five PS-1 constructs (Figure 3.4). Overexpression of the PS-1 ΔEx9 protein induced basal MAO-A activity compared to control cells. The PS-1 Y115H increased Ca^{2+}-sensitive MAO-A activity and the ΔEx9 protein showed a tendency to increase Ca^{2+}-sensitive MAO-A activity compared to their basal activity levels. The PS-1 M146V protein did not alter MAO-A activity compared to vector control. The PS-1 WT and dominant negative D257A proteins decreased the Ca^{2+}-sensitive MAO-A activity, but did not alter basal MAO-A activity.

The effect of overexpression of PS-1 proteins on endogenous MAO-B activity is not altered as much with the five PS-1 constructs (Figure 3.5). Although tendencies (*i.e.* increased with PS-1 ΔEx9 and decreased with PS-1 Y115H and M146V) were observed, these were not statistically significant.

3.4 PS-1 proteins differentially affect intracellular free Ca^{2+} levels in PS-1 transfected HT-22 cells

Because some effects of PS-1 on endogenous MAO-A activity seemed to implicate Ca^{2+}, the effect of PS-1 constructs on intracellular free Ca^{2+} levels was examined. Confocal laser fluorescent microscopy was used to examine Fluo-3AM fluorescence (once inside the cell this compound binds free Ca^{2+} and fluoresces green). With low magnification there was generally no increase in cytoplasmic Ca^{2+} levels in cells expressing the PS-1 constructs compared to wild-type or control (empty vector), although there was an unexpected decrease in Fluo-3AM

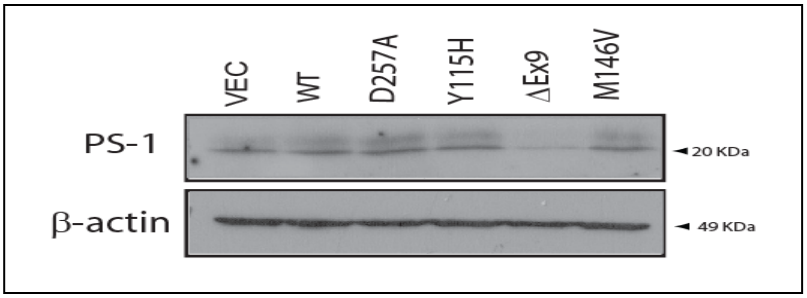

Figure 3.3: Western blot of over-expressed PS-1 constructs. Five PS-1 constructs and the pcDNA3.1 vector were transfected into HT-22 cells for 24 hours and the 20 kDa species of PS-1 was detected by Western blot (the low level of detection in the ΔEx9 sample confirms the absence of Exon 9).

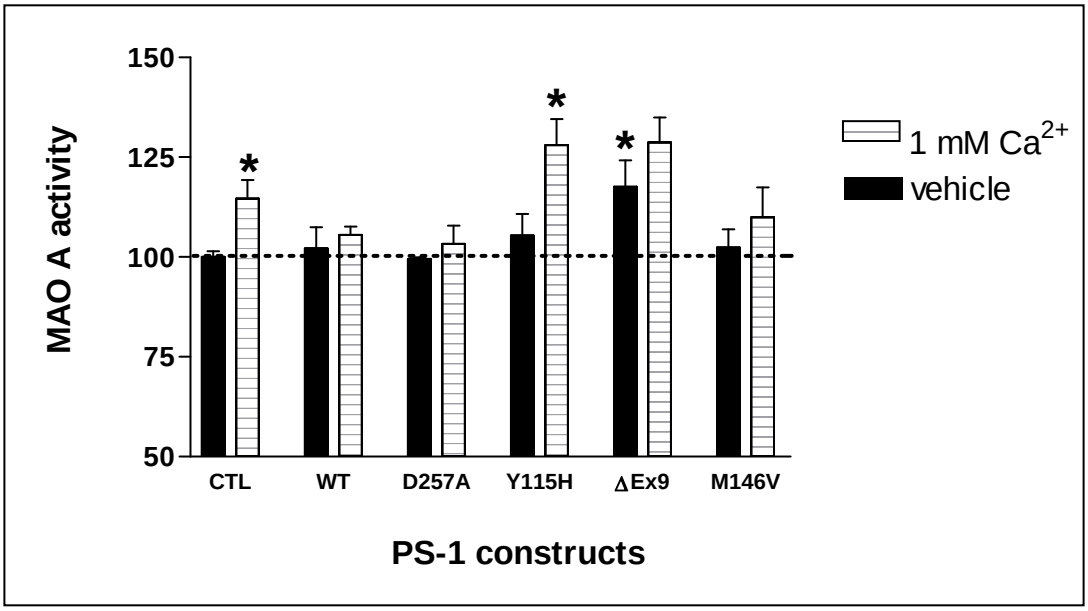

Figure 3.4: Activity assay graph of MAO-A with and without Ca^{2+} in PS-1 transfected HT-22 cells. Endogenous MAO-A activity was measured in HT-22 cells transfected with either the pcDNA3.1 empty vector (control), PS-1 WT, D257A, Y115H, ΔEx9 or M146V constructs (black solid bars) (one-way ANOVA and Bonferroni's *post hoc* test were used; $P<0.05$; n=3). Endogenous MAO-A activity was also measured in the same HT-22 transfected cells but treated with 1 mM Ca^{2+} for 20 min during the assay (horizontal lined bars) (Unpaired t tests were used; two-tailed $P<0.05$; n=3). Significant increases in basal MAO-A activity were found in ΔEx9 expressing cells. MAO-A activity was also enhanced by Ca^{2+} in vector transfected control (CTL) and Y115H samples.

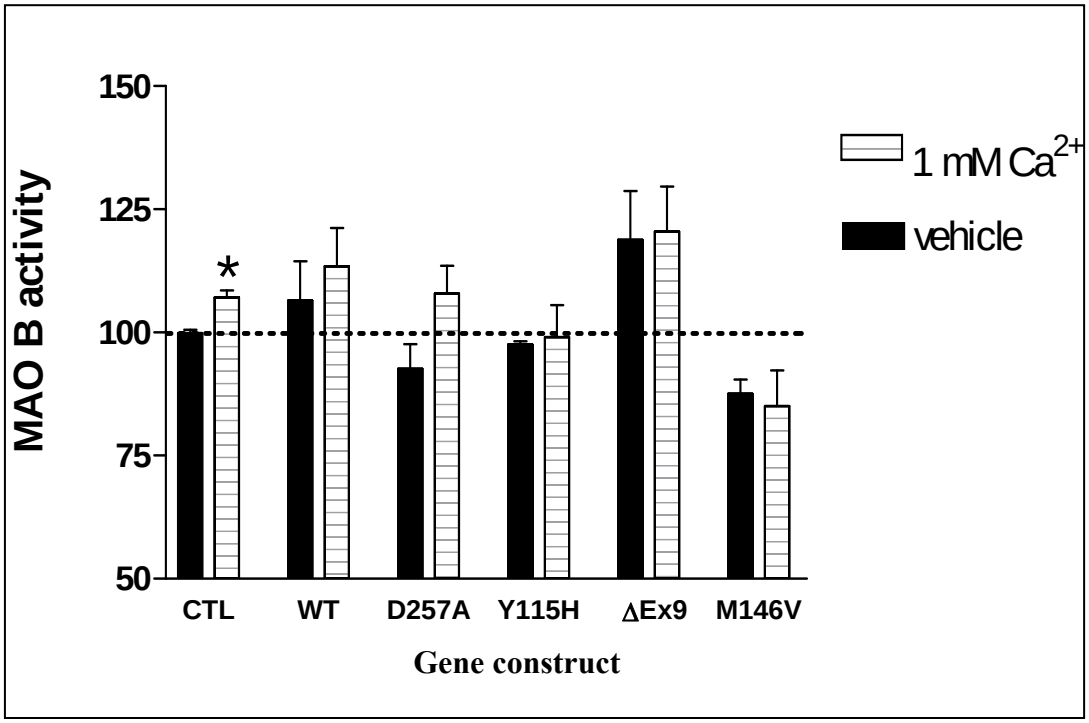

Figure 3.5: Activity assay graph of MAO-B with and without Ca^{2+} in PS-1 transfected HT-22 cells. Endogenous MAO-B activity was measured in HT-22 cells transfected with either the pcDNA3.1 empty vector (control), PS-1 WT, D257A, Y115H, ΔEx9 or M146V constructs (black solid bars) (one-way ANOVA and Bonferroni's *post hoc* test were used; $P<0.05$; n=3). Endogenous MAO-B activity was also measured in the same HT-22 transfected cells but treated with 1 mM Ca^{2+} for 20 min during the assay (horizontal lined bars) (Unpaired t tests were used; two-tailed $P<0.05$; n=3). Only cells expressing the control vector and treated with Ca^{2+} have a significant increase in MAO-B activity compared to basal MAO-B level.

fluorescence in cells expressing the PS-1 ΔEx9 protein (Figure 3.6). Using higher magnification I found that cells expressing the PS-1 Y115H mutant seemed to have more Ca^{2+} concentrated around the nuclear membrane than the other cells and that the dominant negative catalytically inactive PS-1 D257A mutant resulted in a diffuse Ca^{2+} signal- including throughout the nucleus (Figure 3.7). The reasons behind these effects are unclear, but appear to indicate that the effects of PS-1 proteins on MAO-A activity are not restricted to their ability to affect Ca^{2+} availability.

3.5 Overexpression of Calbindin D-28K diminishes the effect of PS-1 proteins on MAO-A activity in HT-22 cells

Basal and Ca^{2+}-sensitive MAO-A activity (only MAO-A was measured because of the lack of Ca^{2+}-related PS-1 effects seen with MAO-B activities) was determined in HT-22 co-expressing the Ca^{2+}-binding protein Calbindin D-28K (CB-28K) and the PS-1 proteins (WT, Y115H, ΔEx9 and M146V). The over-expression of CB-28K, compared to its empty vector pREP, is not as clear as expected; this has been found to be a limitation of the antibody used (Figure 3.8). Figure 3.9 shows that co-expression of CB-28K clearly blocks the Ca^{2+}-sensitive MAO-A activity in control cultures. Its effect on the other cultures is not clear as the individual standard deviations are so large, rendering effects inconclusive.

3.6 Treatment of HT-22 cells expressing PS-1 Y115H proteins with MAO inhibitors decrease reactive oxygen species formation

Given that PS-1-mediated increases in MAO-A activity were observed, proportional increases in peroxy radical production by the cell is expected. The effect of PS-1 on the production of peroxy radical species was examined by DCF

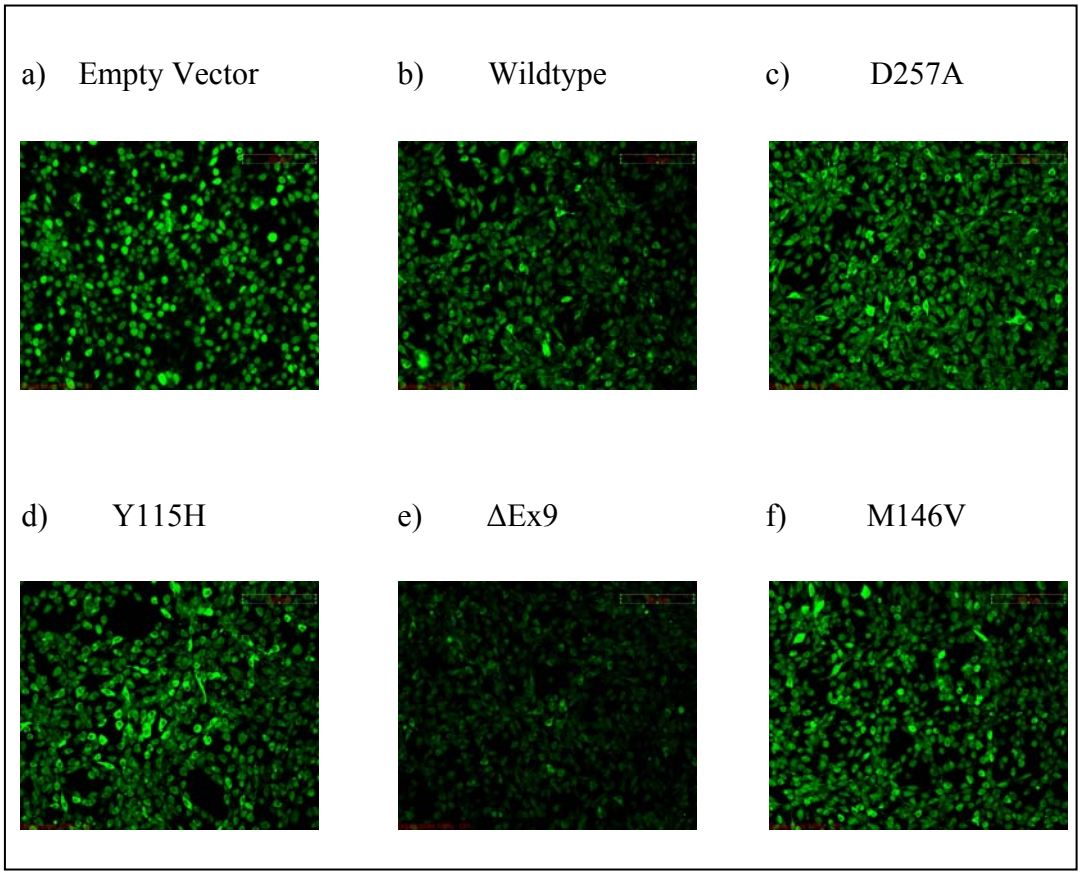

Figure 3.6: Fluo-3AM detection of intracellular free Ca^{2+} in PS-1 transfected HT-22 cells (20X magnification). The empty vector, pcDNA3.1, and five PS-1 proteins, PS-1 WT, D257A, Y115, ΔEx9 and M146V were over-expressed in HT-22 cells for 24 hours. Fluo-3AM was added to the cells and the level of fluorescence (directly correlated to free Ca^{2+}) was observed under 20X magnification using confocal laser fluorescence microscopy. Only ΔEx9 (e) had an obvious decrease in cytosolic Ca^{2+} levels. All other mutated PS-1 constructs (c,d,f) had an increase over WT (b) but not over vector treated cells (a). (n=4)

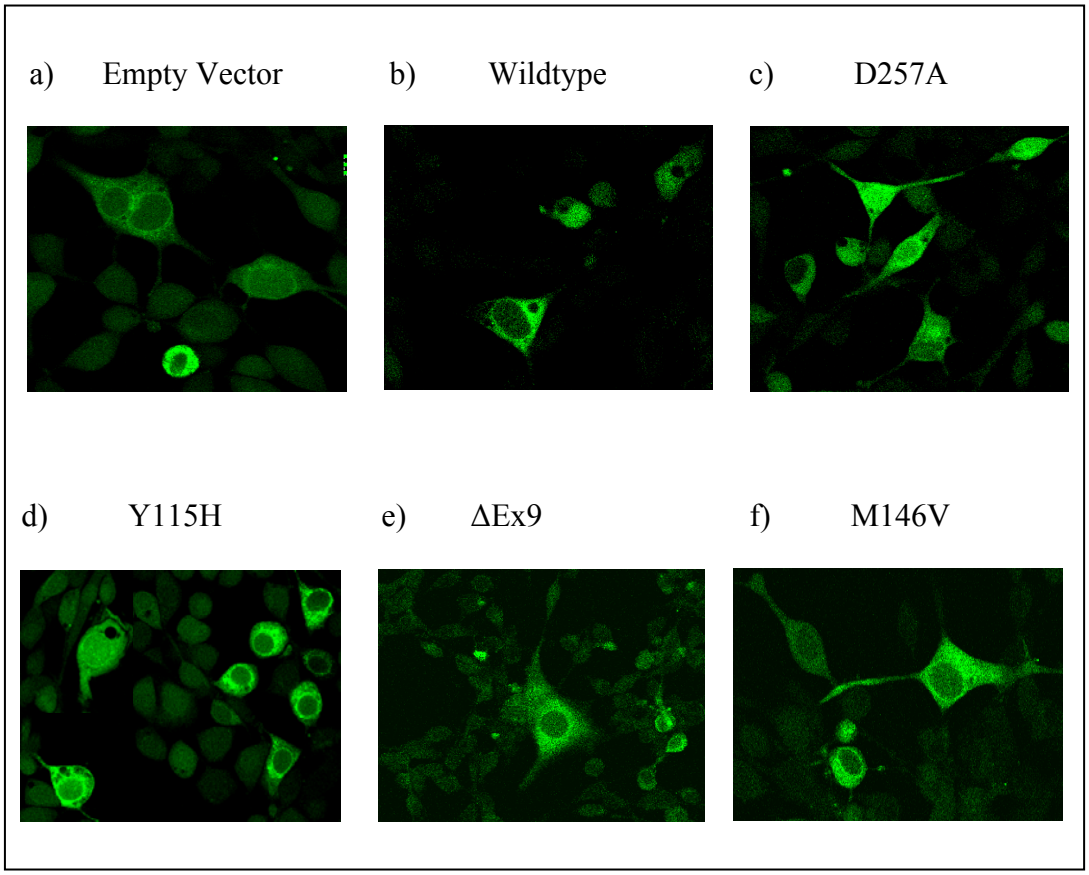

Figure 3.7: Fluo-3AM detection of intracellular free Ca^{2+} in PS-1 transfected HT-22 cells (40X magnification). The empty vector, pcDNA3.1, and five PS-1 proteins, PS-1 WT, D257A, Y115, ΔEx9 and M146V and were over-expressed in HT-22 cells for 24 hours. Fluo-3AM was added to the cells and the level of fluorescence was observed under 40X magnification by a confocal laser fluorescent microscope. Only cells expressing PS-1 Y115H and D257A seemed to affect Ca^{2+} localization in the cell. PS-1 Y115H (d) seemed to have more Ca^{2+} concentrated around the nuclear membrane and PS-1 D257A (c) resulted in a diffuse Ca^{2+} signal including throughout the nucleus. (n=4)

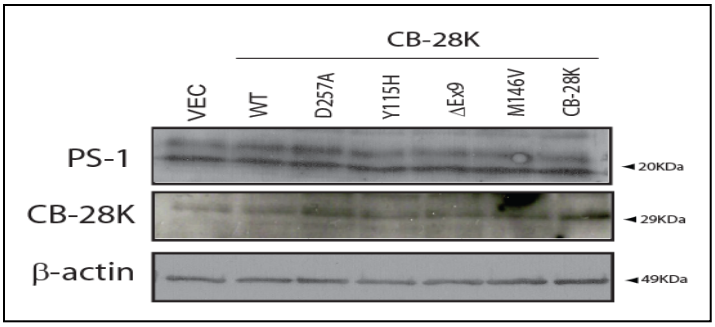

Figure 3.8: Western blot of co-transfected CB-28K and PS-1 constructs. The two vectors, pcDNA3.1 and pREP, and five PS-1 constructs and were transfected into HT-22 cells for 24 hours. The PS-1 constructs were detected with the primary antibody PS-1. At the same time CB-28K was co-transfected in each cell culture dish containing PS-1 WT, the four mutated PS-1 constructs or CB-28K only. The over-expressed CB-28K was detected with the primary antibody Calbindin D28K.

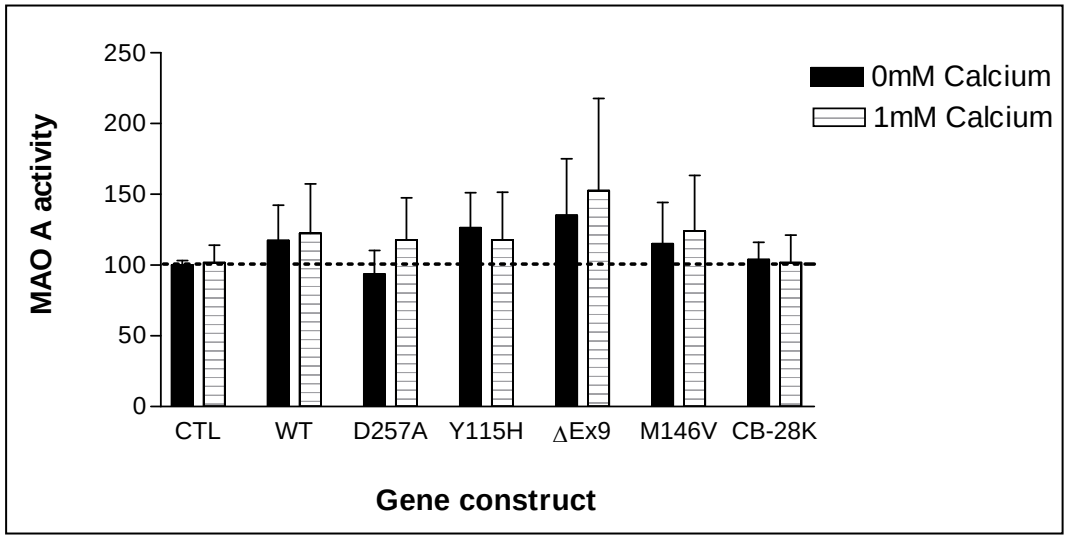

Figure 3.9: Activity assay graph of MAO-A with and without Ca^{2+} in PS-1 and CB-28K co-transfected HT-22 cells. Endogenous MAO-A activity was measured in HT-22 cells transfected with either the pcDNA3.1 and pREP empty vectors (control), PS-1 WT, D257A, Y115H, ΔEx9, M146V or CB-28K constructs (black solid bars) (n=3). Endogenous MAO-A activity was also measured in the same HT-22 transfected cells but treated with 1 mM Ca^{2+} for 20 min during the assay (horizontal lined bars) (n=3). Basal MAO-A activity in familial PS-1 constructs are the same as before but co-transfection of CB-28K in CTL and especially Y115H expressing cells reduce MAO-A activity in the presence of Ca^{2+}.

fluorescence using a laser-scanning confocal fluorescence microscope. PS-1 WT- and ΔEx9-expressing HT-22 cells had less fluorescence than the vector control PS-1 Y115H-expressing cells (Figure 3.10). The effects of clorgyline (MAO-A inhibitor) and deprenyl (MAO-B inhibitor) were marginal in all groups except in cells expressing PS-1 Y115H where both inhibitors prevented peroxy radical production.

3.7 PCR results of wild-type and transgenic PS-1(M146V) mice

To determine if the effects of PS-1 proteins were relevant in vivo, wild-type and PS-1 transgenic mice brains (these mice over-express the PS-1 (M146V) protein) were collected and used to assay both basal and Ca^{2+}-sensitive MAO activities. All mice were genotyped (section 2.2.10) to confirm the presence of the transgene. For purposes of comparison, this portion of the study included mice that were transgenic for the human APP (hAPP) gene carrying the KM670/671NL Swedish familial AD-related mutation.

Figure 3.11 depicts genotyping results (PCR) and reveals that mice assigned numbers 38, 39, 57, 58, 59, 70, 73, 80, 87, 89, 92, 93, 94, 98 were PS-1 positive and the mice assigned numbers 31, 37, 52, 54, 55, 56, 83, 90, 91, 95, 96, 97 were PS-1 negative (wildtype, control). Figure 3.12 depicts genotyping results and reveals that mice numbered with 37, 59, 60, 73, 77, 88, 93, 94, 97 were hAPP positive and the mice numbered with 31, 38, 39, 52, 55, 57, 58, 70, 83, 87, 89, 90, 91, 92, 95, 96, 98 were APP negative (wildtype, control).

3.8 Transgenic PS-1 mice brains and endogenous MAO-A activity

3.8.1 Transgenic PS-1(M146V) cortical MAO-A activity is sensitive to Ca^{2+}

Cortical tissue from WT and transgenic PS-1 (M146V) mice were homogenized in potassium phosphate buffer, and basal and Ca^{2+}-sensitive MAO activity was determined. In WT mouse cortical homogenates MAO-A activity did

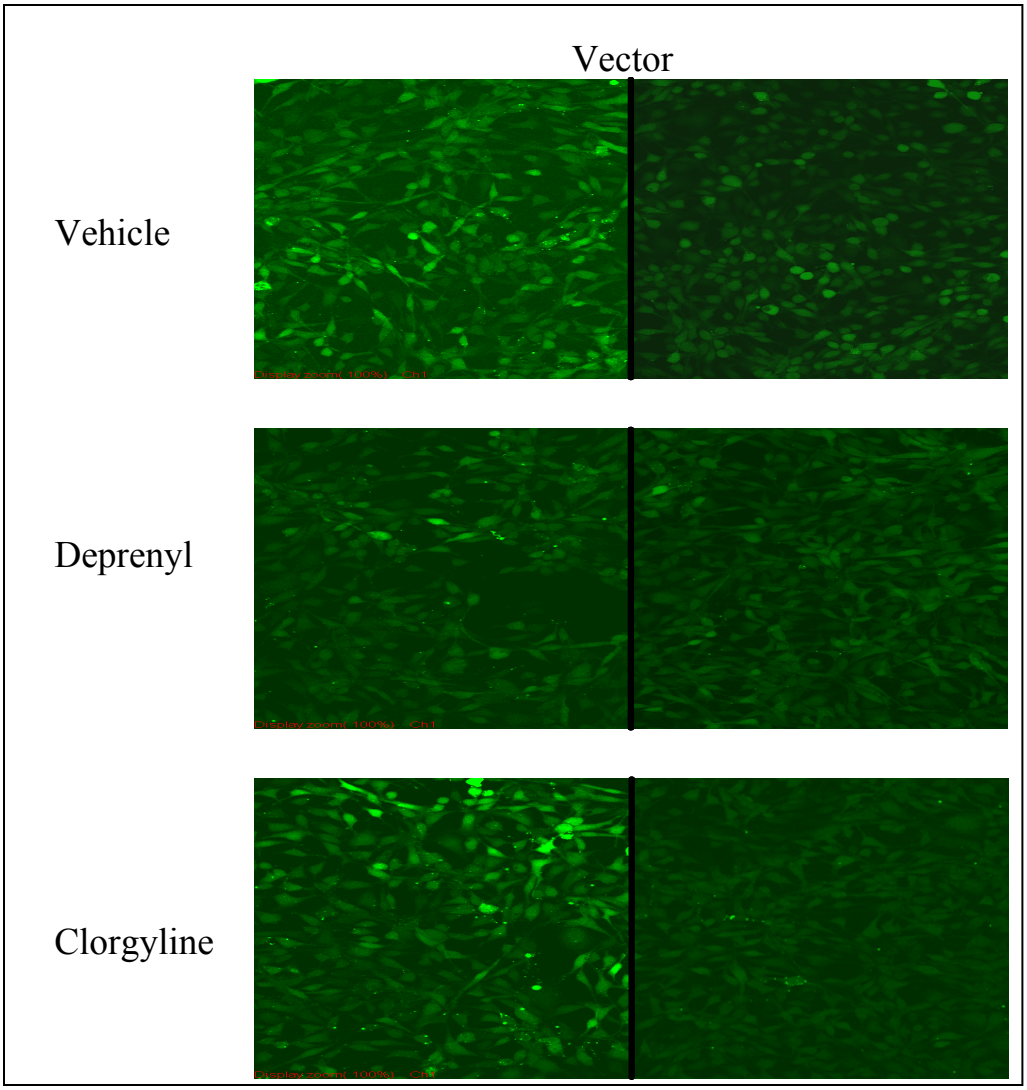

Figure 3.10a: DCF detection of reactive oxygen species in PS-1 transfected HT-22 cells treated with vehicle, clorgyline or deprenyl (continued on the next three pages). Vector and PS-1 proteins, WT, Y115H and ΔEx9, were over-expressed in HT-22 cells for 24 hours and treated with vehicle, clorgyline or deprenyl 4 hours post-transfection. DCF was added to the cells and the level of fluorescence was monitored under 10X magnification by a confocal laser fluorescence microscope. Vehicle-treated PS-1 WT and ΔEx9-expressing cells had less fluorescence than vector-transfected and PS-1 Y115-expressing cells. Clorgyline and deprenyl treatment had little effect in most cultures, but clearly inhibited DCF fluorescence in cells expressing PS-1 Y115H. (n=3; two trials are shown in each picture and all left or right sides correspond to one trial)

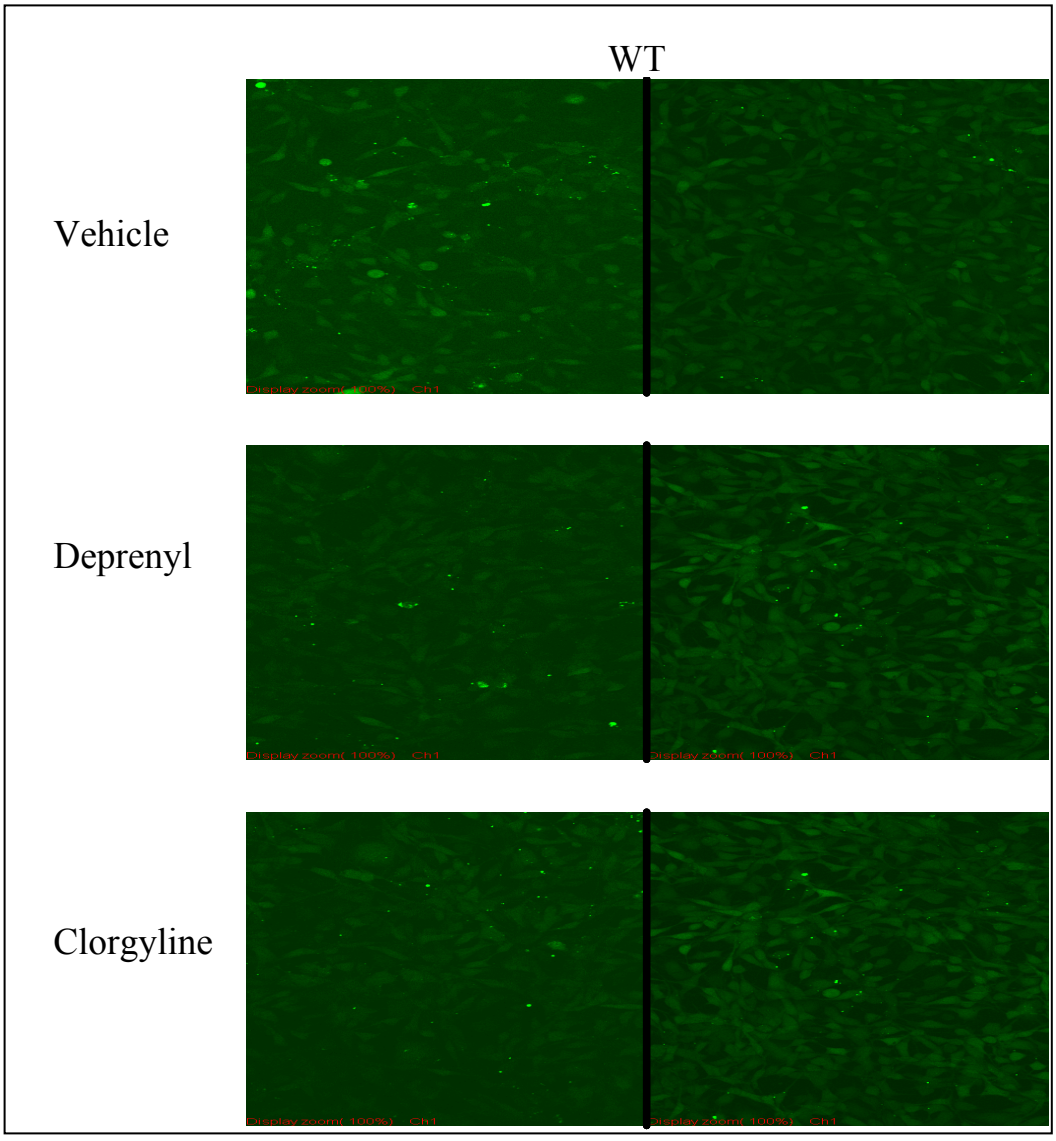

Figure 3.10b: DCF detection of reactive oxygen species in PS-1 transfected HT-22 cells treated with vehicle, clorgyline or deprenyl. (These pictures depict the DCF fluorescence in PS-1 WT-expressing HT-22 cells. This is a continuation of the data presented on page 69.)

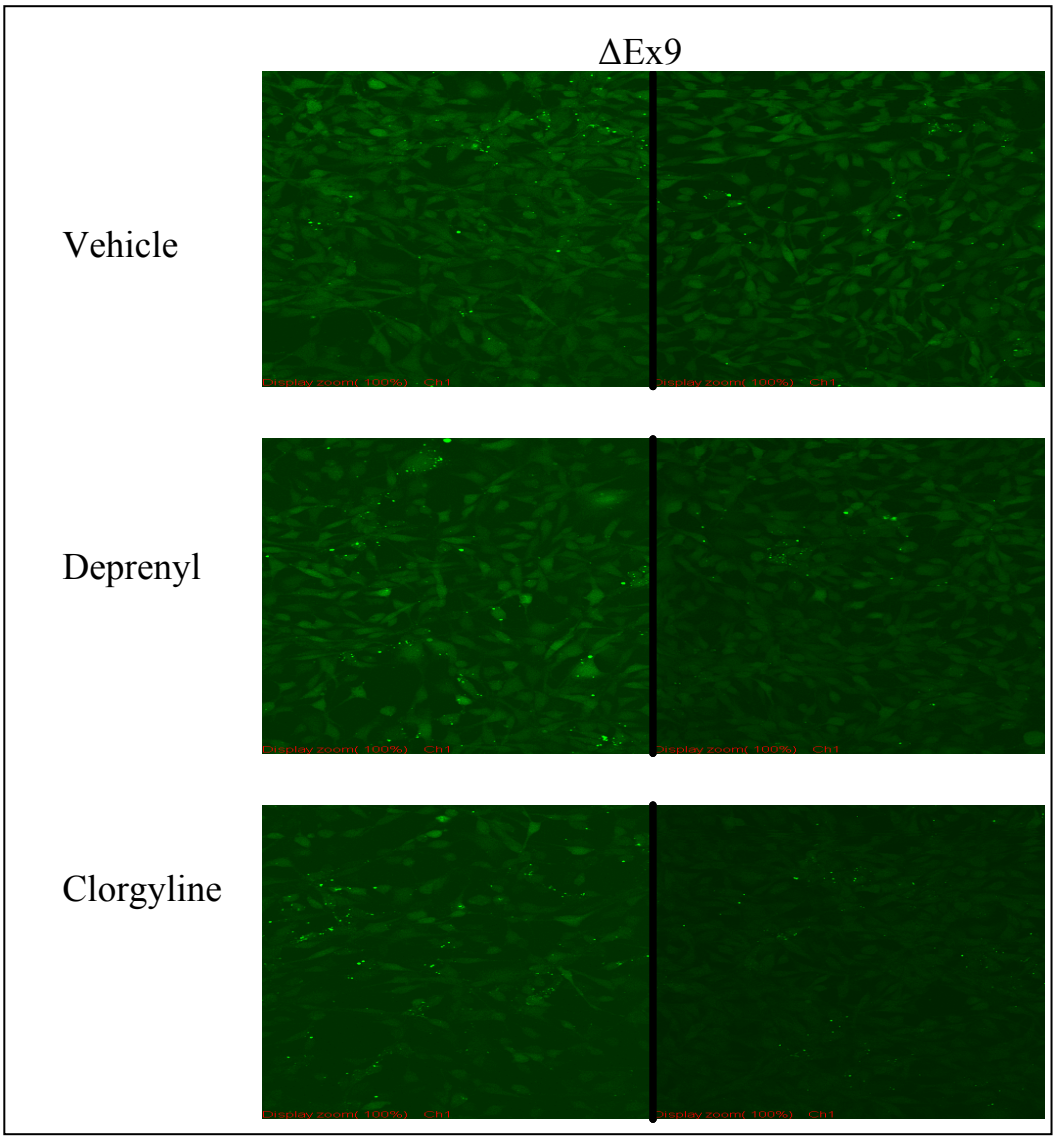

Figure 3.10c: DCF detection of reactive oxygen species in PS-1 transfected HT-22 cells treated with vehicle, clorgyline or deprenyl. (These pictures depict the DCF fluorescence in PS-1 ΔEx9-expressing HT-22 cells. This is a continuation of the data presented on page 69).

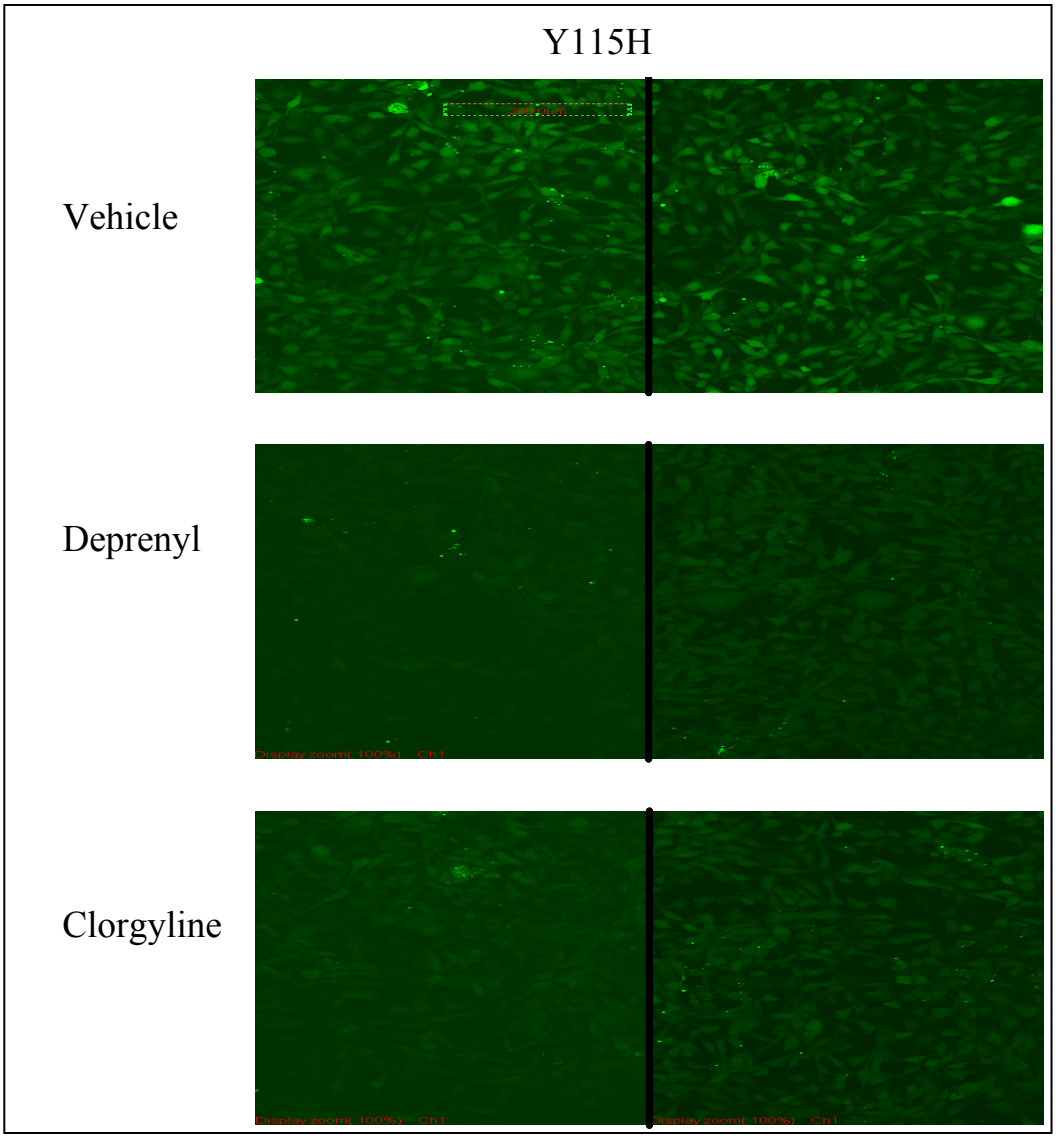

Figure 3.10d: DCF detection of reactive oxygen species in PS-1 transfected HT-22 cells treated with vehicle, clorgyline or deprenyl. (These pictures depict the DCF fluorescence in PS-1 Y115H-expressing HT-22 cells. This is a continuation of the data presented on page 69).

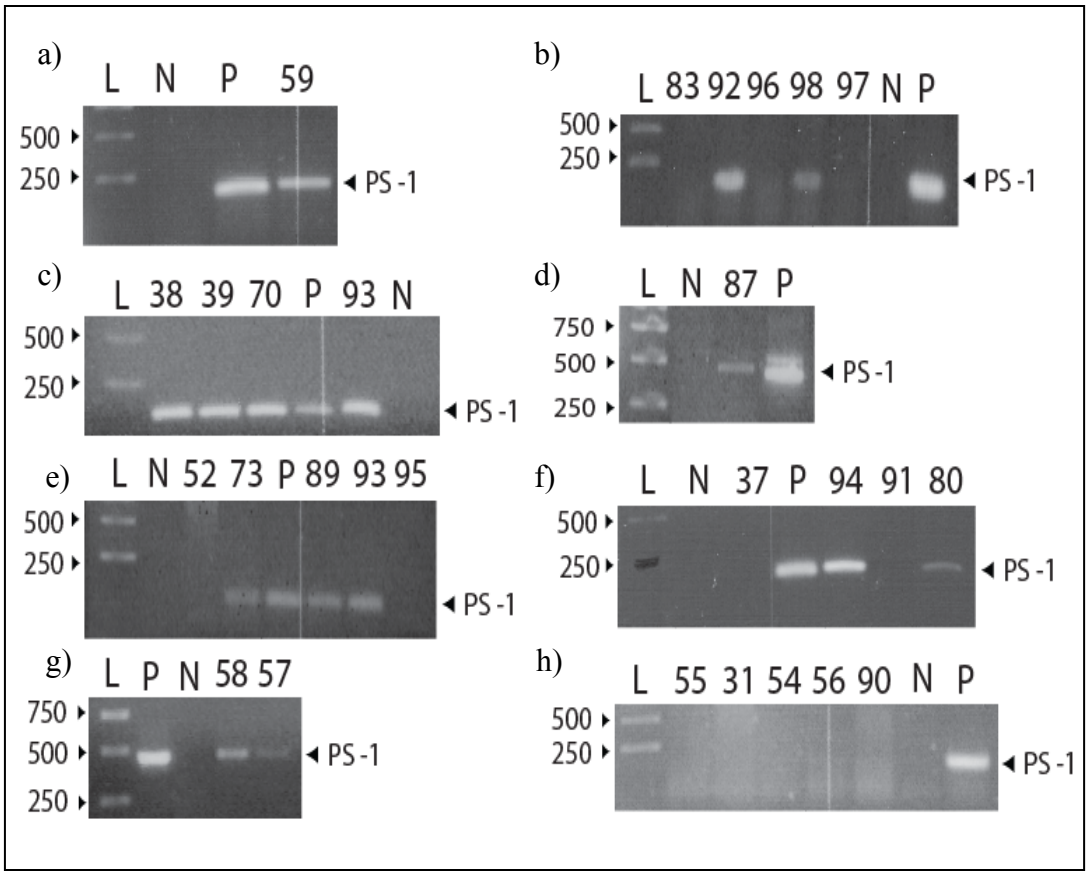

Figure 3.11: PCR results of PS-1 positive mice. The brain tissues of 26 mice were first digested and then PCR was carried out. The mice designated numbers 38, 39, 57, 58, 59, 70, 73, 80, 87, 89, 92, 93, 94, 98 are shown to have a PS-1 positive PCR band comparable to the positive control lane (P) and the mice designated 31, 37, 52, 54, 55, 56, 83, 90, 91, 95, 96, 97 are shown to have no PCR band as in the negative control lane (N).

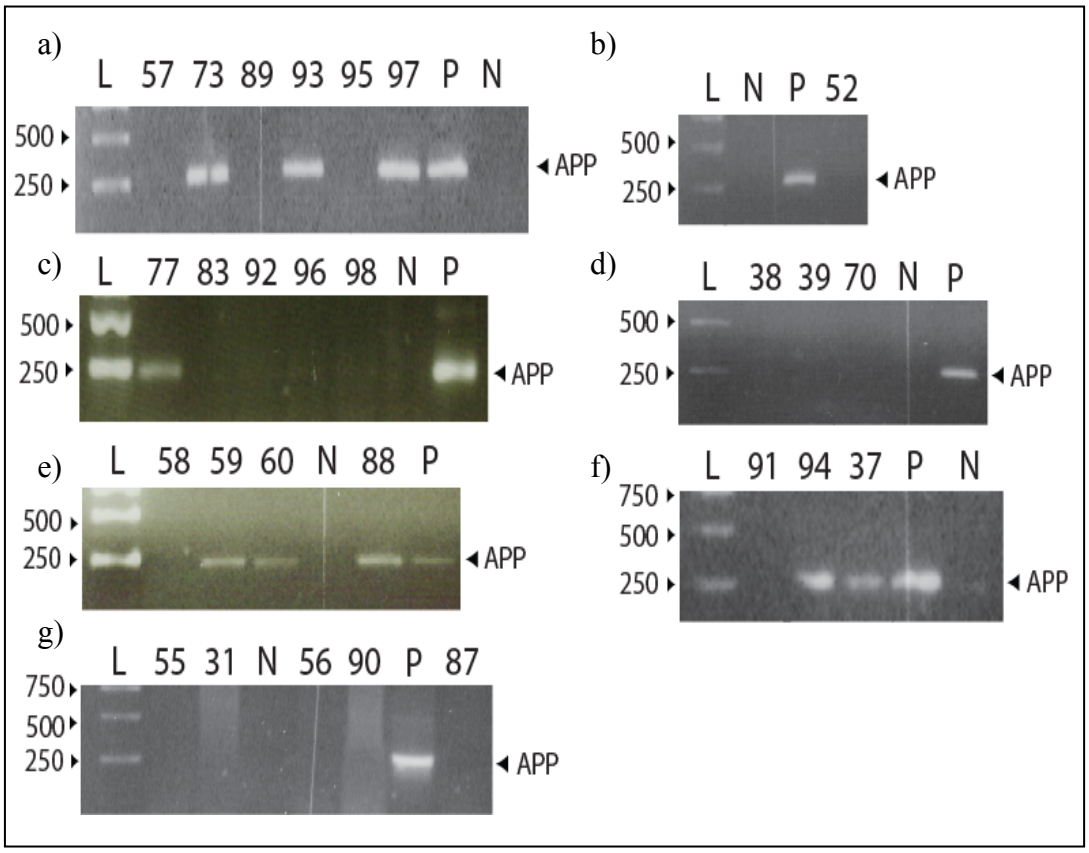

Figure 3.12: PCR results of APP positive mice. The brain tissues of 26 mice were first digested and then PCR was carried out. The mice designated numbers 37, 59, 60, 73, 77, 88, 93, 94, 97 are shown to have a APP positive PCR band comparable to the positive control lane (P) and the mice designated 31, 38, 39, 52, 55, 57, 58, 70, 83, 87, 89, 90, 91, 92, 95, 96, 98 are shown to have no PCR band as in the negative control lane (N).

not respond to incubation with increasing concentrations of Ca^{2+} (Figure 3.13a). In contrast, in transgenic mouse cortical homogenates, there is a tendency for MAO-A activity levels to increase with increasing concentrations of Ca^{2+} (Figure 3.13b).

3.8.2 Transgenic PS-1(M146V) cerebellar MAO-A activity is not sensitive to Ca^{2+}

Cerebellar homogenates from WT and transgenic PS-1 (M146V) mice were also examined for MAO-A activity. Neither WT (Figure 3.14a) nor PS-1(M146V) (Figure 3.14b) cerebellar MAO-A activities responded significantly to Ca^{2+}.

3.9 Transgenic PS-1 mice brains and endogenous MAO-B activity

3.9.1 Transgenic PS-1(M146V) cortical MAO-B activity is sensitive to Ca^{2+}

MAO-B activity in cortical tissue from WT and transgenic PS-1 (M146V) mice were also examined, for purposes of comparison. Figure 3.15 reveals that cortical MAO-B activity in WT mice does not respond to incubation with increasing concentrations of Ca^{2+}, but that cortical MAO-B activity in transgenic PS-1(M146V) mice does respond, although significance is not reached.

3.9.2 Cerebellar MAO-B from transgenic PS-1 mice is not sensitive to Ca^{2+}

Cerebellar homogenates from WT and transgenic PS-1 (M146V) mice were also examined for MAO-B activity. Neither WT (Figure 3.16a) nor PS-1(M146V) ((Figure 3.16b) cerebellar MAO-B activities responded to incubation with Ca^{2+}.

3.10 Biogenic amine levels in the Cortex, Cerebellum and Hippocampus of WT and PS-1 transgenic mice

As the expression of the PS-1(M146V) transgene appears to affect both MAO-A and MAO-B activities in a region-specific manner, regional levels of

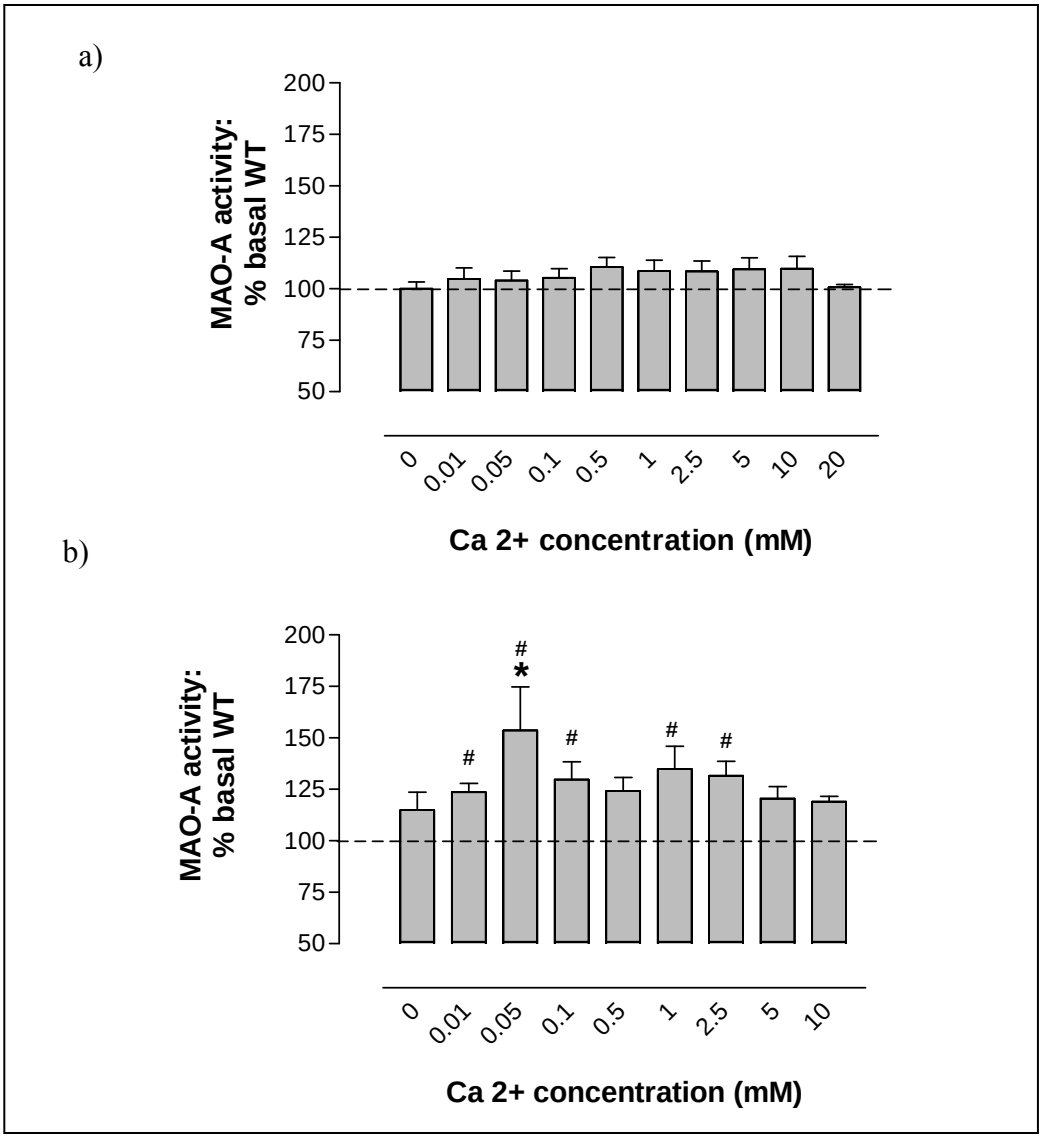

Figure 3.13: MAO-A and Ca^{2+} concentration-response curves from cortical homogenates of WT and PS-1 mice. a) WT mice. Increasing concentrations of Ca^{2+} slightly increase WT MAO-A activity compared to their basal level (0mM Ca^{2+}). b) Transgenic PS-1(M146V) mice. The basal level of PS-1 MAO-A activity (0 mM) compared to the basal level of WT mice (100%) is moderately increased. Increasing concentrations of Ca^{2+} greatly increase PS-1 mice MAO-A activity compared to their basal level (0 mM) (∗: one-way ANOVA and Bonferroni's *post hoc* test was used to compare PS-1 or WT activity with different concentrations of calcium, $P<0.05$; #: unpaired t tests was used to compare activity between PS-1 and WT at each concentration, one-tailed, $P<0.05$; n=3)

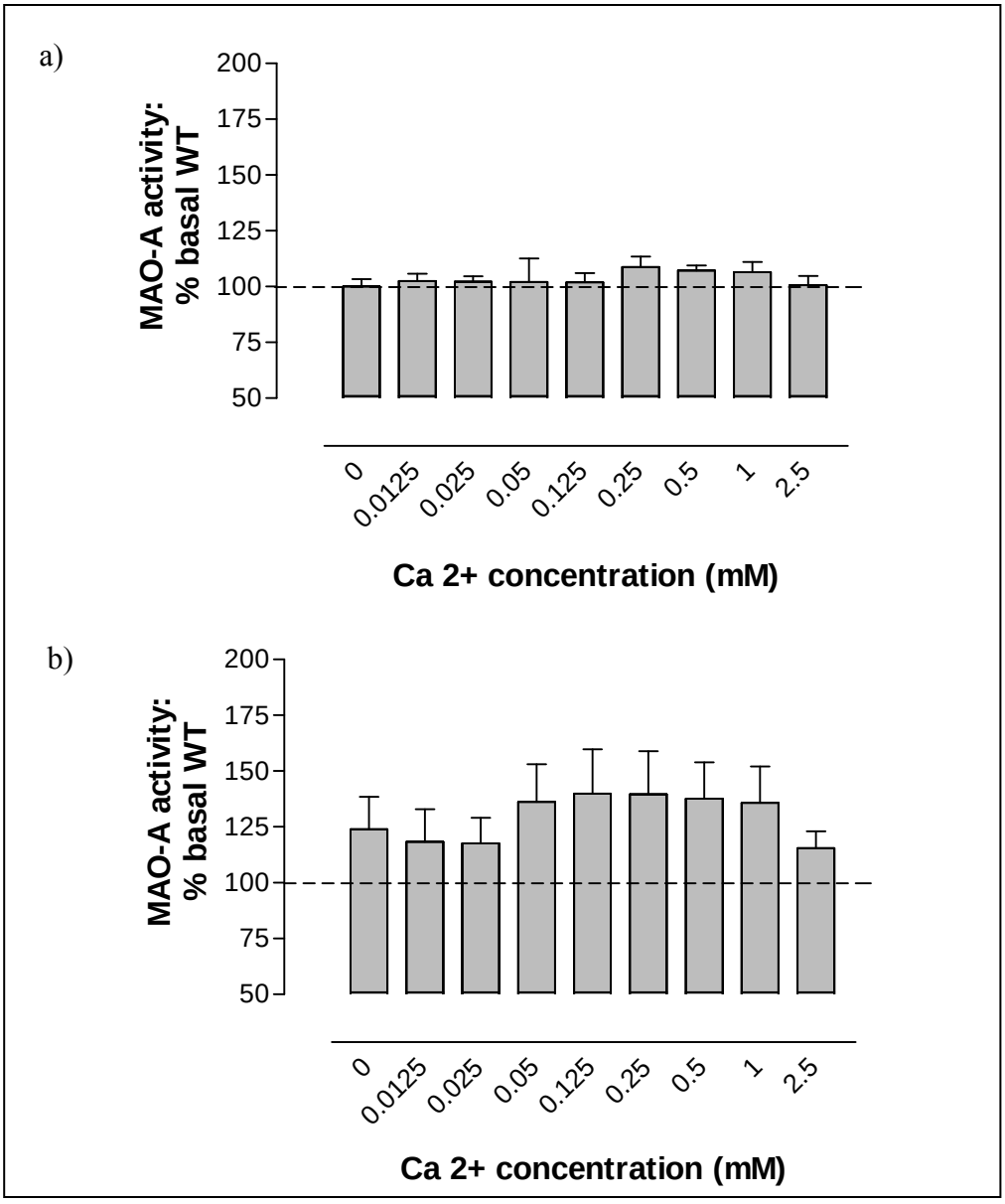

Figure 3.14: MAO-A and Ca^{2+} concentration-response curves from cerebellar homogenates of WT and PS-1 mice. a) WT mice. Increasing concentrations of Ca^{2+} slightly increase WT MAO-A activity compared to their basal level (0 mM Ca^{2+}). b) Transgenic PS-1(M146V) mice. The basal level of PS-1 MAO-A activity (0 mM) compared to the basal level of WT mice (100%) is greatly increased. Increasing concentrations of Ca^{2+} produce a tendency for moderate increases in PS-1 mice MAO-A activity compared to their basal level (0 mM). (n=3).

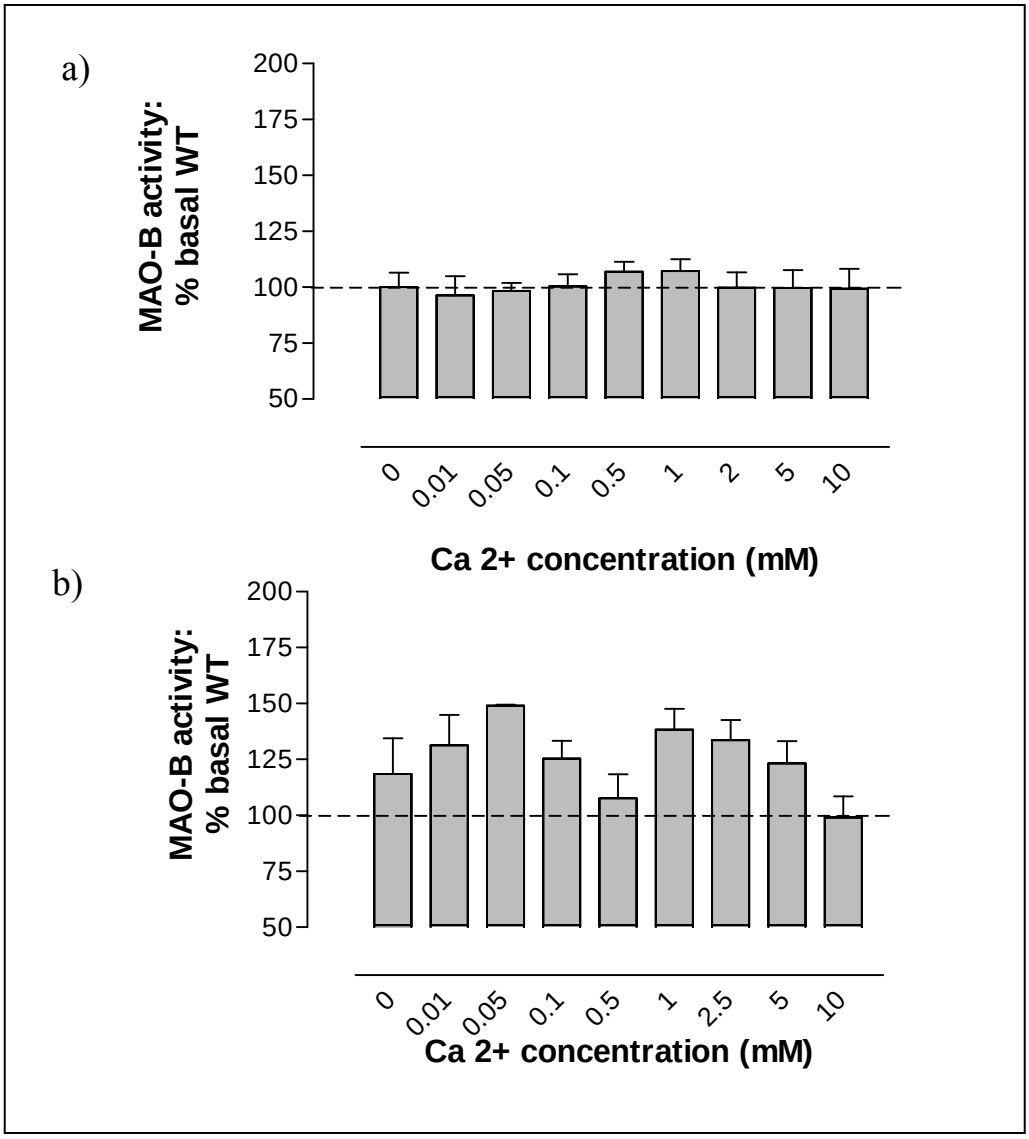

Figure 3.15: MAO-B and Ca^{2+} concentration-response curves from cortical homogenates of WT and PS-1 mice. a) WT mice. Increasing concentrations of Ca^{2+} do not increase WT MAO-B activity compared to their basal level (0 mM Ca^{2+}). b) Transgenic PS-1(M146V) mice. The basal level of PS-1 MAO-B activity (0 mM) compared to the basal level of WT mice (100%) is increased and in the presence of increasing concentrations of Ca^{2+} PS-1 mice increase- in an apparent biphasic manner- MAO-B activity compared to their basal level (0 mM). (n=3).

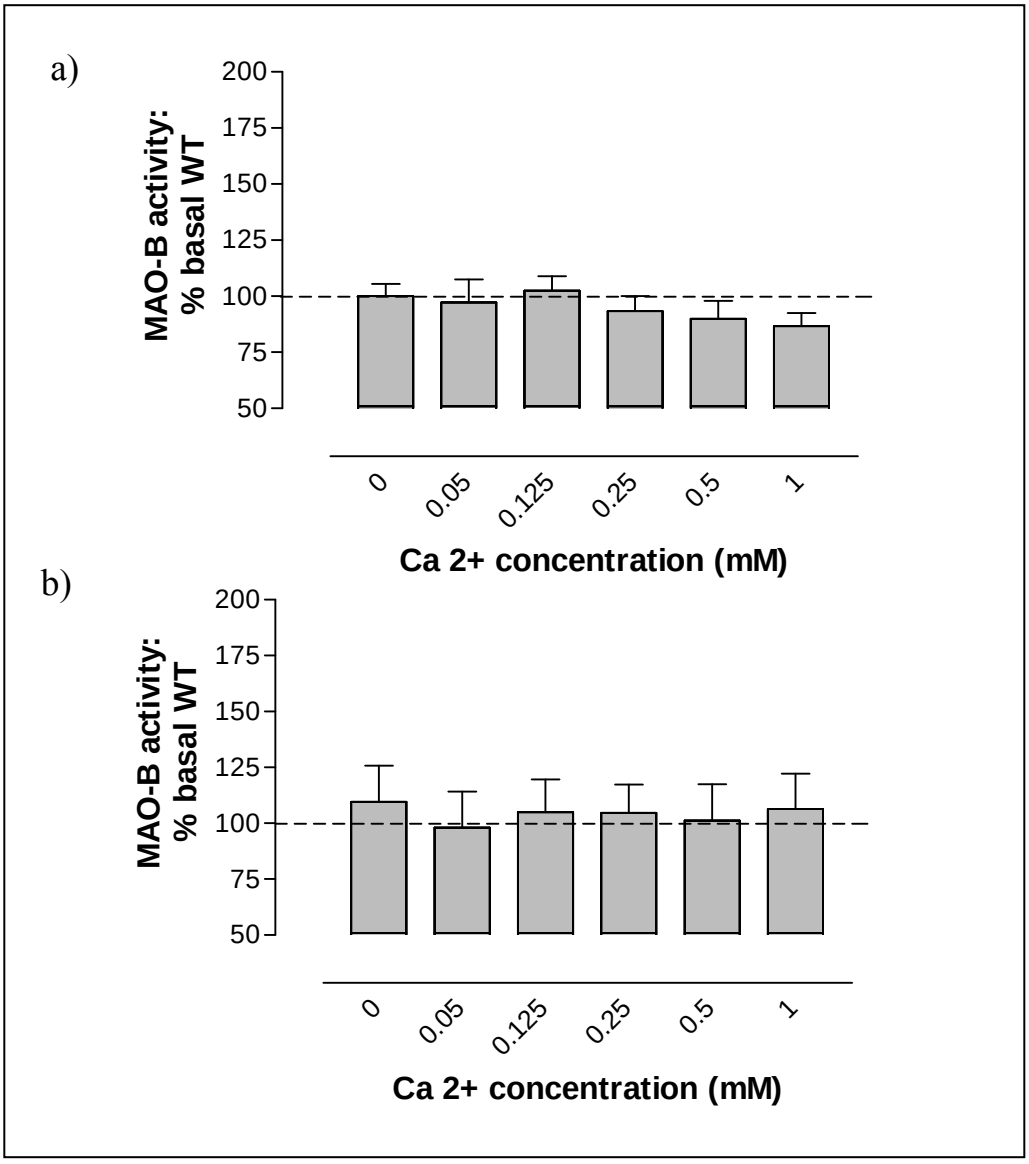

Figure 3.16: MAO-B and Ca^{2+} concentration-response curves from cerebellar homogenates of WT and PS-1 mice. a) WT mice. Increasing concentrations of Ca^{2+} do not increase WT MAO-B activity compared to their basal level (0 mM Ca^{2+}). b) Transgenic PS-1(M146V) mice. The basal level of PS-1 MAO-B activity (0 mM) compared to the basal level of WT mice (100%) is somewhat increased and in the presence of increasing concentrations of Ca^{2+}, PS-1 mice do not increase MAO-B activity compared to their basal level (0 mM). (n=3).

biogenic amine substrates for MAO-A and MAO-B, e.g. 5-HT, dopamine (DA) and noradrenaline (NA) were analyzed (this was in collaboration with Dr. G.B. Baker, University of Alberta).

In the cortex of PS-1 mice it was found that there is a significant decrease in DOPAC compared to WT, which possibly shows that more DA is being metabolized to HVA (Figure 3.17a). There was also an unusual decrease in 5-HT's metabolite 5-HIAA.

In contrast, for the cerebellar region, there was a significantly reduced amount of DA, NA and 5-HT levels, compared to WT. Along with the decreased DA there was a tendency for an increase in its metabolite HVA. Unfortunately I could not verify if the decreased NA was a result of it being metabolized because NA's metabolites were not quantified (Figure 3.17b).

Although the hippocampal MAO activity could not be measured because of inadequate tissue amounts required for the MAO activity assay, I still decided to examine if any changes in the cortex and cerebellum could be found in the hippocampus. Interestingly in PS-1 mice, I found a significantly larger amount of DA compared to WT mice and thus a tendency for more HVA metabolites was observed but this metabolite increase was not statistically significant probably due to the large standard deviation (Figure 3.17c). All other amines measured had similar amounts between WT and PS-1 mice.

3.11 Endogenous MAO protein levels in the Cortex, Cerebellum and Hippocampus of WT and PS-1 transgenic mice

Since the MAO activity was found to be different between WT and transgenic mice and between the cortex and cerebellum, I tested to see if this difference was due to differences in MAO protein levels. Furthermore, because the difference in MAO activity seen between regions of transgenic PS-1 mice brains was in the presence of Ca^{2+}, I tested if some well-known and not so well-known endogenous molecules regulating Ca^{2+} availability were altered.

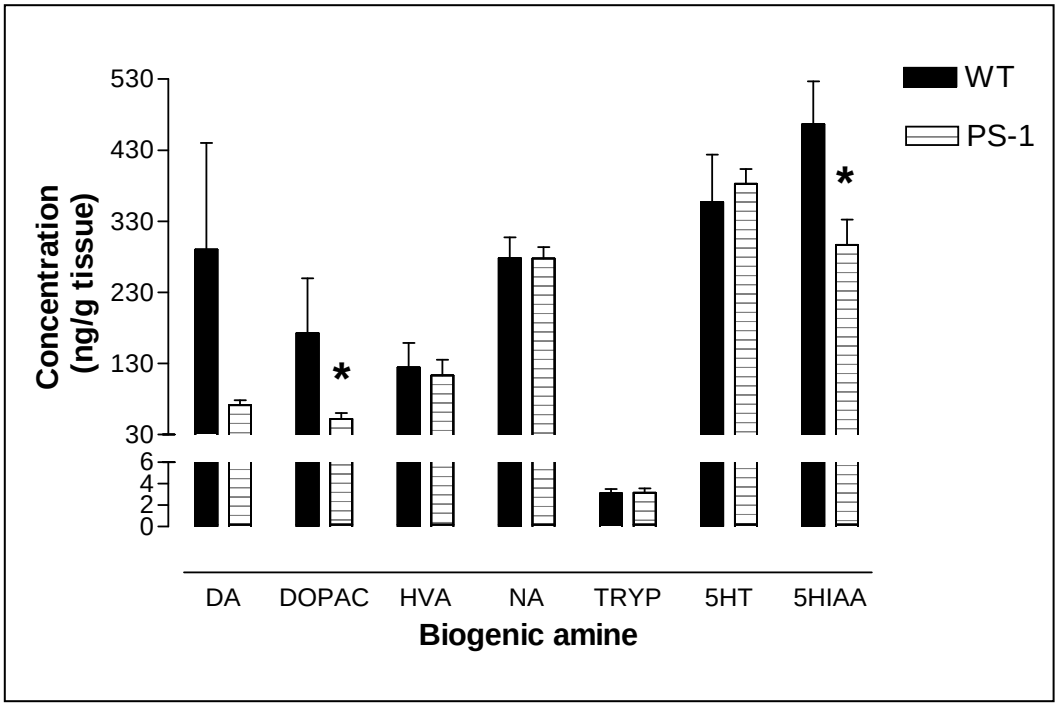

Figure 3.17a: Biogenic amine concentrations from cortical homogenates of WT and PS-1 mice. HPLC was performed on cortical homogenates of WT (black solid bars) and PS-1 (horizontal lined bars) mice and specific biogenic amine levels were measured. DOPAC and 5-HIAA levels were significantly decreased in PS-1(M146V) mice (One-tailed t-tests; *: $P<0.05$; n=6).

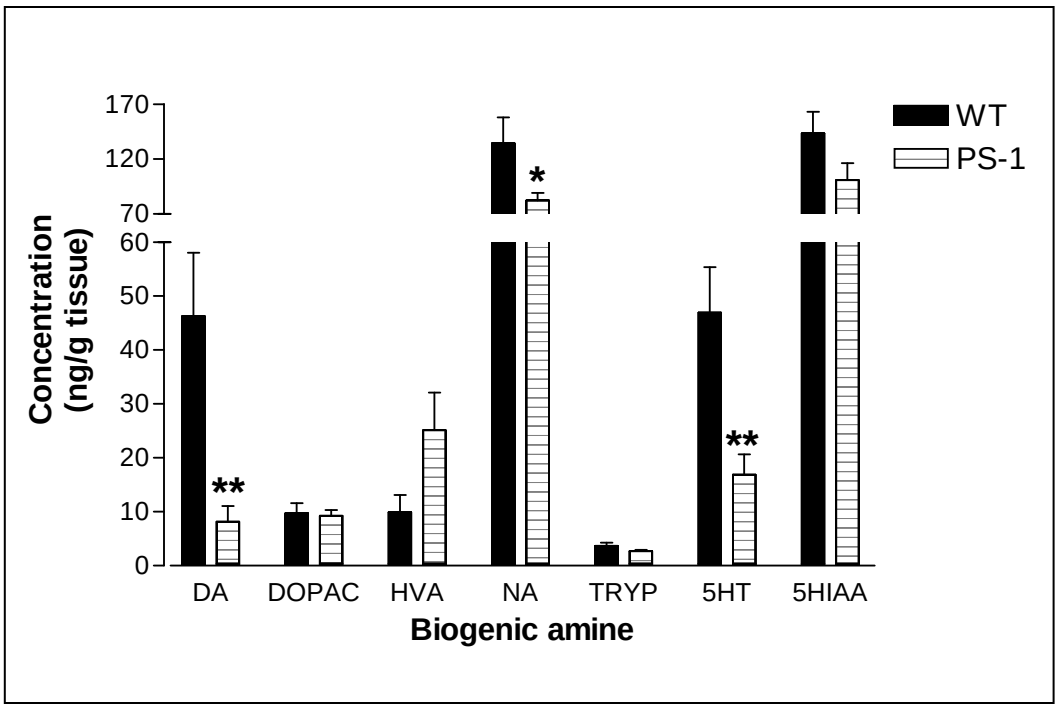

Figure 3.17b: Biogenic amine concentrations from cerebellar homogenates of WT and PS-1 mice. HPLC was performed on cerebellar homogenates of WT (black solid bars) and PS-1 (horizontal lined bars) mice and specific biogenic amine levels were measured. A significantly reduced level of DA, NA and 5-HT were found (One-tailed t-tests: *: $P<0.05$, **: $P<0.01$; n=6).

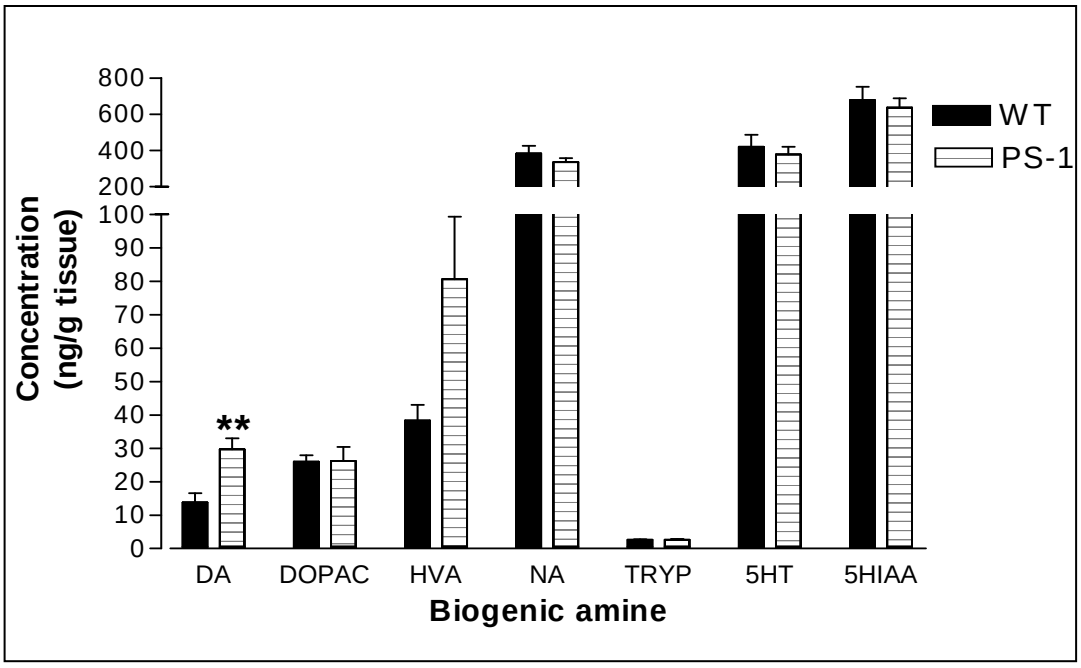

Figure 3.17c: Biogenic amine concentrations from hippocampal homogenates of WT and PS-1 mice. HPLC was performed on hippocampal homogenates of WT (black solid bars) and PS-1 (horizontal lined bars) mice and specific biogenic amine levels were measured. In comparison to WT, an increased level of the DA was found (One-tailed t-tests; **: $P<0.01$; $n=5$).

3.11.1 Endogenous MAO protein levels in the cortex

Genotyped cortex tissue from 6month old WT and transgenic PS-1 (M146V), APP (Swe) or PS-1/APP double transgenic mice were homogenized and a Western blot was carried out as outlined in section 2.2.7. Then the primary antibodies anti-MAO-A (H-70), anti-MAO-B (C-17), anti-CB-28K and anti-phospho-p38 (MAP kinase) were applied. Figure 3.18 unexpectedly shows that the full length MAO-A protein in double transgenic PS-1/APP mice is completely lost in the cortex, and between WT and PS-1 mice the MAO-A protein levels are exactly the same. Therefore the increased response of basal MAO-A in the cortex region of PS-1 mice compared to WT (Figure 3.13) is not due to increased protein levels of MAO-A. Concerning MAO-B, there are no changes observed in protein levels between WT and PS-1 mice. It is likely then that the higher basal MAO-B activity in PS-1 mice is not due to higher MAO-B protein levels since there is no drastic increase in MAO-B. For the other proteins, calbindin (a known inhibitor of Ca^{2+}) and phospho-p38 (recently found in our lab to bind and inhibit Ca^{2+} (data not shown)) they are, respectively, the same amount or not detected. So the increased MAO-A and MAO-B response to Ca^{2+} observed cannot be due to altered protein levels of either calbindin or activated p38.

3.11.2 Endogenous MAO protein levels in the cerebellum

Genotyped cerebellum tissue from 6month old WT and transgenic PS-1 (M146V), APP (Swe) or PS-1/APP double transgenic mice were then prepared and assayed in the same method as the cortex tissue in section 3.11.1. Similar results were obtained in the cerebellum as was seen in the cortex region of all mice tested (Figure 3.19). Specifically, it was found that in cerebellar tissue full-length MAO-A is lost in bigenic APP/PS-1 mice. Also this time compared to WT, PS-1 mice have a slightly smaller amount of MAO-A protein but still this illustrates that the increased MAO-A activity in PS-1 mice, found in section 3.8.2, cannot be due to increased MAO-A protein levels. MAO-B, once again, was observed to have no significant difference in protein levels between WT and PS-1 mice. Lastly in all

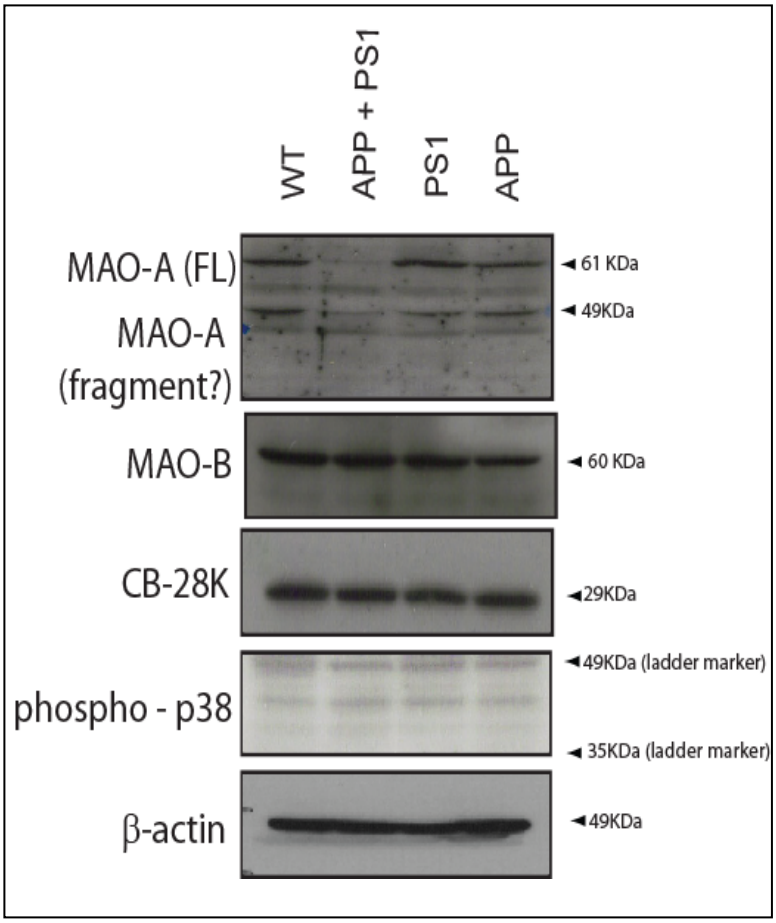

Figure 3.18: Western blot of protein levels in the cortex of 6 month old WT and transgenic PS-1 (M146V), APP (Swe) or PS-1/APP mice. MAO-A was detected with the primary antibody MAO-A (H-70), MAO-B was detected with the primary antibody MAO-B (C-17), CB-28K was detected with the primary antibody Calbindin D28k and activated p38 was detected with phospho-p38 MAP kinase antibody. Full length MAO-A protein in double transgenic PS-1/APP mice is completely lost in the cortex, and between WT and PS-1 mice the MAO-A/B protein levels are exactly the same. (n=3)

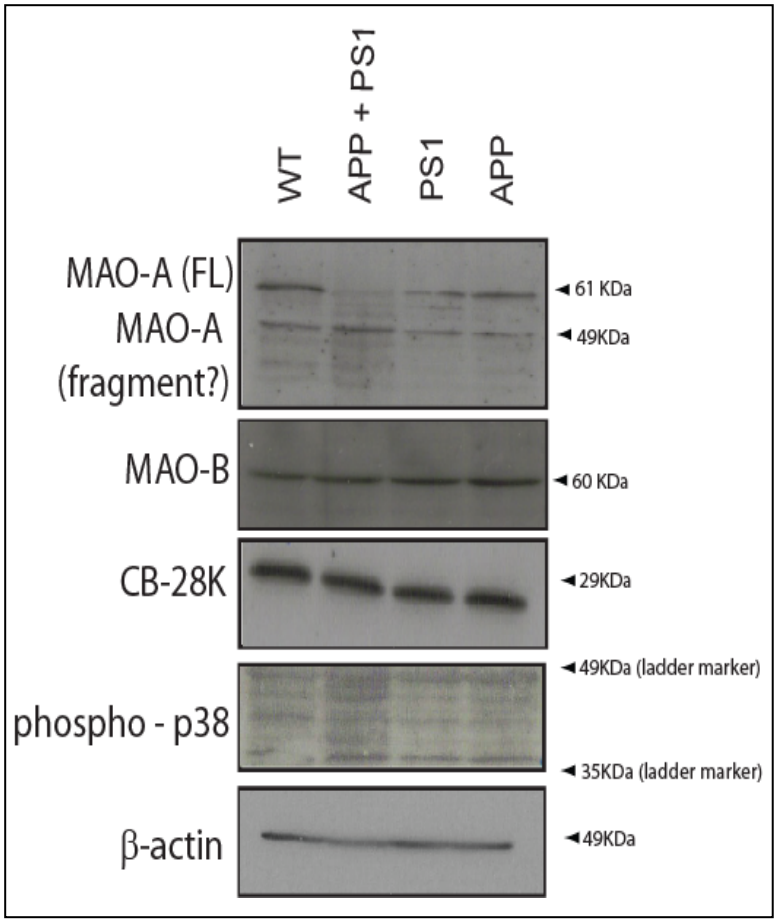

Figure 3.19: Western blot of protein levels in the cerebellum of 6 month old WT and transgenic PS-1 (M146V), APP (Swe) or PS-1/APP mice. MAO-A was detected with the primary antibody MAO-A (H-70), MAO-B was detected with the primary antibody MAO-B (C-17), CB-28K was detected with the primary antibody Calbindin D28k and activated p38 was detected with phospho-p38 MAP kinase antibody. Full-length MAO-A is lost in bigenic APP/PS-1 mice and compared to WT, PS-1 mice have a slightly smaller amount of MAO-A protein. (n=3)

mice, calbindin protein levels are unchanged and there is no activated p38 (MAPK) detected.

3.11.3 Endogenous MAO protein levels in the hippocampus

Next, I chose to look at one last region, the hippocampus, to see if the same protein amounts were also seen there. Once again, I took genotyped hippocampal tissue from 6month old WT and transgenic PS-1 (M146V), APP (Swe) or PS-1/APP double transgenic mice and prepared and assayed the tissue in the same method as described in the past two sections. Concerning MAO-B, CB-28K and activated p38, identical results were obtained in the hippocampus as was seen in the cortex and cerebellum regions of all mice tested but there are some differences in MAO-A protein levels (Figure 3.20). In the hippocampus of the double PS-1/APP transgenic mice there is only a decrease, not a complete loss, of MAO-A full length protein. Also in PS-1 mice there is a slightly smaller amount of full-length MAO-A compared to WT and a large smear of smaller bands appear around and below 49kDa.

Taken together, the activity graphs and immunoblots from the 3 brain regions show that there is an obvious modulation of MAO-A activity in the cortex and cerebellum and/or full-length protein levels all in regions by PS-1 but with respect to MAO-B, there is one PS-1 related change in activity in the cortex, no activity change in the cerebellum and all protein levels seem to be unchanged too. Combining these results with the lack of changes in MAO-B activity in the cell culture studies described previously, I then chose to focus more on characterizing specifically the PS-1 and MAO-A interaction.

3.11.4 MAO activity and biogenic amine levels in bigenic PS-1/APP mice

Preliminary data from the cortical homogenates of PS-1/APP mice show that these mice still have MAO-A and -B activity (Figure 3.21), even though there was little or no observable full-length MAO-A in these mice, but no noticeable changes in biogenic amine levels because of the large standard deviations (Figure 3.22).

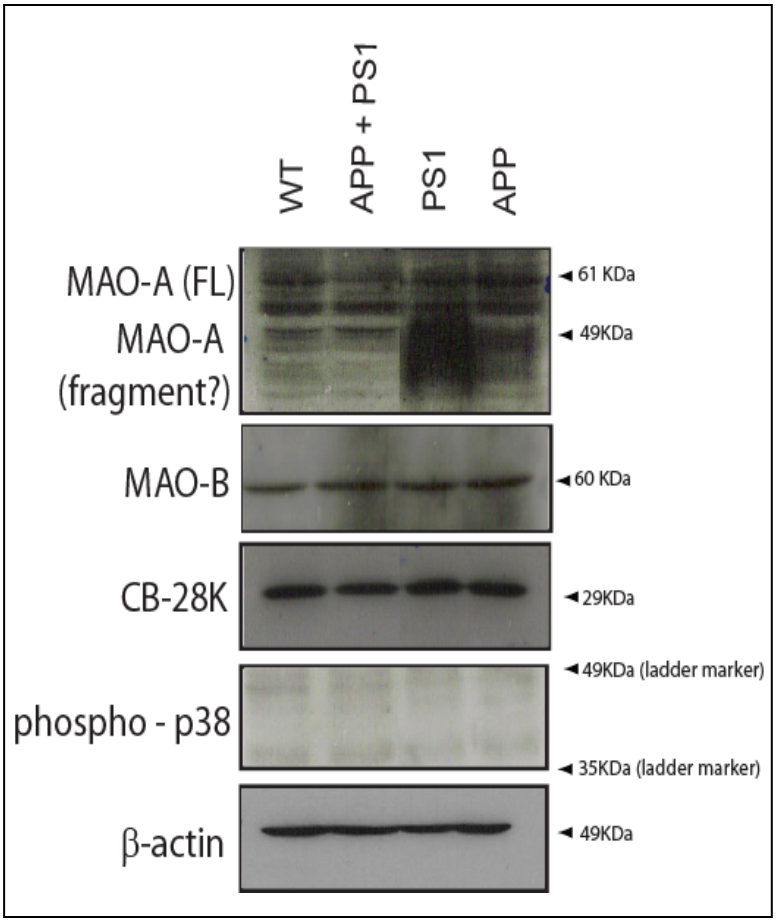

Figure 3.20: Western blot of protein levels in the hippocampus of 6 month old WT and transgenic PS-1 (M146V), APP (Swe) or PS-1/APP mice. MAO-A was detected with the primary antibody MAO-A (H-70), MAO-B was detected with the primary antibody MAO-B (C-17), CB-28K was detected with the primary antibody Calbindin D28k and activated p38 was detected with phospho-p38 MAP kinase antibody. In bigenic APP/PS-1 mice, only a decrease, not a complete loss, of MAO-A full length protein occurs. In PS-1 mice, there is a slightly smaller amount of full-length MAO-A compared to WT and a large smear of smaller bands appear around and below 49kDa. (n=3)

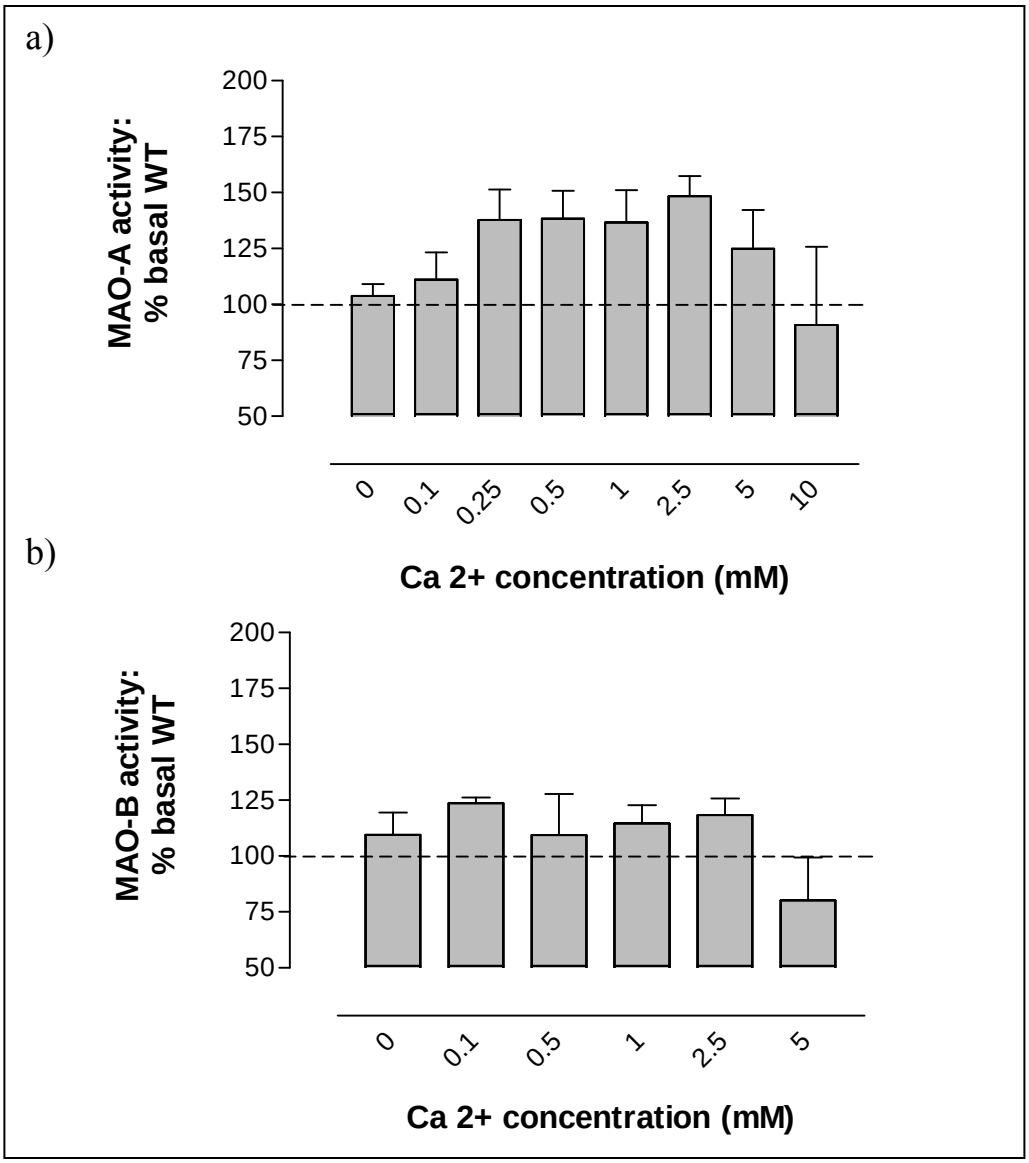

Figure 3.21: MAO and Ca^{2+} concentration-response curves from the cortex of bigenic PS-1/APP mice. a) MAO-A activity. Increasing concentrations of Ca^{2+} greatly increase MAO-A activity compared to their basal level (0 mM Ca^{2+}). b) MAO-B activity. Increasing concentrations of calcium also increase MAO-B activity compared to their basal level (0 mM), but to a lesser extent than MAO-A. (n=1).

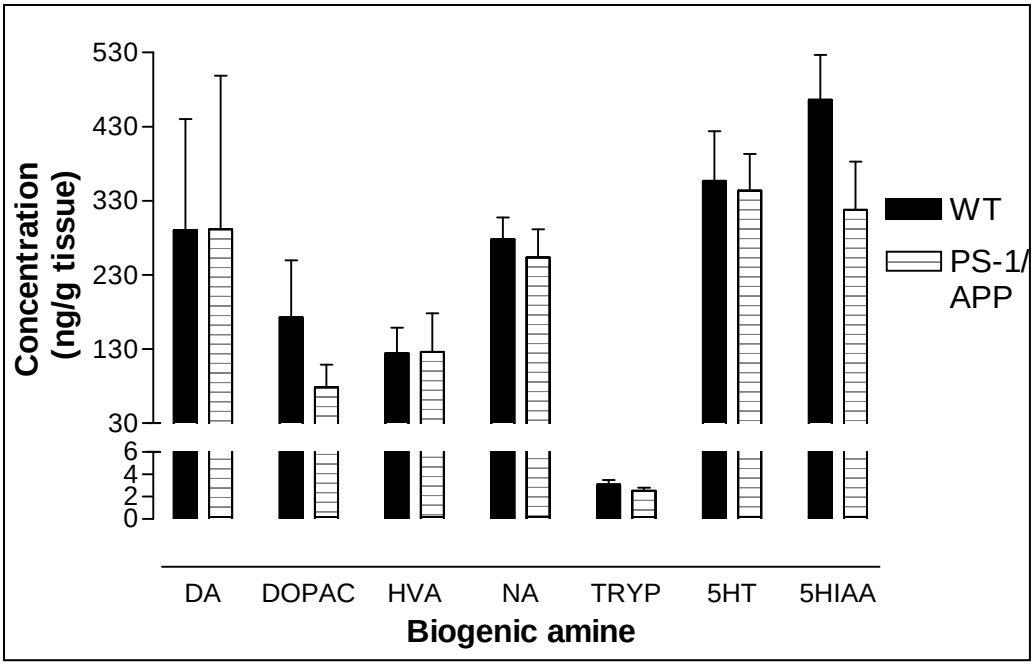

Figure 3.22: Biogenic amine concentrations from cortical homogenates of bigenic PS-1/APP mice. HPLC was performed on cortical homogenates of WT (black solid bars) and bigenic PS-1/APP (horizontal lined bars) mice and specific biogenic amine levels were measured. There was no obvious change in any biogenic amine (n=6).

3.12 Co-transfection of PS-1 and MAO-A DNA results in the disappearance of full length MAO-A protein

So far, from my results, I have found that both PS-1 and Ca^{2+} are somehow altering MAO-A protein and activity. Additionally, my results show that only some of the PS-1 constructs affect MAO-A by altering Ca^{2+} levels therefore the interaction between PS-1 and MAO-A may not always be indirect but sometimes direct. To examine this hypothesis I first looked at three different cell lines, which are the HT-22, PC12 and HEK 293A cell lines (more information about these cell lines can be found in section 2.1.4). Previously we had only observed endogenous MAO so over-expressed PS-1 and MAO should have a more pronounced effect. Thus, in each cell line I co-transfected one of the five PS-1 constructs and the MAO-A construct. The empty vector controls, pcDNA3.1 and pCMV/myc/mito, were also transfected in each cell line. All cells were transfected for 24 hours and the detailed procedure can be found in section 2.2.5. After a Western blot was carried out (outlined in section 2.2.7) and the primary antibodies anti-MAO-A (H-70 and T-19) and anti-PS-1 (MAB5232) were used to measure any changes in protein amounts.

In both the HT-22 (Figure 3.23) and HEK 293A (Figure 3.24) cells there is, for the most part, the same effect. Compared to HT-22 and HEK 293A cells co-transfected with PS-1 WT, the cells expressing PS-1 D257A have a decreased amount of full length MAO-A protein and the cells expressing PS-1 Y115H have very little full length MAO-A protein. In cells expressing the PS-1 ΔEx9 protein there is no change (HT-22 cells) or a very slight increase (HEK 293A) in full length MAO-A protein compared to cells expressing PS-1 WT. Lastly, the cells expressing the PS-1 M146V protein seemed to have an increase in MAO-A full length protein. Surprisingly, in HEK 293A cells the N-terminal MAO-A antibody (T-19) seems to detect an N-terminal fragment around 40 kDa in HEK cells expressing the PS-1 Y115H protein. PC12 cells on the other hand, seem to have the same MAO-A protein amount in cells expressing the PS-1 D257A and ΔEx9 proteins compared to PS-1 WT (Figure 3.25). Also in these cells the PS-1 Y115H construct decreased the full length MAO-A protein less than what was seen in the cell lines HT-22

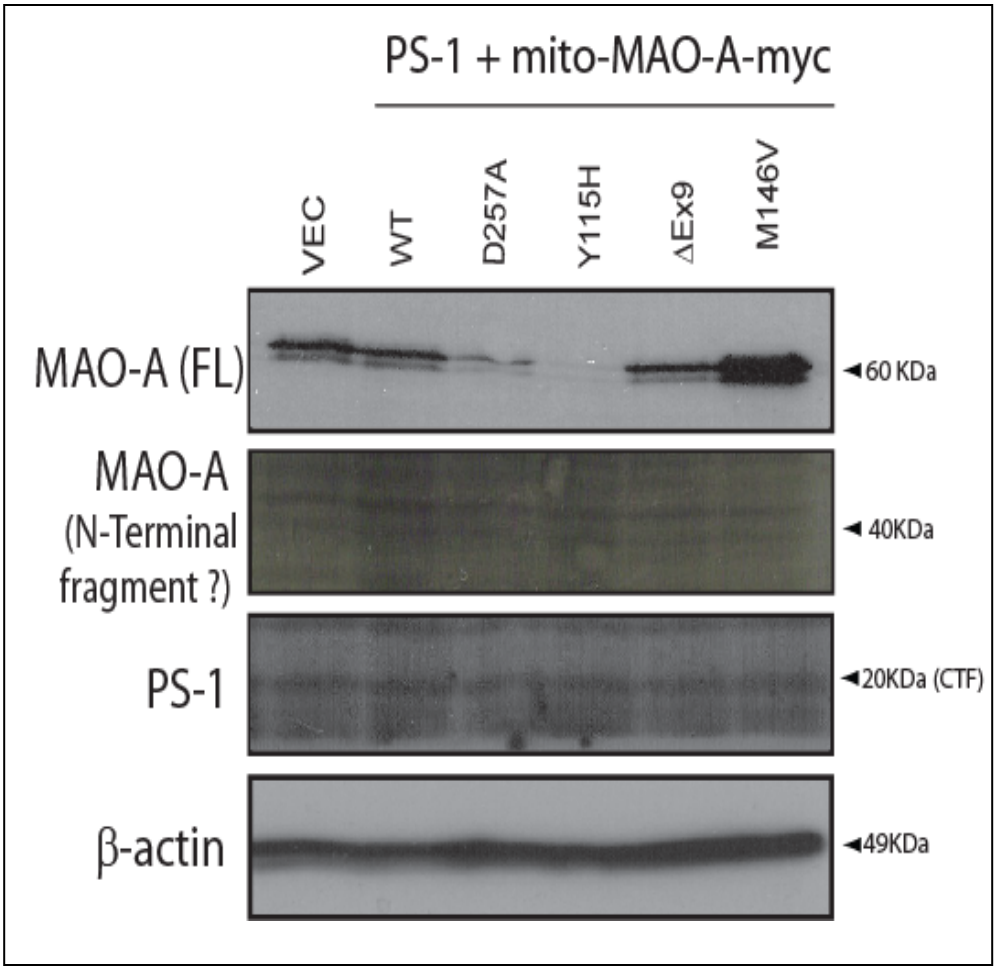

Figure 3.23: Western blot of 24 hour co-transfection of PS-1 and MAO-A cDNA in HT-22 cells. MAO-A was detected with the primary antibody MAO-A (H-70) and the primary antibody MAO-A (T-19). PS-1 was detected with the primary antibody PS-1. Cells expressing PS-1 D257A have a decreased amount of full length MAO-A protein and the cells expressing PS-1 Y115H have very little full length MAO-A protein, while cells expressing the PS-1 M146V protein seemed to have an increase in MAO-A full length protein. (n=1)

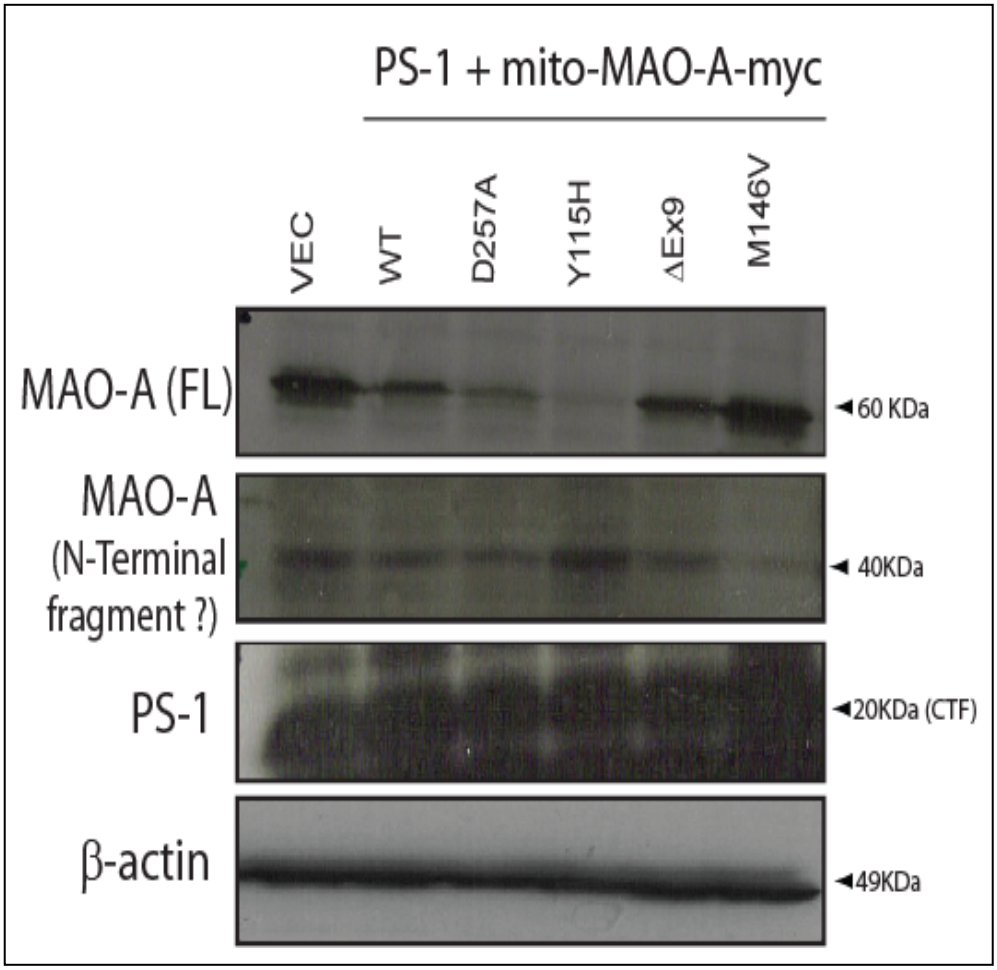

Figure 3.24: Western blot of 24 hour co-transfection of PS-1 and MAO-A DNA in HEK 293 cells. MAO-A was detected with the primary antibody MAO-A (H-70) and the primary antibody MAO-A (T-19). PS-1 was detected with the primary antibody PS-1. Cells expressing PS-1 D257A have a decreased amount of full length MAO-A protein and the cells expressing PS-1 Y115H have very little full length MAO-A protein, while cells expressing the PS-1 ΔEx9 and M146V protein seemed to have an increase in MAO-A full length protein. Also there seems to be an N-terminal fragment around 40 kDa in HEK cells expressing the PS-1 Y115H protein. (n=1)

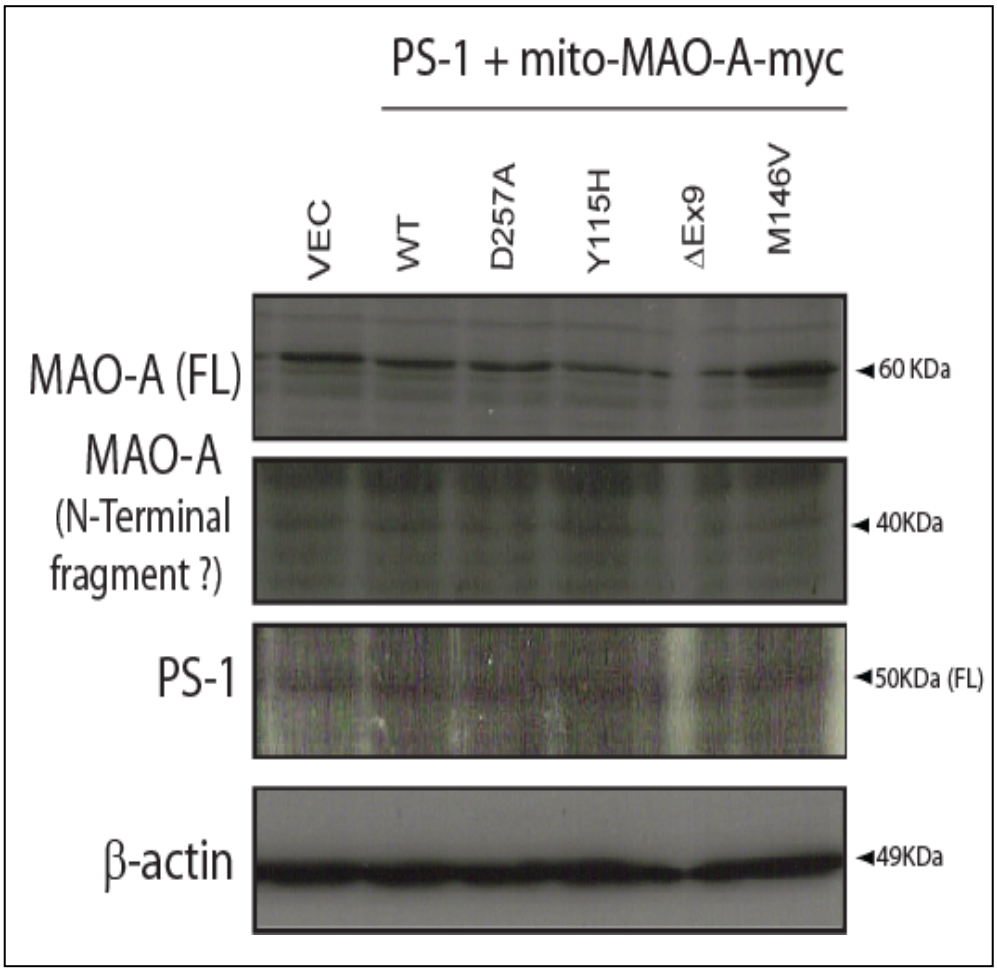

Figure 3.25: Western blot of 24 hour co-transfection of PS-1 and MAO-A DNA in PC12 cells. MAO-A was detected with the primary antibody MAO-A (H-70) and the primary antibody MAO-A (T-19). PS-1 was detected with the primary antibody PS-1. Cells expressing the PS-1 Y115H construct only decrease the full length MAO-A protein and the same increase in full length MAO-A protein, seen in HT-22 and HEK 293 cells expressing the PS-1 M14V protein, is observed. (n=1)

and HEK 293A but the same increase in full length MAO-A protein, seen in HT-22 and HEK 293A cells expressing the PS-1 M14V protein, is observed.

One conclusion from these data is that the PS-1 protein has a dual effect toward MAO-A in that it can indirectly affect MAO-A through its sensitivity to Ca^{2+} and directly affect MAO-A by reducing its full length form.

3.13 Different PS-1 constructs and MAO physically interact to various extents

With possible MAO-A fragment proteins found in hippocampal tissue (Figure 3.20) and now in a cell line (Figure 3.24), it is highly likely that MAO, or at the very least, MAO-A is a novel substrate of PS-1. If this is true, then the two proteins must be able to directly bind to each other in order for this cleavage to occur. The extent of this binding can be detected by immunoprecipitation. All five PS-1 DNA and the empty vector pcDNA3.1 were transfected into HT-22 cells for 24 hours. Then the PS-1 proteins were pulled down (immunoprecipitation protocol is in section 2.2.6) and MAO-A and MAO-B proteins were detected through Western blot (protocol is in section 2.2.7). Figure 3.26 shows that PS-1 WT, Y115H, ΔEx9 and M146V all interact with MAO-A to the same extent but PS-1 D257A interacts very little. Concerning MAO-B, all of the PS-1 DNA interact with this isoform very little except for PS-1 Y115H. This result is intriguing because in the previous section the PS-1 Y115H mutant was the only protein which could cause the complete loss of full length MAO-A protein. So this stronger interaction between PS-1 Y115H and MAO, as found by this immunoprecipitation assay, could be one reason as to why this mutant can cause a loss of full-length MAO-A.

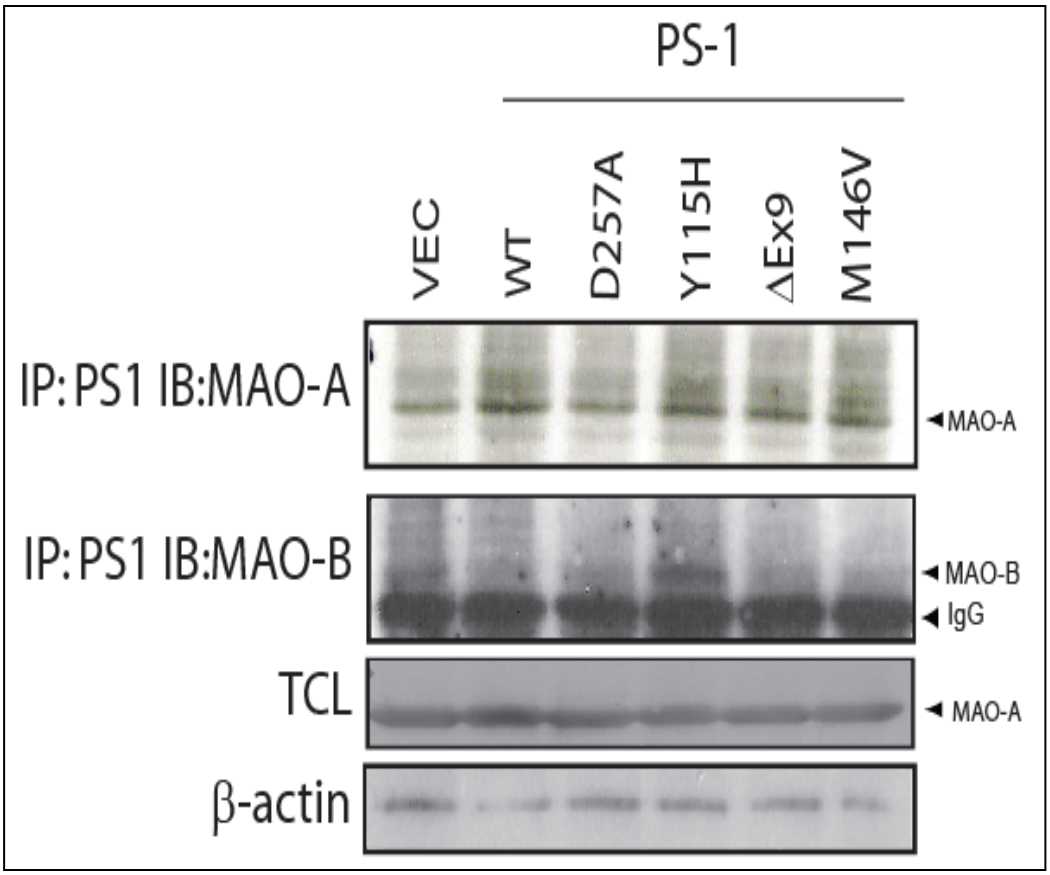

Figure 3.26: Western blot of Immunoprecipitation assay between PS-1 and MAO-A in HT-22 cells. PS-1 proteins were expressed in HT-22 cells for 24 hours then PS-1 was pulled down, and MAO-A and MAO-B proteins were detected. MAO-A was detected with the primary antibody MAO-A (H-70) and MAO-B was detected with the primary antibody MAO-B (C-17). PS-1 WT, Y115H, ΔEx9 and M146V all interact with MAO-A to the same degree and PS-1 D257A interacts very litttle. All of the PS-1 proteins interacted very little with the B isoform except for PS-1 Y115H. (n=3)

3.14 DAPT, a γ-secretase inhibitor, can increase MAO-A activity

3.14.1 DAPT-treated HT-22 cells overexpressing PS-1 have an increased MAO-A activity

If PS-1 is mediating the loss of full length MAO-A protein (by a cleavage reaction), then MAO-A, as a novel substrate for PS-1/γ-secretase, must bind to the PS-1 substrate binding site and then be transferred to the catalytically active site to be cleaved. To test this hypothesis I used DAPT, a chemical that is hypothesized to inhibit γ-secretase activity by preventing the passage of the substrate from PS-1's binding site to its catalytic site.

Briefly, HT-22 cells were transfected with the pcDNA3.1 vector, PS-1 WT and M146V DNA for 24 hours according to the transfection protocol in section 2.2.5. After, the cells, radiolabelled serotonin substrate solution and DAPT solutions (with concentraton ranging from 100 nM-1 mM) were prepared and the MAO-A activity assay was carried out (procedure is in section 2.2.8). The graph in Figure 3.27 shows that the cells transfected with the pcDNA3.1 and PS-1 WT constructs have a similar MAO-A activity response to the increasing DAPT concentrations. That is, they seem to peak at around 10 nM then decrease and peak again at 10 μM. The cells expressing the PS-1 M146V protein have an increase in MAO-A activity with increases in the DAPT concentration and this increase peaks at around 1 μM. At all concentrations though, except at 10 nM, the PS-1 M146V expressing cells have the higher MAO-A activity.

3.14.2 DAPT-treated transgenic PS-1 mouse cortical homogenates have an increased MAO-A activity

We next took the cortex tissue of WT and transgenic PS-1 (M146V) 6 month old mice and tested the endogenous MAO-A activity after 20 min of DAPT treatment. All of the tissue, radiolabelled serotonin substrate solution and DAPT solutions were prepared in a similar manner, as in section 3.14.1, and the MAO-A activity assay procedure was the same too.

With the 6 month old cortical homogenates we found that the MAO-A activity decreases with increasing concentrations of DAPT in the WT mice, and the PS-1 cortical homogenates have the exact opposite effect (Figure 3.28). As the DAPT concentrations increase, the MAO-A activity in the PS-1 mice tissue increase and peak at around 10 μM. Therefore, in PS-1 transfected cells and now in PS-1 transgenic mice tissue there is a consistent increase in MAO-A activity, with increasing concentrations of DAPT. Because of the short treatment with DAPT, this increase cannot be due to protein synthesis or post-translational processing but is probably be due to a possible competitive interaction between these three molecules.

3.15 PS-1 transgenic mice have a slightly inferior short term memory

To determine if PS-1 (M146V) transgenic mice had any deficits in short-term memory the Water maze test was carried out. After one day of training, according to the method described in section 2.2.12, each mouse was placed in the pool only at the South direction and the swimming pattern was recorded for 1 min. Figure 3.29 illustrates that PS-1 mice do not perform as well as WT mice on the test day. When frequency of entrance was measured, PS-1 mice (horizontal lined bars) enter the hidden platform area less than WT mice (black solid bars) mice, and spent a considerably larger time entering the corresponding platform area in the southeast quadrant. When duration of time spent in each platform area was measured, PS-1 mice (horizontal lined bars) swam mostly in the southeast and southwest quadrant platform areas while the WT mice (black solid bars) swam mostly in the northwest quadrant.

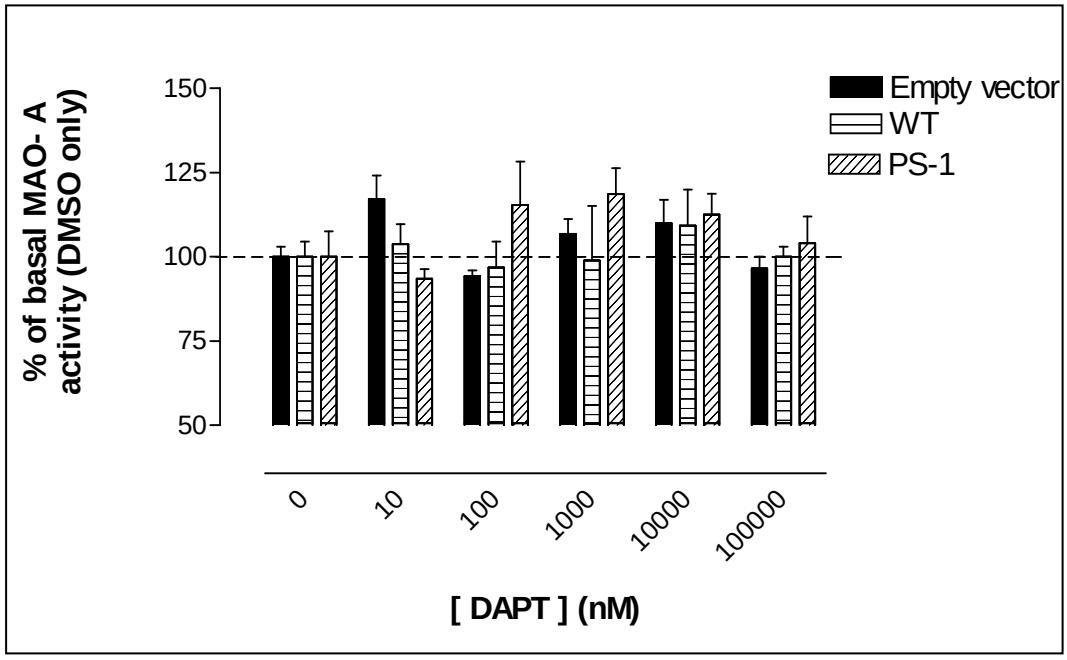

Figure 3.27: MAO-A and DAPT concentration-response curves from HT-22 cells transfected with pcDNA3.1, PS-1 WT and M146V. Endogenous MAO-A activity was measured in HT-22 cells transfected for 24 hours with either the pcDNA3.1 empty vector (control) (black solid bars), PS-1 WT (horizontal lined bars) or PS-1 M146V (diagonal lined bars) constructs, in the presence of DAPT (20 min treatment) (n=3). Vector and WT expressing cells have a peak MAO-A activity around 10 nM then decrease and peak again at 10 μM. PS-1 M146V expressing cells increase in MAO-A activity with increases in DAPT concentration and this increase peaks at around 1 μM.

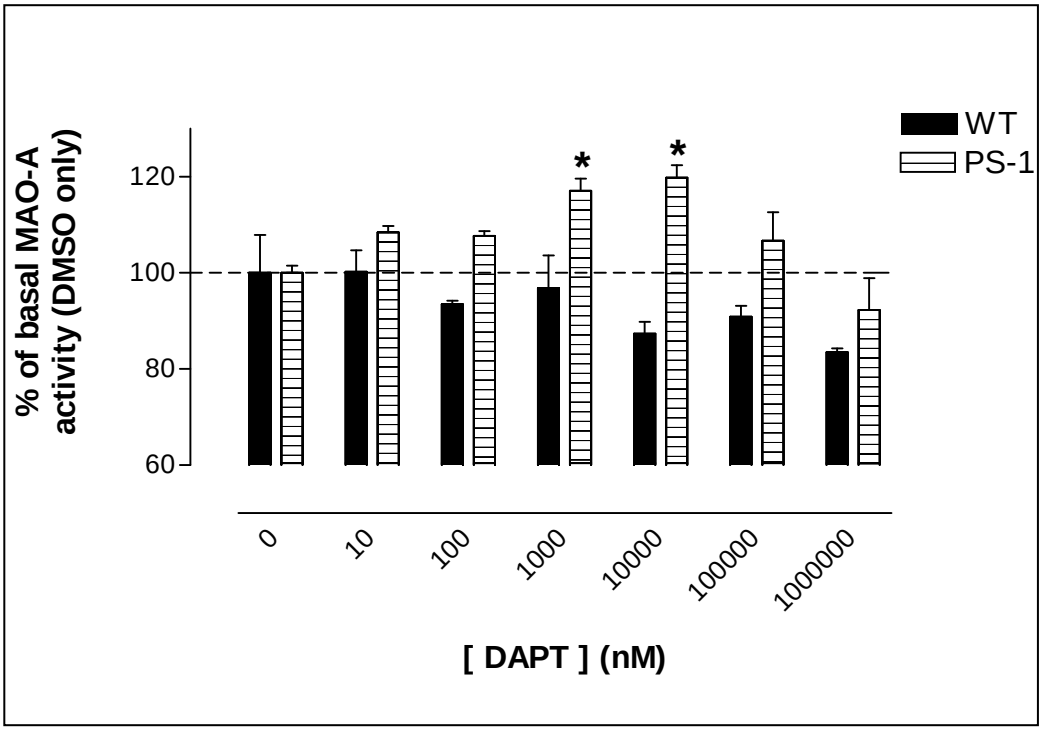

Figure 3.28: MAO-A and DAPT concentration-response curves from PS-1 WT and M146V cortical tissue homogenates. Endogenous MAO-A activity was measured in cortical homogenates from 6 month old WT (black solid bars) or PS-1 (M146V) (horizontal lined bars) mice, in the presence of DAPT (20 min treatment). PS-1 cortical homogenates have a consistently higher, and sometimes significant increase, in MAO-A activity compared to WT cortical homogenates, with increasing concentrations of DAPT (Two-way ANOVA and Bonferroni's *post hoc* test were used; $P<0.05$; n=3).

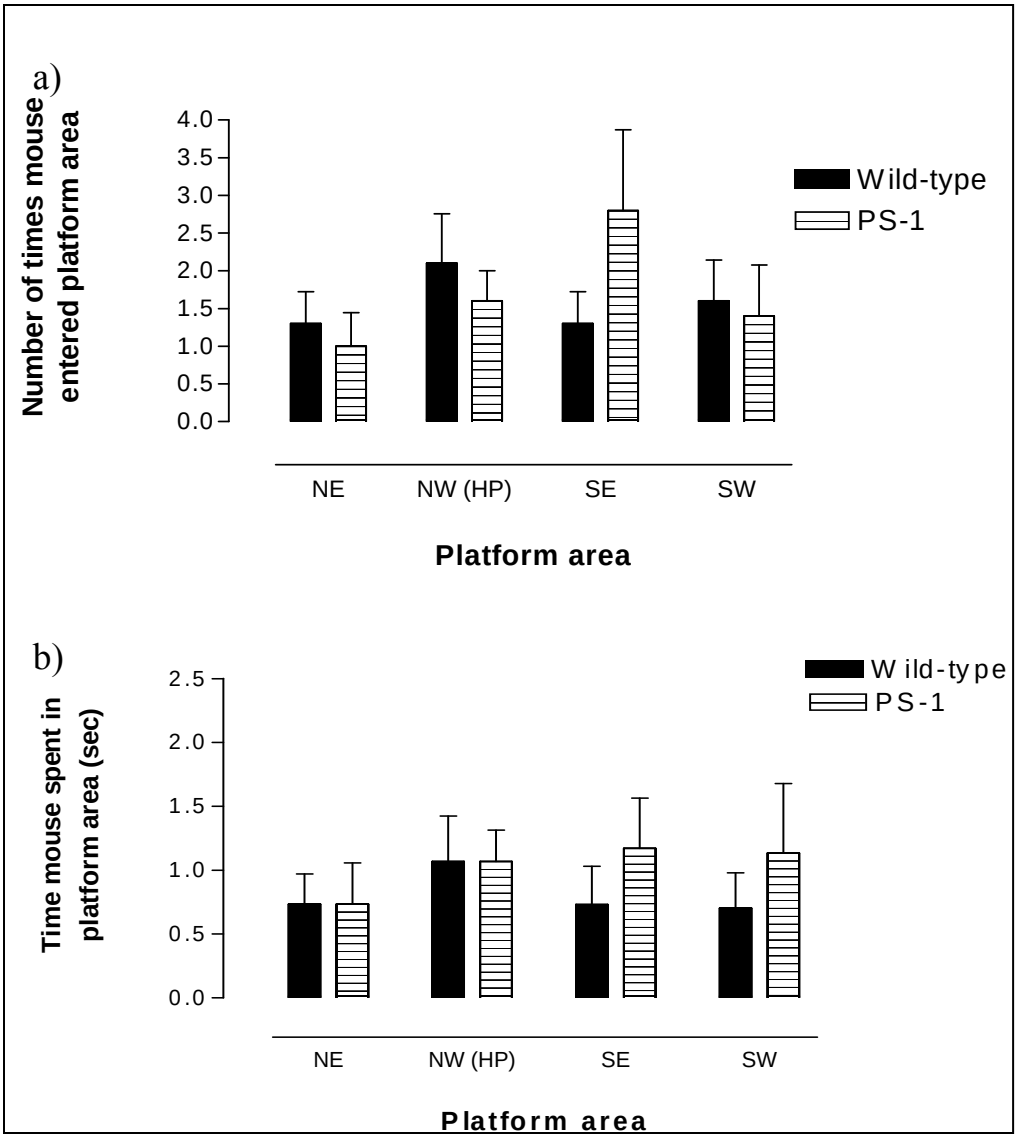

Figure 3.29: Behaviour data for WT and PS-1 (M146V) mice. After one day of training each mouse was placed in the "South" part of the pool (water maze) and their swimming pattern was recorded for 1 min. a) PS-1 mice (horizontal lined bars) enter the hidden platform (HP) area (in NorthWest (NW) quadrant) marginally less than WT mice (black solid bars) mice, and spent a considerably larger time entering the corresponding platform area in the SouthEast (SE) quadrant. b) PS-1 mice (horizontal lined bars) swam mostly in the SE and SW quadrants while the WT mice (black solid bars) swam mostly in the NW quadrant. (n=5)

4 DISCUSSION

4.1 Indirect effects of PS-1

Aside from cancer and cardiovascular disease, AD is one of the most prevalent disorders affecting the elderly (1, 2). The human life span is increasing making this disease much more prominent and widespread than ever before, yet the exact mechanisms involved in AD-related pathology still remain unclear. Looking at cellular models, including familial AD models, which reflect the more aggressive forms of AD (*cf.* sporadic AD), is of utmost importance to understanding how the disease progresses and to developing better treatments. Moreover because clinical symptoms in AD occur 20-30 years after neurodegeneration begins (3), prophylactic measures taken before or during the neurodegeneration phase may be a better approach than attempting to reverse an already existing AD pathology. This study was undertaken to examine one of these neurodegenerative pathways in the brain. Based on the literature and previous work from our laboratory, a hypothesis suggesting a relation between PS-1, MAO and Ca^{2+} in AD was forwarded.

The expression of PS-1 in the mitochondrial-enriched fraction (which contains the majority of the cell's MAO) was confirmed (13, 14). Radioenzymatic MAO assays revealed that in comparison to WT PS-1, familial AD-related PS-1 mutations (e.g. bearing Y115H, ΔEx9 and M146V mutations) cause an increase in basal and/or Ca^{2+}-sensitive MAO-A activity in the hippocampal-derived HT-22 cells. These effects were most prominent in cells expressing the more aggressive PS-1 Y115H and ΔEx9 mutants. In contrast to MAO-A, only basal MAO-B activity in PS-1 ΔEx9-expressing cells was higher and there was no sensitivity to Ca^{2+} in cells expressing any of the three familial AD mutations. This Ca^{2+} specificity for the

MAO-A isoform was also observed by Kosenko *et al* (110) in non-synaptic mitochondria of rat forebrain and in HT-22 cells by Cao *et al* (111). Co-expression of the PS-1 proteins with CB-28K revealed mutant-specific effects on MAO-A activities. For example, the vector- and PS-1 Y115H-expressing cells had their previous Ca^{2+}-sensitive MAO-A response blocked, but this was less evident in PS-1 ΔEx9-expressing cells. The PS-1 M146V (100, 103, 124, 126) and PS-1 ΔEx9 (102, 118) proteins are known to affect Ca^{2+} levels; perhaps the persistence of the effect of PS-1 ΔEx9 on MAO-A activity in the presence of CB-28K could be due to an increase in intracellular Ca^{2+} levels beyond the capacity of overexpressed CB-28K. Examination of free intracellular Ca^{2+}, using the Ca^{2+}-specific FLUO-3AM, revealed an unexpected decrease in Fluo-3AM fluorescence in cells expressing the PS-1 ΔEx9 protein and no other obvious changes with the other PS-1 mutated proteins. Higher magnification revealed changes in the distribution of Ca^{2+} throughout the cell; for example, cells expressing the PS-1 Y115H protein seemed to have more Ca^{2+} concentrated around the nuclear membrane and cells expressing the PS-1 D257A protein had a diffuse Ca^{2+} signal- including throughout the nucleus. The differences observed between the present and published data (wherein intracellular Ca^{2+} increases are associated with familial AD-related PS-1 proteins) could be attributed to the sensitivity of the reagent we used and/or because of our assay method, which did not allow for the proper quantitation of changes. If quantitative methods were used, subtle changes in HT-22 cell Ca^{2+} between the PS-1 constructs might be revealed. Yet, Smith *et al* (104) have also observed that dissociated neurons in culture are not able to evoke increases in intracellular Ca^{2+} unless first depolarized. Thus, future experiments are required to confirm the effect of the familial AD-related PS-1 constructs used herein on altering Ca^{2+} levels in HT-22 cells.

To determine if the cellular effects of PS-1 proteins could be even more apparent in constitutively expressing transgenic (T*g*) animals, we used wild-type and PS-1 transgenic mice brains (these mice over-express the PS-1 M146V protein). We chose to use 6 month-old mice as Aβ levels are non-existent at this time point (in fact, these PS-1 mice do not develop appreciable Aβ deposits even at 18 months of age (130)); all observed effects are then assumed to be APP/Aβ-independent. The

cortex, hippocampus and cerebellum represent three brain regions affected during AD. Cortical homogenates from PS-1 mice had increased basal MAO-A and MAO-B activities compared to age-matched WT littermates. These results reflect the findings of Sparks *et al* (94) who used specific cortical areas from human AD brains. Moreover, in the presence of increasing concentrations of Ca^{2+} there was approximately a 25% increase in sensitivity of both MAO isoforms to Ca^{2+}. This increased MAO activity in the cortex would be expected to affect the levels of aminergic substrate of the enzyme (Figure 4.1 illustrates the MAO biogenic amine substrates that should be affected). Indeed, levels of DA had a tendency to decrease in PS-1 cortices, but the levels of NA and 5-HT did not. In PS-1 T*g* mouse cerebellar extracts there was an increase in basal and Ca^{2+}-sensitive MAO-A activity (approximately 12% increase), but MAO-B remained unaltered. In corresponding homogenates there was a significant decrease in DA, NA and 5-HT and increases in the DA metabolite HVA. The decreased 5-HIAA could be indicative of lower 5-HT synthesis (reflecting the tendency for the lower availability of tryptophan, the precursor for 5-HT) in PS-1 T*g* mouse samples. Even though the cerebellum had only an increased MAO-A activity, as opposed to the cortex which had increases in both MAO-A and MAO-B, there seems to be more of an effect occurring in PS-1 T*g* mice within this area. This occurrence could be attributed to the fact that basal MAO-A activity is increased approximately 25% in the cerebellum compared to WT, while in the cortex basal activity was only increased by approximately 12% compared to WT. Combining this with the fact that both brain regions have Ca^{2+}-sensitive increases in MAO-A activity and that MAO-A is more predominant in noradrenergic neurons (59), then it would not be unreasonable to assume that MAO-A substrates could presumably be affected more in the cerebellum of PS-1 T*g* mice. Although MAO activity was not determined in hippocampal extracts because of the limited quantity of tissue, analysis of biogenic amine levels revealed equal or larger amounts of DOPAC and HVA, perhaps reflecting the significantly higher levels of DA in this tissue.

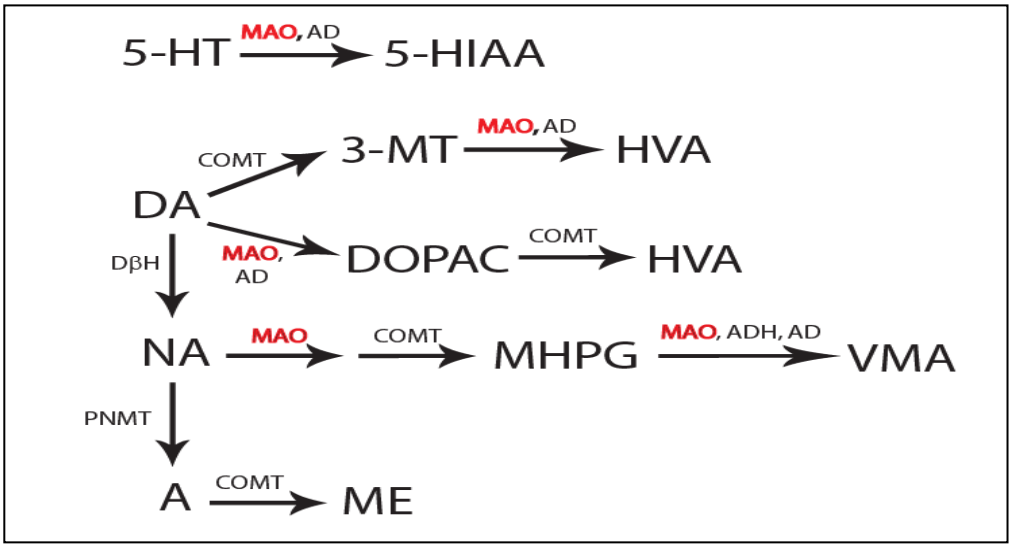

Figure 4.1: Biogenic amine metabolism. MAO catalyzed biogenic amine metabolism is noted in red. (Enzymes abbreviations are AD (aldehyde dehydrogenase), ADH (alcohol dehydrogenase), COMT (catechol-*o*-methyl transferase), DβH (dopamine β-hydroxylase), MAO (monamine oxidase), PNMT (phenylethanolamine-*N*-methyltransferase); amine abbreviations are 3-MT (3-methoxytyramine), 5-HIAA (5-hydroxyindole acetic acid), 5-HT (serotonin), A (adrenaline), DA (dopamine), DOPAC (3, 4-dihydroxyphenylacetic acid), HVA (homovanillic acid), MHPG (3-Methoxy-4-hydroxyphenylethyleneglycol), ME (Metanephrine), NA (noradrenaline), and VMA (vanillylmandelic acid).

Even though the exact relationship between specific familial AD PS-1 mutations and Ca^{2+} remains unclear, it is apparent that the individual PS-1 proteins do affect MAO-A (and MAO-B) basal and Ca^{2+}-sensitive activities, both in cell cultures and *ex vivo*, thus indicating that the effects of PS-1 proteins on MAO are not simply restricted to their ability to affect Ca^{2+} levels.

4.2 Direct PS-1 effects

The differences in MAO activity between WT and PS-1 T*g* mice and between different brain regions could be indicating differences in protein levels. This, however, did not appear to be the case as cortical and cerebellar protein extracts from PS-1 T*g* mice have similar, or even slightly less, respectively, MAO-A protein levels than did WT mouse extracts. MAO-B protein levels were the same in PS-1 T*g* and WT mice. Therefore, the increased MAO activity in PS-1 T*g* mice cannot be attributed to corresponding increases in MAO protein levels. Interestingly, examination of protein levels in hippocampal extracts revealed a slight decrease in full-length MAO-A proteins levels and an increase in MAO-A protein fragments migrating at approximately 49 kDa. Even more surprising was that in all three brain regions full length MAO-A was almost completely lost in bigenic APP/PS-1 mice (a commonly used model for AD-related pathology). Therefore it is possible that mutated PS-1 proteins are able to cleave full-length MAO-A proteins through proteolytic processing.

As the regionally-specific effects in PS-1 T*g* mice brains was only observed with the Ca^{2+}-sensitive component of MAO activity, the expression levels of two proteins known to affect either PS-1 function and/or MAO function were examined. These were calbindin (which was shown by Guo *et al* (124) to suppress any PS-1-mediated toxicity and by Cao *et al* (111) to inhibit MAO-A activity) and activated p38 MAPK (which was recently found in our laboratory to phosphorylate MAO-A and to inhibit Ca^{2+}-sensitive MAO-A activity). Although the expression levels of both proteins were not detectably different between WT and PS-1 brain extracts,

their influence on MAO-A activity *in vivo* can not be conclusively excluded; for example, their influence might have occurred at a much earlier time (*note*, the animals tested were already six months of age) or their subcellular distribution, and hence their influence, might have changed, although this would not be readily detectable by western blot analysis.

The observation that MAO-A protein could be cleaved in PS-1 T*g* mouse brain was very exciting as this would be the first time that this would have been observed. To determine if this could be reproduced in cell cultures, a peripheral cell line, HEK 293A, and two neuronal cell lines, HT-22 and PC12, were used. Co-expression of MAO-A with our original five PS-1 constructs revealed that the overexpression of the PS-1 Y115H mutant resulted in an almost complete loss of full length MAO-A in HT-22 and HEK 293A cells; MAO-A was only modestly diminished in PC12 cells. This loss of full-length MAO-A was not accompanied by a loss of MAO-A activity, suggesting that it is not the full length MAO-A species that is the active species (or not exclusively). In HEK 293A cells this loss was accompanied by the conspicuous appearance of an N-terminal fragment. It is interesting to note that the catalytically inactive PS-1 D257A protein could also reduce full-length MAO-A (although to a lesser extent than the PS-1 Y115H mutant) in HT-22 and HEK 293A cells (which was reflected in a loss in MAO-A activity).

The reduced MAO-A full-length protein found in various PS-1 M146V T*g* mouse brain regions and in three different cell lines suggest that MAO-A might be a putative substrate of PS-1. If this is true, then the two proteins must associate in order for this cleavage to occur. Immunoprecipitation of overexpressed PS-1 proteins revealed that the three familial AD-related mutants (Y115H, ΔEx9 and M146V) and PS-1 WT all directly interacted with MAO-A; the PS-1 Y115H protein was the only one to also associate strongly with MAO-B. As the PS-1 D257A protein associated very weekly with either of the MAO isoforms, it suggests that it either binds very weakly with MAO proteins or that the PS-1 and MAO association is not direct, but rather in a larger complex. This possibility is reasonable as previous work from our laboratory indicates that the MAO-A protein exists in a

large molecular weight complex (> 200 kDa), which could include several proteins including PS-1/γ-secretase.

If PS-1 is proteolytically processing the MAO-A protein, then MAO-A must bind to the PS-1 substrate binding site. Both tissue extracts and cell culture extracts were incubated with DAPT, a chemical that is believed to allosterically or directly modulate γ-secretase activity by preventing the passage of substrate from PS-1's binding site to its catalytic site (131). DAPT treatment consistently increased MAO-A activity in PS-1 M146V-transfected cells and in PS-1 M146V T*g* mice cortical homogenates, in a DAPT concentration-dependent manner. As this occurred *in vitro* (with a maximum incubation time of 10 min), the increase in MAO-A activity can not be the result of either *de novo* protein synthesis or post-translational processing. A more acceptable explanation is that DAPT is acting as a competitive antagonist. In other words, DAPT is competing with MAO-A for access to the PS-1 binding site and releasing MAO-A from the PS-1/MAO-A complex. The subsequent increase in MAO-A activity suggests that the association between PS-1 and MAO-A inhibits MAO-A activity. If this is true, then this would represent a novel endogenous means of regulating MAO-A activity.

The potential clinical relevance of this work needs to be addressed. While the implications to AD and related neurodegenerative diseases are obvious, this work also provides a basis for the depression that is often associated with AD. MAO-A is known to play a role in several mental disorders (132) and relatively modest changes in MAO-A activity/function can have important neuropsychiatric consequences as demonstrated by the fact a 34% increase in [^{11}C]-harmine-labeled MAO-A is observed in brains of untreated depressed patients compared to controls, yet MAO-A appears to be the major contributor to neurotransmitter metabolism in these same patients (133). Furthermore, and perhaps most relevant to the present work, depression might promote cognitive impairment and be a risk factor for AD (134). Perhaps subtle changes in PS-1 function that might not be sufficient to promote aberrant APP processing to the toxic Aβ peptide and any AD-related pathology, could affect MAO function (and its sensitivity to Ca^{2+}). This, in turn, could predispose to depression not only in the sub-clinical AD population, but perhaps

more importantly, could also predispose to depression in the general psychiatric population itself. Thus, a simple genetic screening for PS-1 mutations might be useful for AD-related neurodegeneration as well as for other MAO-related psychiatric disorders, including depression.

Taken together, this thesis work provides the groundwork for a relationship between PS-1 and MAO-A function. Specifically, PS-1 (i) can indirectly affect MAO-A through its sensitivity to Ca^{2+}, and (ii) can directly affect MAO-A by a possible PS-1/γ-secretase-mediated proteolytic event. The latter not only suggests that MAO-A is a novel substrate for PS-1/γ-secretase, but that the association between PS-1 and MAO-A seems to inhibit MAO-A activity. If PS-1 is mutated, such as in familial AD, then it increases its tendency to cleave MAO-A into smaller (active?) fragments.

In summary, from all our experiments, we conclude that:

1) PS-1 is able to alter intracellular Ca^{2+} levels and PS-1 Y115H and PS-1 D257A may also be involved in altering Ca^{2+} distribution.
2) In cells, the PS-1 mutations, particularly the Y115H and ΔEx9 variants, increase basal and Ca^{2+}-sensitive MAO-A activities. The Ps-1 M146V mutation specifically affects Ca^{2+}-sensitive MAO activity. Only the effects of PS-1 Y115H are calbindin-sensitive.
3) In transgenic mice, expressing the PS-1 M146V mutant protein, there is an increase in basal and Ca^{2+}-sensitive MAO-A (cerebellum>cortex). Cortical MAO-B activity appears to respond to Ca^{2+} in these same mice.
4) Full-length MAO-A is lost in cells co-expressing PS-1 Y115H and MAO-A. MAO-A fragments are evident in the hippocampus of PS-1 mice and in HEK 293A cells co-expressing PS-1 Y115H and MAO-A.
5) The PS-1 Y115H protein is the only protein that can directly interact with both MAO isoforms.
6) Inhibition of PS-1 M146V by DAPT causes an increase in MAO-A activity, suggesting a competitive inhibition of the PS-1 binding site could release MAO-A and allow for its activation.

4.3 Future directions

Because many of the findings from this work have never been presented before there are still many *in vitro* and *in vivo* experiments that are necessary. First it would be important to quantitate the effects of the PS-1 constructs on Ca^{2+} levels or distribution within the cell. Second, it is necessary to know to what extent, if any, MAO-A cleavage is similar to other familiar PS-1 substrates such as APP and Notch. Based on this, MAO-A truncation mutants could be generated to see if truncated MAO-A protein retains activity. Lastly, it would be critical to determine how much of the increased MAO-A activity (by full-length or smaller MAO-A peptides) contributes to hydroxyl radical production and oxidative stress in the brain. Well-known reagents such as the hydrogen peroxide-binding DCFDA can be used for this purpose. These experiments should elucidate the mechanism(s) by which PS-1 (and Ca^{2+}) affects MAO activity and to what degree this increased MAO activity (and sensitivity to Ca^{2+}) is implicated in the neurodegeneration occurring in AD.

5 REFERENCES

1. Chamandy N, Wolfson C. 2005. Underlying cause of death in demented and non-demented elderly Canadians. *Neuroepidemiology* 25: 75-84
2. Kochanek KD, Murphy SL, Anderson RN, Scott C. 2004. Deaths: final data for 2002. *Natl Vital Stat Rep* 53: 1-115
3. Goedert M, Spillantini MG. 2006. A century of Alzheimer's disease. *Science* 314: 777-81
4. Selkoe DJ, Podlisny MB. 2002. Deciphering the genetic basis of Alzheimer's disease. *Annu Rev Genomics Hum Genet* 3: 67-99
5. Roberson ED, Mucke L. 2006. 100 years and counting: prospects for defeating Alzheimer's disease. *Science* 314: 781-4
6. Sherrington R, Rogaev EI, Liang Y, Rogaeva EA, Levesque G, et al. 1995. Cloning of a gene bearing missense mutations in early-onset familial Alzheimer's disease. *Nature* 375: 754-60
7. Rogaev EI, Sherrington R, Wu C, Levesque G, Liang Y, et al. 1997. Analysis of the 5' sequence, genomic structure, and alternative splicing of the presenilin-1 gene (PSEN1) associated with early onset Alzheimer disease. *Genomics* 40: 415-24
8. Rogaev EI, Sherrington R, Rogaeva EA, Levesque G, Ikeda M, et al. 1995. Familial Alzheimer's disease in kindreds with missense mutations in a gene on chromosome 1 related to the Alzheimer's disease type 3 gene. *Nature* 376: 775-8
9. Cook DG, Sung JC, Golde TE, Felsenstein KM, Wojczyk BS, et al. 1996. Expression and analysis of presenilin 1 in a human neuronal system:

localization in cell bodies and dendrites. *Proc Natl Acad Sci U S A* 93: 9223-8

10. Kovacs DM, Fausett HJ, Page KJ, Kim TW, Moir RD, et al. 1996. Alzheimer-associated presenilins 1 and 2: neuronal expression in brain and localization to intracellular membranes in mammalian cells. *Nat Med* 2: 224-9
11. Dewji NN, Singer SJ. 1997. Cell surface expression of the Alzheimer disease-related presenilin proteins. *Proc Natl Acad Sci U S A* 94: 9926-31
12. Li J, Xu M, Zhou H, Ma J, Potter H. 1997. Alzheimer presenilins in the nuclear membrane, interphase kinetochores, and centrosomes suggest a role in chromosome segregation. *Cell* 90: 917-27
13. Ankarcrona M, Hultenby K. 2002. Presenilin-1 is located in rat mitochondria. *Biochem Biophys Res Commun* 295: 766-70
14. Hansson CA, Frykman S, Farmery MR, Tjernberg LO, Nilsberth C, et al. 2004. Nicastrin, presenilin, APH-1, and PEN-2 form active gamma-secretase complexes in mitochondria. *J Biol Chem* 279: 51654-60
15. Kimberly WT, LaVoie MJ, Ostaszewski BL, Ye W, Wolfe MS, Selkoe DJ. 2003. Gamma-secretase is a membrane protein complex comprised of presenilin, nicastrin, Aph-1, and Pen-2. *Proc Natl Acad Sci U S A* 100: 6382-7
16. Hardy J, Selkoe DJ. 2002. The amyloid hypothesis of Alzheimer's disease: progress and problems on the road to therapeutics. *Science* 297: 353-6
17. Brunkan AL, Goate AM. 2005. Presenilin function and gamma-secretase activity. *J Neurochem* 93: 769-92
18. Medina M, Dotti CG. 2003. RIPped out by presenilin-dependent gamma-secretase. *Cell Signal* 15: 829-41
19. Selkoe DJ, Wolfe MS. 2007. Presenilin: running with scissors in the membrane. *Cell* 131: 215-21
20. Moreira PI, Honda K, Liu Q, Santos MS, Oliveira CR, et al. 2005. Oxidative stress: the old enemy in Alzheimer's disease pathophysiology. *Curr Alzheimer Res* 2: 403-8

21. Iwatsubo T, Odaka A, Suzuki N, Mizusawa H, Nukina N, Ihara Y. 1994. Visualization of A beta 42(43) and A beta 40 in senile plaques with end-specific A beta monoclonals: evidence that an initially deposited species is A beta 42(43). *Neuron* 13: 45-53
22. Zhao B, Yu M, Neitzel M, Marugg J, Jagodzinski J, et al. 2008. Identification of {gamma}-Secretase Inhibitor Potency Determinants on Presenilin. *J Biol Chem* 283: 2927-38
23. Pan D, Rubin GM. 1997. Kuzbanian controls proteolytic processing of Notch and mediates lateral inhibition during Drosophila and vertebrate neurogenesis. *Cell* 90: 271-80
24. Brou C, Logeat F, Gupta N, Bessia C, LeBail O, et al. 2000. A novel proteolytic cleavage involved in Notch signaling: the role of the disintegrin-metalloprotease TACE. *Mol Cell* 5: 207-16
25. Mumm JS, Schroeter EH, Saxena MT, Griesemer A, Tian X, et al. 2000. A ligand-induced extracellular cleavage regulates gamma-secretase-like proteolytic activation of Notch1. *Mol Cell* 5: 197-206
26. Thinakaran G, Borchelt DR, Lee MK, Slunt HH, Spitzer L, et al. 1996. Endoproteolysis of presenilin 1 and accumulation of processed derivatives in vivo. *Neuron* 17: 181-90
27. Podlisny MB, Citron M, Amarante P, Sherrington R, Xia W, et al. 1997. Presenilin proteins undergo heterogeneous endoproteolysis between Thr291 and Ala299 and occur as stable N- and C-terminal fragments in normal and Alzheimer brain tissue. *Neurobiol Dis* 3: 325-37
28. Kim H, Ki H, Park HS, Kim K. 2005. Presenilin-1 D257A and D385A mutants fail to cleave Notch in their endoproteolyzed forms, but only presenilin-1 D385A mutant can restore its gamma-secretase activity with the compensatory overexpression of normal C-terminal fragment. *J Biol Chem* 280: 22462-72
29. Wolfe MS, Xia W, Ostaszewski BL, Diehl TS, Kimberly WT, Selkoe DJ. 1999. Two transmembrane aspartates in presenilin-1 required for presenilin endoproteolysis and gamma-secretase activity. *Nature* 398: 513-7

30. Yamasaki A, Eimer S, Okochi M, Smialowska A, Kaether C, et al. 2006. The GxGD motif of presenilin contributes to catalytic function and substrate identification of gamma-secretase. *J Neurosci* 26: 3821-8
31. Fraering PC, LaVoie MJ, Ye W, Ostaszewski BL, Kimberly WT, et al. 2004. Detergent-dependent dissociation of active gamma-secretase reveals an interaction between Pen-2 and PS1-NTF and offers a model for subunit organization within the complex. *Biochemistry* 43: 323-33
32. Tu H, Nelson O, Bezprozvanny A, Wang Z, Lee SF, et al. 2006. Presenilins form ER Ca2+ leak channels, a function disrupted by familial Alzheimer's disease-linked mutations. *Cell* 126: 981-93
33. Yoo AS, Cheng I, Chung S, Grenfell TZ, Lee H, et al. 2000. Presenilin-mediated modulation of capacitative calcium entry. *Neuron* 27: 561-72
34. Wang R, Wang B, He W, Zheng H. 2006. Wild-type presenilin 1 protects against Alzheimer disease mutation-induced amyloid pathology. *J Biol Chem* 281: 15330-6
35. Dumanchin C, Brice A, Campion D, Hannequin D, Martin C, et al. 1998. De novo presenilin 1 mutations are rare in clinically sporadic, early onset Alzheimer's disease cases. French Alzheimer's Disease Study Group. *J Med Genet* 35: 672-3
36. Mehta ND, Refolo LM, Eckman C, Sanders S, Yager D, et al. 1998. Increased Abeta42(43) from cell lines expressing presenilin 1 mutations. *Ann Neurol* 43: 256-8
37. Scheuner D, Eckman C, Jensen M, Song X, Citron M, et al. 1996. Secreted amyloid beta-protein similar to that in the senile plaques of Alzheimer's disease is increased in vivo by the presenilin 1 and 2 and APP mutations linked to familial Alzheimer's disease. *Nat Med* 2: 864-70
38. Blurton-Jones M, Laferla FM. 2006. Pathways by which Abeta facilitates tau pathology. *Curr Alzheimer Res* 3: 437-48
39. Gomez-Isla T, Growdon WB, McNamara MJ, Nochlin D, Bird TD, et al. 1999. The impact of different presenilin 1 andpresenilin 2 mutations on amyloid deposition, neurofibrillary changes and neuronal loss in the familial

Alzheimer's disease brain: evidence for other phenotype-modifying factors. *Brain* 122 (Pt 9): 1709-19

40. Larner AJ, Doran M. 2006. Clinical phenotypic heterogeneity of Alzheimer's disease associated with mutations of the presenilin-1 gene. *J Neurol* 253: 139-58
41. Dovey HF, John V, Anderson JP, Chen LZ, de Saint Andrieu P, et al. 2001. Functional gamma-secretase inhibitors reduce beta-amyloid peptide levels in brain. *J Neurochem* 76: 173-81
42. Wong GT, Manfra D, Poulet FM, Zhang Q, Josien H, et al. 2004. Chronic treatment with the gamma-secretase inhibitor LY-411,575 inhibits beta-amyloid peptide production and alters lymphopoiesis and intestinal cell differentiation. *J Biol Chem* 279: 12876-82
43. Schmidt B, Baumann S, Braun HA, Larbig G. 2006. Inhibitors and modulators of beta- and gamma-secretase. *Curr Top Med Chem* 6: 377-92
44. Weggen S, Eriksen JL, Das P, Sagi SA, Wang R, et al. 2001. A subset of NSAIDs lower amyloidogenic Abeta42 independently of cyclooxygenase activity. *Nature* 414: 212-6
45. Hare ML. 1928. Tyramine oxidase: A new enzyme system in liver. *Biochem J* 22: 968-79
46. Blaschko H, Richter D, Schlossmann H. 1937. The oxidation of adrenaline and other amines. *Biochem J* 31: 2187-96
47. Slotkin TA. 1999. Mary Bernheim and the discovery of monoamine oxidase. *Brain Res Bull* 50: 373
48. Bach AW, Lan NC, Johnson DL, Abell CW, Bembenek ME, et al. 1988. cDNA cloning of human liver monoamine oxidase A and B: molecular basis of differences in enzymatic properties. *Proc Natl Acad Sci U S A* 85: 4934-8
49. Hsu YP, Weyler W, Chen S, Sims KB, Rinehart WB, et al. 1988. Structural features of human monoamine oxidase A elucidated from cDNA and peptide sequences. *J Neurochem* 51: 1321-4
50. Powell JF, Hsu YP, Weyler W, Chen SA, Salach J, et al. 1989. The primary structure of bovine monoamine oxidase type A. Comparison with peptide

sequences of bovine monoamine oxidase type B and other flavoenzymes. *Biochem J* 259: 407-13

51. Lan NC, Heinzmann C, Gal A, Klisak I, Orth U, et al. 1989. Human monoamine oxidase A and B genes map to Xp 11.23 and are deleted in a patient with Norrie disease. *Genomics* 4: 552-9
52. Levy ER, Powell JF, Buckle VJ, Hsu YP, Breakefield XO, Craig IW. 1989. Localization of human monoamine oxidase-A gene to Xp11.23-11.4 by in situ hybridization: implications for Norrie disease. *Genomics* 5: 368-70
53. Grimsby J, Chen K, Wang LJ, Lan NC, Shih JC. 1991. Human monoamine oxidase A and B genes exhibit identical exon-intron organization. *Proc Natl Acad Sci U S A* 88: 3637-41
54. De Colibus L, Li M, Binda C, Lustig A, Edmondson DE, Mattevi A. 2005. Three-dimensional structure of human monoamine oxidase A (MAO A): relation to the structures of rat MAO A and human MAO B. *Proc Natl Acad Sci U S A* 102: 12684-9
55. Binda C, Li M, Hubalek F, Restelli N, Edmondson DE, Mattevi A. 2003. Insights into the mode of inhibition of human mitochondrial monoamine oxidase B from high-resolution crystal structures. *Proc Natl Acad Sci U S A* 100: 9750-5
56. Binda C, Newton-Vinson P, Hubalek F, Edmondson DE, Mattevi A. 2002. Structure of human monoamine oxidase B, a drug target for the treatment of neurological disorders. *Nat Struct Biol* 9: 22-6
57. Pintar JE, Breakefield XO. 1982. Monoamine oxidase (MAO) activity as a determinant in human neurophysiology. *Behav Genet* 12: 53-68
58. Levitt P, Pintar JE, Breakefield XO. 1982. Immunocytochemical demonstration of monoamine oxidase B in brain astrocytes and serotonergic neurons. *Proc Natl Acad Sci U S A* 79: 6385-9
59. Westlund KN, Denney RM, Kochersperger LM, Rose RM, Abell CW. 1985. Distinct monoamine oxidase A and B populations in primate brain. *Science* 230: 181-3

60. Thorpe LW, Westlund KN, Kochersperger LM, Abell CW, Denney RM. 1987. Immunocytochemical localization of monoamine oxidases A and B in human peripheral tissues and brain. *J Histochem Cytochem* 35: 23-32
61. Cotzias GC, Dole VP. 1951. Metabolism of amines. II. Mitochondrial localization of monoamine oxidase. *Proc Soc Exp Biol Med* 78: 157-60
62. Rodriguez De Lores Arnaiz G, De Robertis ED. 1962. Cholinergic and non-cholinergic nerve endings in the rat brain. II. Subcellular localization of monoamine oxidase and succinate dehydrogenase. *J Neurochem* 9: 503-8
63. Oswald EO, Strittmatter CF. 1963. Comparative Studies in the Characterization of Monoamine Oxidases. *Proc Soc Exp Biol Med* 114: 668-73
64. Gorkin VZ. 1966. Monoamine oxidases. *Pharmacol Rev* 18: 115-20
65. Schnaitman C, Erwin VG, Greenawalt JW. 1967. The submitochondrial localization of monoamine oxidase. An enzymatic marker for the outer membrane of rat liver mitochondria. *J Cell Biol* 32: 719-35
66. Greenawalt JW, Schnaitman C. 1970. An appraisal of the use of monoamine oxidase as an enzyme marker for the outer membrane of rat liver mitochondria. *J Cell Biol* 46: 173-9
67. Youdim MB, Bakhle YS. 2006. Monoamine oxidase: isoforms and inhibitors in Parkinson's disease and depressive illness. *Br J Pharmacol* 147 Suppl 1: S287-96
68. Johnston JP. 1968. Some observations upon a new inhibitor of monoamine oxidase in brain tissue. *Biochem Pharmacol* 17: 1285-97
69. Cases O, Seif I, Grimsby J, Gaspar P, Chen K, et al. 1995. Aggressive behavior and altered amounts of brain serotonin and norepinephrine in mice lacking MAOA. *Science* 268: 1763-6
70. Grimsby J, Toth M, Chen K, Kumazawa T, Klaidman L, et al. 1997. Increased stress response and beta-phenylethylamine in MAOB-deficient mice. *Nat Genet* 17: 206-10

71. Liebowitz MR, Hollander E, Schneier F, Campeas R, Welkowitz L, et al. 1990. Reversible and irreversible monoamine oxidase inhibitors in other psychiatric disorders. *Acta Psychiatr Scand Suppl* 360: 29-34

72. Chiba K, Trevor A, Castagnoli N, Jr. 1984. Metabolism of the neurotoxic tertiary amine, MPTP, by brain monoamine oxidase. *Biochem Biophys Res Commun* 120: 574-8

73. Burns RS, Chiueh CC, Markey SP, Ebert MH, Jacobowitz DM, Kopin IJ. 1983. A primate model of parkinsonism: selective destruction of dopaminergic neurons in the pars compacta of the substantia nigra by N-methyl-4-phenyl-1,2,3,6-tetrahydropyridine. *Proc Natl Acad Sci U S A* 80: 4546-50

74. Blackwell B. 1963. Hypertensive Crisis Due to Monoamine-Oxidase Inhibitors. *Lancet* 2: 849-50

75. Knoll J. 1986. The pharmacology of (-)deprenyl. *J Neural Transm Suppl* 22: 75-89

76. Birkmayer W, Riederer P, Ambrozi L, Youdim MB. 1977. Implications of combined treatment with 'Madopar' and L-deprenil in Parkinson's disease. A long-term study. *Lancet* 1: 439-43

77. Birkmayer W, Knoll J, Riederer P, Youdim MB, Hars V, Marton J. 1985. Increased life expectancy resulting from addition of L-deprenyl to Madopar treatment in Parkinson's disease: a longterm study. *J Neural Transm* 64: 113-27

78. Finberg JP, Wang J, Bankiewicz K, Harvey-White J, Kopin IJ, Goldstein DS. 1998. Increased striatal dopamine production from L-DOPA following selective inhibition of monoamine oxidase B by R(+)-N-propargyl-1-aminoindan (rasagiline) in the monkey. *J Neural Transm Suppl* 52: 279-85

79. Mandel S, Weinreb O, Amit T, Youdim MB. 2005. Mechanism of neuroprotective action of the anti-Parkinson drug rasagiline and its derivatives. *Brain Res Brain Res Rev* 48: 379-87

80. Fowler JS, Volkow ND, Wang GJ, Pappas N, Logan J, et al. 1996a. Inhibition of monoamine oxidase B in the brains of smokers. *Nature* 379: 733-6

81. Haefely W, Burkard WP, Cesura AM, Kettler R, Lorez HP, et al. 1992. Biochemistry and pharmacology of moclobemide, a prototype RIMA. *Psychopharmacology (Berl)* 106 Suppl: S6-14

82. Sieradzan K, Channon S, Ramponi C, Stern GM, Lees AJ, Youdim MB. 1995. The therapeutic potential of moclobemide, a reversible selective monoamine oxidase A inhibitor in Parkinson's disease. *J Clin Psychopharmacol* 15: 51S-9S

83. Bonnet U. 2003. Moclobemide: therapeutic use and clinical studies. *CNS Drug Rev* 9: 97-140

84. Fowler JS, Volkow ND, Wang GJ, Pappas N, Logan J, et al. 1996b. Brain monoamine oxidase A inhibition in cigarette smokers. *Proc Natl Acad Sci U S A* 93: 14065-9

85. Mega MS, Cummings JL, Fiorello T, Gornbein J. 1996. The spectrum of behavioral changes in Alzheimer's disease. *Neurology* 46: 130-5

86. Agbayewa MO. 1986. Earlier psychiatric morbidity in patients with Alzheimer's disease. *J Am Geriatr Soc* 34: 561-4

87. Berger AK, Fratiglioni L, Forsell Y, Winblad B, Backman L. 1999. The occurrence of depressive symptoms in the preclinical phase of AD: a population-based study. *Neurology* 53: 1998-2002

88. Shalat SL, Seltzer B, Pidcock C, Baker EL, Jr. 1987. Risk factors for Alzheimer's disease: a case-control study. *Neurology* 37: 1630-3

89. Ringman JM, Diaz-Olavarrieta C, Rodriguez Y, Chavez M, Paz F, et al. 2004. Female preclinical presenilin-1 mutation carriers unaware of their genetic status have higher levels of depression than their non-mutation carrying kin. *J Neurol Neurosurg Psychiatry* 75: 500-2

90. Braak H, Braak E. 1991. Neuropathological stageing of Alzheimer-related changes. *Acta Neuropathol* 82: 239-59

91. Mejia S, Giraldo M, Pineda D, Ardila A, Lopera F. 2003. Nongenetic factors as modifiers of the age of onset of familial Alzheimer's disease. *Int Psychogeriatr* 15: 337-49

92. Emson PC, Lindvall O. 1986. Neuroanatomical aspects of neurotransmitters affected in Alzheimer's disease. *Br Med Bull* 42: 57-62

93. Emilsson L, Saetre P, Balciuniene J, Castensson A, Cairns N, Jazin EE. 2002. Increased monoamine oxidase messenger RNA expression levels in frontal cortex of Alzheimer's disease patients. *Neurosci Lett* 326: 56-60

94. Sparks DL, Woeltz VM, Markesbery WR. 1991. Alterations in brain monoamine oxidase activity in aging, Alzheimer's disease, and Pick's disease. *Arch Neurol* 48: 718-21

95. Smith MA, Perry G, Richey PL, Sayre LM, Anderson VE, et al. 1996. Oxidative damage in Alzheimer's. *Nature* 382: 120-1

96. Sayre LM, Zelasko DA, Harris PL, Perry G, Salomon RG, Smith MA. 1997. 4-Hydroxynonenal-derived advanced lipid peroxidation end products are increased in Alzheimer's disease. *J Neurochem* 68: 2092-7

97. Smith MA, Harris PL, Sayre LM, Perry G. 1997. Iron accumulation in Alzheimer disease is a source of redox-generated free radicals. *Proc Natl Acad Sci U S A* 94: 9866-8

98. Zheng H, Gal S, Weiner LM, Bar-Am O, Warshawsky A, et al. 2005. Novel multifunctional neuroprotective iron chelator-monoamine oxidase inhibitor drugs for neurodegenerative diseases: in vitro studies on antioxidant activity, prevention of lipid peroxide formation and monoamine oxidase inhibition. *J Neurochem* 95: 68-78

99. Anandatheerthavarada HK, Biswas G, Robin MA, Avadhani NG. 2003. Mitochondrial targeting and a novel transmembrane arrest of Alzheimer's amyloid precursor protein impairs mitochondrial function in neuronal cells. *J Cell Biol* 161: 41-54

100. Leissring MA, Paul BA, Parker I, Cotman CW, LaFerla FM. 1999. Alzheimer's presenilin-1 mutation potentiates inositol 1,4,5-trisphosphate-mediated calcium signaling in Xenopus oocytes. *J Neurochem* 72: 1061-8

101. Guo Q, Furukawa K, Sopher BL, Pham DG, Xie J, et al. 1996. Alzheimer's PS-1 mutation perturbs calcium homeostasis and sensitizes PC12 cells to death induced by amyloid beta-peptide. *Neuroreport* 8: 379-83

102. Cedazo-Minguez A, Popescu BO, Ankarcrona M, Nishimura T, Cowburn RF. 2002. The presenilin 1 deltaE9 mutation gives enhanced basal phospholipase C activity and a resultant increase in intracellular calcium concentrations. *J Biol Chem* 277: 36646-55

103. Leissring MA, Akbari Y, Fanger CM, Cahalan MD, Mattson MP, LaFerla FM. 2000. Capacitative calcium entry deficits and elevated luminal calcium content in mutant presenilin-1 knockin mice. *J Cell Biol* 149: 793-8

104. Smith IF, Hitt B, Green KN, Oddo S, LaFerla FM. 2005. Enhanced caffeine-induced Ca2+ release in the 3xTg-AD mouse model of Alzheimer's disease. *J Neurochem* 94: 1711-8

105. Schneider I, Reverse D, Dewachter I, Ris L, Caluwaerts N, et al. 2001. Mutant presenilins disturb neuronal calcium homeostasis in the brain of transgenic mice, decreasing the threshold for excitotoxicity and facilitating long-term potentiation. *J Biol Chem* 276: 11539-44

106. Begley JG, Duan W, Chan S, Duff K, Mattson MP. 1999. Altered calcium homeostasis and mitochondrial dysfunction in cortical synaptic compartments of presenilin-1 mutant mice. *J Neurochem* 72: 1030-9

107. Navarro A. 2004. Mitochondrial enzyme activities as biochemical markers of aging. *Mol Aspects Med* 25: 37-48

108. Casley CS, Land JM, Sharpe MA, Clark JB, Duchen MR, Canevari L. 2002. Beta-amyloid fragment 25-35 causes mitochondrial dysfunction in primary cortical neurons. *Neurobiol Dis* 10: 258-67

109. Boitier E, Rea R, Duchen MR. 1999. Mitochondria exert a negative feedback on the propagation of intracellular Ca2+ waves in rat cortical astrocytes. *J Cell Biol* 145: 795-808

110. Kosenko EA, Venediktova NI, Kaminsky Yu G. 2003. [Calcium and ammonia stimulate monoamine oxidase A activity in brain mitochondria]. *Biology bulletin of the Russian Academy of Sciences* 30: 449-52

111. Cao X, Wei Z, Gabriel GG, Li X, Mousseau DD. 2007. Calcium-sensitive regulation of monoamine oxidase-A contributes to the production of peroxyradicals in hippocampal cultures: implications for Alzheimer disease-related pathology. *BMC Neurosci* 8: 73

112. Satrustegui J, Villalba M, Pereira R, Bogonez E, Martinez-Serrano A. 1996. Cytosolic and mitochondrial calcium in synaptosomes during aging. *Life Sci* 59: 429-34

113. Tollefson GD. 1990. Short-term effects of the calcium channel blocker nimodipine (Bay-e-9736) in the management of primary degenerative dementia. *Biol Psychiatry* 27: 1133-42

114. Bullock R. 2006. Efficacy and safety of memantine in moderate-to-severe Alzheimer disease: the evidence to date. *Alzheimer Dis Assoc Disord* 20: 23-9

115. Perez-Tur J, Froelich S, Prihar G, Crook R, Baker M, et al. 1995. A mutation in Alzheimer's disease destroying a splice acceptor site in the presenilin-1 gene. *Neuroreport* 7: 297-301

116. Citron M, Eckman CB, Diehl TS, Corcoran C, Ostaszewski BL, et al. 1998. Additive effects of PS1 and APP mutations on secretion of the 42-residue amyloid beta-protein. *Neurobiol Dis* 5: 107-16

117. Steiner H, Romig H, Grim MG, Philipp U, Pesold B, et al. 1999. The biological and pathological function of the presenilin-1 Deltaexon 9 mutation is independent of its defect to undergo proteolytic processing. *J Biol Chem* 274: 7615-8

118. Smith IF, Boyle JP, Vaughan PF, Pearson HA, Cowburn RF, Peers CS. 2002. Ca(2+) stores and capacitative Ca(2+) entry in human neuroblastoma (SH-SY5Y) cells expressing a familial Alzheimer's disease presenilin-1 mutation. *Brain Res* 949: 105-11

119. Campion D, Flaman JM, Brice A, Hannequin D, Dubois B, et al. 1995. Mutations of the presenilin I gene in families with early-onset Alzheimer's disease. *Hum Mol Genet* 4: 2373-7

120. Campion D, Dumanchin C, Hannequin D, Dubois B, Belliard S, et al. 1999. Early-onset autosomal dominant Alzheimer disease: prevalence, genetic heterogeneity, and mutation spectrum. *Am J Hum Genet* 65: 664-70
121. Hebert SS, Godin C, Levesque G. 2003. Oligomerization of human presenilin-1 fragments. *FEBS Lett* 550: 30-4
122. Hatchett CS, Tyler S, Armstrong D, Dawbarn D, Allen SJ. 2007. Familial Alzheimer's disease presenilin 1 mutation M146V increases gamma secretase cutting of p75NTR in vitro. *Brain Res* 1147: 248-55
123. Pigino G, Pelsman A, Mori H, Busciglio J. 2001. Presenilin-1 mutations reduce cytoskeletal association, deregulate neurite growth, and potentiate neuronal dystrophy and tau phosphorylation. *J Neurosci* 21: 834-42
124. Guo Q, Christakos S, Robinson N, Mattson MP. 1998. Calbindin D28k blocks the proapoptotic actions of mutant presenilin 1: reduced oxidative stress and preserved mitochondrial function. *Proc Natl Acad Sci U S A* 95: 3227-32
125. LaFontaine MA, Mattson MP, Butterfield DA. 2002. Oxidative stress in synaptosomal proteins from mutant presenilin-1 knock-in mice: implications for familial Alzheimer's disease. *Neurochem Res* 27: 417-21
126. Guo Q, Fu W, Sopher BL, Miller MW, Ware CB, et al. 1999. Increased vulnerability of hippocampal neurons to excitotoxic necrosis in presenilin-1 mutant knock-in mice. *Nat Med* 5: 101-6
127. Kim SH, Leem JY, Lah JJ, Slunt HH, Levey AI, et al. 2001. Multiple effects of aspartate mutant presenilin 1 on the processing and trafficking of amyloid precursor protein. *J Biol Chem* 276: 43343-50
128. Capell A, Steiner H, Romig H, Keck S, Baader M, et al. 2000. Presenilin-1 differentially facilitates endoproteolysis of the beta-amyloid precursor protein and Notch. *Nat Cell Biol* 2: 205-11
129. Baker GB, Wong JT, Coutts RT, Pasutto FM. 1987. Simultaneous extraction and quantitation of several bioactive amines in cheese and chocolate. *J Chromatogr* 392: 317-31

130. van Groen T, Kiliaan AJ, Kadish I. 2006. Deposition of mouse amyloid beta in human APP/PS1 double and single AD model transgenic mice. *Neurobiol Dis* 23: 653-62

131. Morohashi Y, Kan T, Tominari Y, Fuwa H, Okamura Y, et al. 2006. C-terminal fragment of presenilin is the molecular target of a dipeptidic gamma-secretase-specific inhibitor DAPT (N-[N-(3,5-difluorophenacetyl)-L-alanyl]-S-phenylglycine t-butyl ester). *J Biol Chem* 281: 14670-6

132. Shih JC, Chen K, Ridd MJ. 1999. Monoamine oxidase: from genes to behavior. *Annu Rev Neurosci* 22: 197-217

133. Meyer JH, Ginovart N, Boovariwala A, Sagrati S, Hussey D, et al. 2006. Elevated monoamine oxidase a levels in the brain: an explanation for the monoamine imbalance of major depression. *Arch Gen Psychiatry* 63: 1209-16

134. Thorpe L, Groulx B. 2001. Depressive syndromes in dementia. *Can J Neurol Sci* 28 Suppl 1: S83-95

6 APPENDIX

A. Permission letters for reproduced PS-1 figure

Science
AAAS

Permissions Letter

Ref # 08-25510

DATE: 24 March 2008
TO: Geraldine Gabriel
University of Saskatchewan
103 Wiggins Road
Saskatoon, Sa S7N 5E4
Canada

FROM: Emilie David, Rights and Permissions
RE: Your request for permission dated 03/23/08

Regarding your request, we are pleased to grant you non-exclusive, non-transferable permission to use the AAAS material identified below in your dissertation or thesis identified below, but limited to the formats identified below, and provided that you meet the conditions / requirements below. Such permission is for one time use and therefore does not include permission for future editions, revisions, additional printings, updates, ancillaries, other formats, translations, or promotional pieces, unless otherwise permitted below. This permission does not apply to figures / artwork that are credited to non-AAAS sources. This permission does not include the right to modify AAAS material.

The following credit line must be printed along with the AAAS material: "From [Insert Full Reference Citation]. Reprinted with permission from AAAS."

This permission covers the use of the AAAS material identified herein in the following format versions of your dissertation/thesis:
[x] print
[x] microform
[x] Digitized / electronic versions , provided the reprinted AAAS material remains in situ and is not made digitally available separated from your dissertation/thesis

AAAS agrees that ProQuest/UMI may supply copies of the dissertation/thesis on demand.

If the requested material is sourced to or references non-AAAS sources, you must obtain authorization from that source as well.

You must obtain approval from the author for any modifications you wish to make to the AAAS content covered by this permission.

AAAS must publish the full paper prior to use of any text.

AAAS does not supply photos or artwork. AAAS material must not be used in a derogatory manner. Use of the AAAS material must not imply any endorsement by the American Association for the Advancement of Science. This permission is not valid for the use of the AAAS and/or SCIENCE logos.

Permission is valid for use of the following AAAS material only:
Fig 2 (modified) from Hardy J and Selkoe, SCIENCE 297:353-356 (July 2002)
In the following work only:
Chapter: 1.2.3.1 Catalytic core of the ?-secretase complex, CHARACTERIZATION OF A NOVEL INTERACTION BETWEEN PRESENILIN-1 AND MONOAMINE OXIDA published by University of Saskatchewan in 2008

Thank you for writing. If you have any questions please call me at (202) 326-7074 or write to me via fax at (202) 682-0816. For international calls, +1 is the country code for the United States.

Headquarters:
1200 New York Avenue, NW, Washington, D.C. 20005 USA

Date: Wed, 26 Mar 2008 13:14:57 -0400
From: "Nicole Boucher" <nboucher@rics.bwh.harvard.edu> **Block Address**
Subject: **Re: Request for permission to reproduce one figure in a M.Sc. thesis**
To: "Geraldine Gabriel" <ggg658@mail.usask.ca>

Reply | Reply All | Forward | Print | Delete

No problem - as long as you did not change anything that would change the scientific facts, I approve the use of an adapted version, with appropriate credit.

Dennis Selkoe

On Mar 24, 2008, at 1:56 PM, Geraldine Gabriel wrote:

> To whom it may concern,
>
> I forgot to mention that the figure discussed below (in the previous email) will be modified in my M.Sc. dissertation. The final modified version is attached in this email. Can you please grant me permission to use this modified version of the figure described below in my M.Sc. thesis only? Thank you again.
>
> Sincerely,
> Geraldine Gabriel
>
> Nicole Boucher wrote:
>
> This email confirms that I give my permission for you to use "Fig. 2. Amyloid-beta production by putative intramembranous processing of APP at the proposed active site of the gamma-secretase/PS1 aspartyl protease" from: Hardy J, Selkoe DJ. 2002 - The amyloid hypothesis of Alzheimer's disease: progress and problems on the road to therapeutics. Science 297:353-356,
>
> Dennis J. Selkoe, MD
> Co-Director
> Center for Neurologic Diseases
> Brigham and Women's Hospital
> 77 Avenue Louis Pasteur,HIM 730
> Boston MA 02115
> Ph: 617-525-5200
> Fx: 617525-5252

B. Permission letters for reproduced APP processing figure

Date: Tue, 25 Mar 2008 10:54:33 +0000
From: "Journals Rights" <jrights@wiley.com> **Block Address**
Subject: **FW: Requesting permission to reproduce a modified version of a figur in a M.Sc. thesis dissertation**
To: "ggg658@mail.usask.ca" <ggg658@mail.usask.ca>

Reply | Reply All | Forward | Print | Delete

Dear Geraldine Gabriel,

Thank you for your email request. Permission is granted for you to use the material below for your thesis/dissertation, subject to the usual acknowledgements and on the understanding that you will reapply for permission if you wish to distribute or publish your thesis/dissertation commercially.

With best wishes,
Sally

Sally Byers
Permissions Assistant
Wiley-Blackwell Publishing Ltd.
PO Box 805
9600 Garsington Road
Oxford OX4 2DQ
UK
Tel.01865 476149
Fax. 01865 471149

-----Original Message-----
From: Geraldine Gabriel [mailto:ggg658@mail.usask.ca]
Sent: 24 March 2008 02:08
To: Journals Rights
Subject: Requesting permission to reproduce a modified version of a figure in a M.Sc. thesis dissertation

To whom it may concern,

My name is Geraldine Gabriel and I am a M.Sc. student at the University of Saskatchewan, Canada. I would like to reproduce a modified version of the figure titled "Fig. 1 APP and Notch metabolism" from:

Brunkan AL, Goate AM. 2005. Presenilin function and gamma-secretase activity. J Neurochem 93:769-792,

in my M.Sc. thesis dissertation titled 'Characterization of a novel interaction between presenilin-1 and monoamine oxidase-A'. My final modified version of the aforementioned figure is attached in this email. I would greatly appreciate it if you would grant me permission to use this one figure for my thesis paper only. Thank you for your consideration.

Kind regards,

Geraldine Gabriel

Date: Mon, 03 Mar 2008 21:13:37 -0600 (CST)
From: "Alison Goate" <goate@icarus.wustl.edu> **Block Address**
Subject: **Re: Requesting permission to use one figure in a M.Sc. thesis**
To: "Geraldine Gabriel" <ggg658@mail.usask.ca>

Reply Reply All Forward Print Delete

>Geraldine
This is fine with me.
Alison Goate

To Dr. Goate,
>
> My name is Geraldine Gabriel and I am a M.Sc. student at the University
> of Saskatchewan, Canada. I would like to use your figure titled "Fig.
> 1 APP and Notch metabolism" from:
>
> Brunkan AL, Goate AM. 2005. Presenilin function and gamma-secretase
> activity. J Neurochem 93:769-792,
>
> as part of my M.Sc. thesis. I would greatly appreciate it if you would
> grant me permission to use this one figure for my thesis paper only.
> Thank you for your consideration.
>
> Kind regards,
> Geraldine Gabriel
>

C. Permission letters for reproduced MAO A and B figures

Date: Mon, 24 Mar 2008 10:00:35 -0400
From: "PNAS Permissions" <PNASPermissions@nas.edu> **Block Address**
Subject: **RE: Requesting permission to reproduce two figures in an M.Sc. thesis dissertation**
To: "Geraldine Gabriel" <ggg658@mail.usask.ca>

Reply | Reply All | Forward | Print | Delete

Dear Dr. Gabriel,

Permission is granted for your use of the figures as described in your message below. Please cite the full journal references and "Copyright (copyright year) National Academy of Sciences, U.S.A."

Best regards,
Ariana Raveica for
Diane Sullenberger
Executive Editor
PNAS

-----Original Message-----
From: Geraldine [mailto:ggg658@mail.usask.ca]
Sent: Sunday, March 23, 2008 10:38 PM
To: PNAS Permissions
Subject: Requesting permission to reproduce two figures in an M.Sc. thesis dissertation

To whom it may concern,

My name is Geraldine Gabriel and I am a M.Sc. student at the University of Saskatchewan, Canada. I would like to reproduce Figure 2A (page 12686) titled "Fig. 2. Overall structure of hMAO A....(A) Ribbon representation of the monomer" from:

De Colibus L, Li M, Binda C, Lustig A, Edmondson DE, Mattevi A. 2005. Three-dimensional structure of human monoamine oxidase A (MAO A): relation to the structures of rat MAO A and human MAO B. Proc Natl Acad Sci U S A 102 (36):12684-12689,

and the figure titled "Fig. 1. Overall three-dimensional structure of human MAO-B monomeric unit in complex with 1,4-diphenyl-2-butene" on page 9751 from:

Binda C, Li M, Hubalek F, Restelli N, Edmondson DE, Mattevi A. 2003. Insights into the mode of inhibition of human mitochondrial monoamine oxidase B from high-resolution crystal structures. Proc Natl Acad Sci U S A 100 (17):9750-9755,

in my M.Sc. thesis dissertation titled 'Characterization of a novel interaction between presenilin-1 and mononamine oxidase-A.' I would greatly appreciate it if you would grant me permission to reproduce these two figures in my thesis paper only (ie. use of figures is not for profit). Thank you for your consideration.

Regards,
Geraldine Gabriel

Date: Thu, 07 Feb 2008 09:25:12 -0500
From: "dale e. edmondson" <deedmon@emory.edu> **Block Address**
Subject: **Re: Requesting permission to use two figures in a M.Sc. thesis**
To: "Geraldine Gabriel" <ggg658@mail.usask.ca>

Reply | Reply All | Forward | Print | Delete

Dear Ms. Gabriel: Thank you for your email message. You certainly have my permission to use the figures listed below in your thesis. Let me know if I can be of any further assistance. Best wishes for a successful defense.

Sincerely yours,

Dale E. Edmondson

>To Dr. Edmondson,
>
>My name is Geraldine Gabriel and I am a M.Sc. student at the University
>of Saskatchewan, Canada. I would like to use your figure titled "Fig.
>2. Overall structure of hMAO A....(A) Ribbon representation of the
>monomer" from:
>
>De Colibus L, Li M, Binda C, Lustig A, Edmondson DE, Mattevi A. 2005.
>Three-dimensional structure of human monoamine oxidase A (MAO A):
>relation to the structures of rat MAO A and human MAO B. Proc Natl Acad
>Sci U S A 102:12684-12689,
>
>and the figure titled "Fig. 1. Overall three-dimensional structure of
>human MAO-B monomeric unit in complex with 1,4-diphenyl-2-butene" from:
>
>Binda C, Li M, Hubalek F, Restelli N, Edmondson DE, Mattevi A. 2003.
>Insights into the mode of inhibition of human mitochondrial monoamine
>oxidase B from high-resolution crystal structures. Proc Natl Acad Sci U
>S A 100:9750-9755,
>
>as part of my M.Sc. thesis. I would greatly appreciate it if you would
>grant me permission to use these two figures for my thesis paper only.
>
>Thank you for your consideration.
>
>Kind regards,
>Geraldine Gabriel

--
Dale E. Edmondson
Department of Biochemistry
Emory University School of Medicine
1510 Clifton Rd.
Atlanta, Georgia 30322
404-727-5972
Fax 404-727-2738